Aus dem Lehrstuhl Anatomie III – Zellbiologie
Biomedizinisches Centrum Martinsried
Lehrstuhl der Ludwig-Maximilians-Universität München
Vorstand: Prof. Dr. Michael Kiebler

"The role of the kinase mechanistic Target Of Rapamycin – mTOR – and the RNA-binding protein Pumilio2 in epileptogenesis"

Dissertation
zum Erwerb des Doktorgrades der Medizin
an der Medizinischen Fakultät der
Ludwig-Maximilians-Universität zu München

vorgelegt von
Helena Franziska Pernice

aus
Bad Soden

2021

Mit Genehmigung der Medizinischen Fakultät
der Universität München

Berichterstatter:	Prof. Dr. Michael Kiebler
Mitberichterstatter:	Prof. Dr. Soheyl Noachtar
Mitbetreuung durch den promovierten Mitarbeiter:	Dr. Bastian Popper
Dekan:	Prof. Dr. med. Thomas Gudermann
Tag der mündlichen Prüfung:	25.11.2021

Table of Contents

Summary

Genetic factors contributing to epilepsy are still poorly understood. Furthermore, there is no available, effective treatment for many kinds of genetic epilepsy. Recent insights have sparked considerable interest into the role of synaptically translated proteins, in particular their regulation by RNA binding proteins (RBPs), in the pathogenesis of neurologic disorders. At the same time, there is increasing appreciation for the role of the kinase mTOR for neuronal overexcitability, presenting a valuable target for new therapeutic approaches towards intractable epilepsies. To address this important question, I studied the role of mTOR in the epileptogenesis of mice lacking the RBP Pumilio2 ($Pum2^{GT}$). To this end, I first compared protein expression and localization of mTOR by Western Blot and immunohistochemistry of murine hippocampus of pre-symptomatic and symptomatic $Pum2^{GT}$ animals. Weaned $Pum2^{GT}$ mice, not yet exhibiting an epileptic phenotype, showed decreased mTOR protein levels, while adult $Pum2^{GT}$ mice, which typically experience seizures, did not. Strikingly, $Pum2^{GT}$ mice that underwent memory training and cognitive stress experiments, showed up to five-fold elevations of mTOR protein levels. In addition, expression of targets regulated by Pum2 and mTOR that are associated with epileptogenesis, such as the voltage gated potassium channels $K_v1.1$ and $K_v4.2$, were significantly altered in $Pum2^{GT}$ murine hippocampus, pointing to a possible contribution to the epileptic phenotype. Finally, I investigated a possible interaction of Pum2 and mTOR in both murine hippocampus, cultured rat primary hippocampal neurons, and an immortalized neuroblastoma cell line (HN10e). I found a rapamycin-dependent partial colocalization of the Pum2 and mTOR suggesting a potential interplay between both proteins.

Collectively, my results provide experimental evidence for disturbed mTOR regulation and function in our mouse model of genetic epilepsy caused by Pum2 deficiency. In particular and consistent with previous studies, the low expression of mTOR in pre-symptomatic mice, and the aberrantly high expression of mTOR in symptomatic animals suggests that decreasing mTOR expression or activity may be protective in epilepsy. Finally, a possible interaction of Pum2 and mTOR proteins and the effect of rapamycin provide a promising foundation for future research on RBP and mTOR in the pathophysiology and potential new treatment options of genetic epilepsy.

Zusammenfassung

Noch heute herrscht ein geringes Verständnis und großteils ein gravierender Mangel an effektiven Behandlungsmöglichkeiten genetischer Epilepsien. Neue Erkenntnisse zur Bedeutung von RNA-Bindeproteinen (RBPs) in der Pathogenese neurologischer Erkrankungen wie Epilepsie haben allerdings beträchtliche Aufmerksamkeit erregt. Gleichzeitig findet die Rolle der mTOR Kinase in der neuronalen Hypererregbarkeit zunehmend Anerkennung, wodurch diese zu einem wertvollen Ansatzpunkt für neue therapeutische Konzepte für therapieresistente Epilepsien wird. Ob mTOR in RBP-vermittelter Epileptogenese eine Rolle spielt, ist jedoch bislang unklar. Um dieser Frage anzugehen, untersuchte ich hier die Rolle von mTOR in der Epileptogenese bei Mäusen, die eine verminderte Expression des RBPs Pumilio2 aufweisen ($Pum2^{GT}$). Zu diesem Zweck verglich ich zunächst mithilfe von Western Blot und Immunhistochemie die Proteinexpression und Lokalisierung von mTOR sowie mehrerer relevanter Zielproteine von Pum2 und mTOR im Hippocampus von präsymptomatischen und symptomatischen $Pum2^{GT}$ Mäusen. Nachwuchs von $Pum2^{GT}$-Mäusen, die noch keinen epileptischen Phänotyp aufweisen, zeigen eine verminderte mTOR-Proteinexpression, im Gegensatz zu erwachsenen Mäusen, die typischerweise an Anfällen leiden und normale mTOR-Proteinexpression aufweisen. Bemerkenswerterweise zeigen $Pum2^{GT}$ Mäuse, die Gedächtnistraining und kognitivem Stress ausgesetzt wurden, fünffach erhöhte mTOR-Proteinmengen. Zusätzlich fand ich im Hippocampus von $Pum2^{GT}$ Mäusen signifikante Veränderungen der Proteinexpression von Zielproteinen, die durch Pum2 und mTOR reguliert werden, wie etwa die spannungsgesteuerten Kaliumkanäle $K_v1.1$ und $K_v4.2$. Zuletzt untersuchte ich eine mögliche Interaktion zwischen Pum2 und mTOR sowohl im Maus-Hippocampus sowie in primären hippocampalen Neuronen der Ratte. Zusätzlich prüfte ich den Effekt einer Rapamycin-Behandlung auf mTOR und Pum2 in einer Neuroblastom-Zellinie (HN10e). Hier kolokalisieren Rapamycin-abhängig mTOR und Pum2, was auf mögliches Zusammenspiel der beiden Proteine hindeutet.

Aus diesen Ergebnissen ergeben sich direkte Beweise dafür, dass in unserem Mausmodell für genetische Epilepsie aufgrund von Pum2-Defizienz eine gestörte mTOR-Regulation und Funktion vorliegen. Insbesondere die niedrige Expression von mTOR in präsymptomatischen Mäusen und die unverhältnismäßig hohe Expression von mTOR in stressexponierten, symptomatischen Mäusen weisen darauf hin, dass

eine verminderte mTOR-Expression oder -Aktivität protektiv sein könnte, was zu den Ergebnissen anderer Forschungsgruppen passt. Schließlich bieten die mögliche Interaktion zwischen Pum2 und mTOR und der festgestellte Effekt von Rapamycin eine vielversprechende Grundlage für zukünftige Forschungen an RBP und mTOR in der Pathophysiologie und möglicherweise auch für neue Behandlungsoptionen der genetischen Epilepsie.

1. Introduction

1.1. Epilepsy and RNA-binding proteins

Epilepsy is a heterogenous group of disorders, affecting about 70 million people worldwide (Shakirullah et al. 2014). Presentations, as well as therapeutic options vary depending on etiology: There are structural, infectious, metabolic, immune, genetic, and unknown epilepsies (Scheffer et al. 2017), and while more than 20 different drugs for epilepsy treatment exist, about 30% of affected patients are still refractory to drug treatment (Löscher et al. 2020). Most genetic epilepsies are still of unknown underlying molecular basis (Scheffer et al. 2017), making a targeted treatment difficult, although possibilities of genetic diagnosis have been rising greatly since the availability of whole-genome sequencing (Dhiman 2017). Furthermore, genetic risk factors are believed to contribute to almost all epilepsies that are not clearly acquired, i.e. caused by brain injury (Hildebrand et al. 2013). Knowledge of the molecular bases of epilepsy, therefore, is of paramount importance in the process of exploring causal treatment options. Recent findings have shown the importance of RNA-binding proteins (RBPs) as such genetic risk factors in disorders associated with epilepsy (Ravanidis 2018). In the following, the function and relevance of RBPs, especially the RBP Pumilio2 (Pum2), will be explained.

1.1.1. RNA-binding proteins

The unique shape of neurons allows them to functionally separate cellular compartments, including cell body, axon, dendrites, and synapses, the contact sites between neurons. To allow functional segregation, proteins need to be differentially localized. In general, proteins are sorted from the cell body to their final destination by the use of sorting signals (Blobel 1980). However, another elegant mechanism exists, allowing local protein synthesis at the site of demand: Nerve cells exploit posttranscriptional gene regulation mechanisms comprising mRNA splicing, transport, and localized translation to achieve polarity as well as spatially defined and lasting composition of protein expression that can be triggered by synaptic stimulation (Doyle and Kiebler 2011). For this to occur, *cis*-acting localization elements, often localized in the 3'-untranslated region (3'-UTR) of certain mRNAs, direct mRNAs to these distal

sites of the nerve cell (Kiebler and DesGroseillers 2000; Doyle and Kiebler 2011). These sorting signals are recognized by RNA-binding proteins (RBPs) forming so-called ribonucleoprotein particles (RNPs), which then are transported along microtubules to their specific destination (Doyle and Kiebler 2011). This is a dynamic process leading to long-term changes in protein composition and, in turn, alters transmission at synapses (Liu-Yesucevitz et al. 2011). RBPs can act as suppressors of translation (Dahm and Kiebler 2005) or as activators of protein synthesis, yielding long-term changes that underlie mechanisms such as long-term potentiation (LTP) and long-term depression (LTD) (Linden 1996; Klein et al. 2015). Although specific signals causing RNA release from their suppressing RBPs to activate translation are still largely unknown, studies propose that a possible mechanism is synaptic activation, that increases synaptic protein synthesis (Yoon et al. 2016; Biever et al. 2019; Narayanan et al. 2007). However, the relevance of the dynamic regulation of localized RNPs for synaptic plasticity in learning, memory and disease has been ascertained (Jung et al. 2014). Diseases such as autism spectrum disorders and epilepsy have been associated with disruption in RBP function: Examples of RBP dysfunction in disease are the cytoplasmic polyadenylation binding protein 4 (CPEB4), which modifies the poly-A tail of mRNA and is associated with autism (Parras et al. 2018), the RBP Fox1 homolog 1 (RBFOX1), a splicing regulator that is involved in epilepsy (Gehman et al. 2011), and the fragile X mental retardation protein (FMRP), a translational repressor that causes the Fragile X Syndrome, a condition leading to intellectual disability and, in many cases, seizures (Kidd et al. 2014). The role of the RBP Pumilio2 in epileptogenesis will be examined in this study.

1.1.2. Pumilio2

Pumilio2 (Pum2) belongs to the Pumilio and FBF repressor protein (PUF) family (Jenkins et al. 2009). Its ability to bind RNA is conserved from yeast to humans (Wickens et al. 2002). In mammals, Pumilio1 (Pum1) and Pum2 have been described (Bohn et al. 2018). Pum1 and Pum2 bind distinct RNA targets even though a significant overlap was observed (Zhang et al. 2017). Pum2 is believed to bind to dendritically located RNA, where it functions mainly through translational repression (Vessey et al. 2006, 2010; Menon et al. 2004). Different mechanisms have been proposed how Pum2 regulates protein expression, including control of RNA stability, translation initiation,

and possibly elongation (Goldstrohm et al. 2018). RNA stability and translation initiation rely both on the polyA tail at the 3'-end (Jackson et al. 2010). It is generally believed that shortening polyA tails leads to decreased translation initiation, and deadenylation of mRNAs is a prerequisite for degradation (Goldstrohm and Wickens 2008). The main deadenylase complex in the cell is the CCR4-Not complex (Collart 2016). Pum2 interacts with components of the CCR4-Not complex to accelerate the degradation of certain target RNAs (Van Etten et al. 2012; Goldstrohm et al. 2006). Since the polyA tail also regulates translation initiation (Shirokikh and Preiss 2018), it is plausible that Pum2 controls translation activity via the polyA tail length as well (Van Etten et al. 2012). Another theory suggests that Pum2 binding to the 7-methyl guanosine cap of mRNA leads to translation repression (Cao et al. 2010). Thereby, Pum2 competes with the eukaryotic translation initiation factor 4e (eIF4e) for cap recognition, a prerequisite for translation initiation (Shirokikh and Preiss 2018). Although it has yet to be shown that these mechanisms apply to dendritically localized translation control, some targets of Pum2 in neurons already suggest that Pum2 regulates mRNA localization and expression in neurons: Axonal growth is enabled by Pum2-mediated retention of mRNA from the axon (Martínez et al. 2019). Furthermore, one of the mRNAs regulated by Pum2 is the voltage gated sodium channel 1.6 ($Na_v1.6$) (Driscoll et al. 2013), which contributes to neuronal hyperexcitability in epilepsy (Hargus et al. 2013). These findings strongly suggest a role of Pum2 in regulating neuronal excitability.

1.1.3. Pumilio2 and temporal lobe epilepsy

Mice lacking Pum2 tend to develop late onset epilepsy (Follwaczny et al. 2017). Interestingly, also in humans suffering from idiopathic temporal lobe epilepsy (TLE), a reduction in Pum2 expression has been detected (Wu et al. 2015). Temporal lobe epilepsy is the most common form of human epilepsy. Specifically, the hippocampus is an area likely to be involved in TLE pathogenesis, since often, hippocampal sclerosis is seen in patients with TLE (Alexander et al. 2016). Pum2 is localized in hippocampal dendrites (Vessey et al. 2006), regulates epileptic markers like $Na_v1.6$ (Driscoll et al. 2013), and has been shown to regulate dendritic branching and the number of excitatory synapses in the hippocampus (Vessey et al. 2010). Interestingly, Follwaczny *et al.* have shown that adult Pum2-deficient mice show region-specific expression

changes of Pum2 targets such as $Na_v1.6$ within the hippocampus (Follwaczny et al. 2017). In this context, it is important to note how different areas of the hippocampus interplay during epileptogenesis (Jarero-Basulto et al. 2018; Alexander et al. 2016). A simplified model of hippocampal circuitry is depicted in **Figure 1**: Perforant tract neurons from the entorhinal cortex target dentate gyrus (DG) neurons and partly conduct signals to cornu ammonis (CA)3 neurons. Axons deriving from the DG project as the mossy fiber tract towards CA3 pyramidal neurons, which carry signals to CA1/2 pyramidal neurons, as well as outside the hippocampus to areas such as the fornix. CA1/2 pyramidal neurons target out of the hippocampus to the entorhinal cortex. In epilepsy, abnormal neuronal firing ultimately promotes severe cellular death of hilar neurons and interneurons (Alexander et al. 2016). The loss of afferences leads to an abnormal growth of projections deriving from the dentate gyrus (DG), referred to as “mossy fiber sprouting” (Navidhamidi et al. 2017). Here, dentate gyrus cell (DGC) axons, called mossy fibers, are believed to build *de novo* recurrent excitatory circuits by projecting to neighboring DGCs (Godale and Danzer 2018). Other theories are the formation of abnormal backprojections of CA3 to DGCs or sprouting of CA1, increasing their excitability (Navidhamidi et al. 2017). Interestingly, in denervated hyperactive CA1 regions, no changes in mRNA levels were seen despite changes in ion channel reduction (Tang and Thompson 2010), suggesting posttranscriptional regulation, for example through RBP-mediated local translation. Additionally, local translation is a crucial player in axonal guidance (Shigeoka et al. 2013), a process that underlies axonal sprouting (Koyama and Ikegaya 2018). Since Pum2 is abundantly expressed in the hippocampus (Follwaczny et al. 2017) and loss of Pum2 leads to increased branching and synapse density of CA1 dendrites (Dong et al. 2018), Pum2 is a potential contributor to the described processes leading to TLE. The hippocampus will therefore be the main target of this thesis.

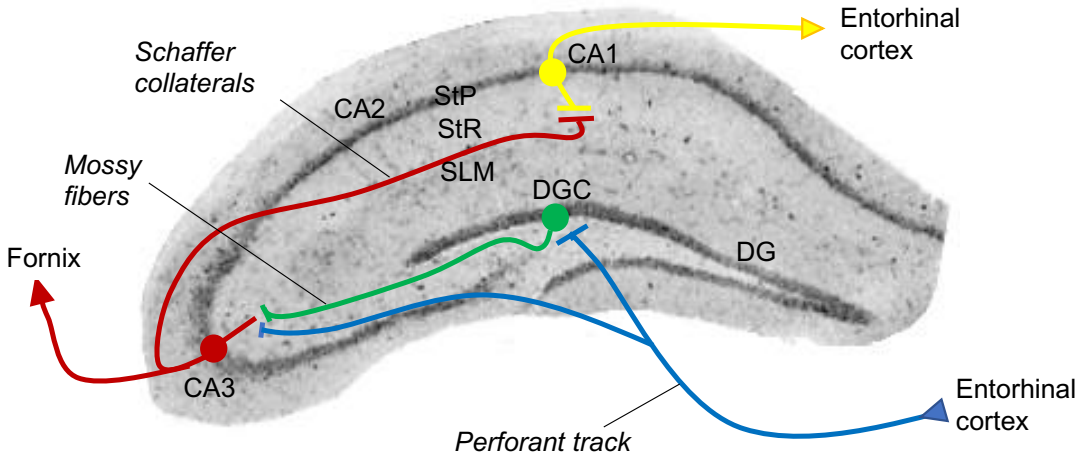

Figure 1: Schematic overview of hippocampal circuitry. Perforant tract neurons from the entorhinal cortex (blue) target DG neurons CA3 neurons (red). DGCs project as the mossy fiber tract (green) towards CA3 pyramidal neurons. CA3 pyramidal neurons target CA1/2 pyramidal neurons (yellow), as well as outside the hippocampus to areas such as the fornix. CA1/2 pyramidal neurons project back to the entorhinal cortex. StP, stratum pyramidale; StR, stratum radiatum; SLM, stratum lacunosum moleculare; CA, cornu ammonis; DG, dentate gyrus. (Figure adapted from Jarero-Basulto et al. 2018).

1.2. Mechanistic target of rapamycin and its role in epileptogenesis

1.2.1. mTOR function and underlying signaling pathways

mTOR is a serine-threonine kinase that is involved in numerous metabolic and stimulatory pathways (Laplante and Sabatini 2009). There are two mTOR complexes, mTORC1 and mTORC2. The two complexes share the common subunits mTOR, the mammalian lethal with sec-13 (mLST8) complex, the Tti1/Tel2 complex, and the DEP domain containing mTOR-interacting protein (DEPTOR) complex. Additional two (in the case of mTORC1) and three (in the case of mTORC2) individual components characterize the two complexes: mTORC1 is defined by its components regulatory protein associated with mTOR (Raptor) and the proline-rich Akt substrate 40kDa (PRAS40). The catalytic subunits mTOR and Raptor, which is the scaffolding protein promoting mTORC1 activity and rapamycin sensitivity, are especially important for function and inhibition. mTORC2 is a rapamycin insensitive complex that consist of rapamycin-insensitive companion of mTOR (Rictor), protein observed with rictor 1 and 2 (protor1/2), and mammalian stress-activated map kinase-interacting protein 1

(mSin1) as defining components. Here, especially mSin1 is important for direct activation of protein kinase B (PKB or AKT) (Laplante and Sabatini 2012; Saxton and Sabatini 2017). Most of the knowledge about mTOR is based on its inhibition by the antibacterial macrolide rapamycin. Rapamycin binds to the FK506 binding protein of 12 kDa (FKBP12), which then binds to mTOR, thereby inhibiting mTOR's ability to bind substrates (Saxton and Sabatini 2017).

An important function of mTOR is the regulation of metabolism is the response to environmental changes, being involved in a broad spectrum of functions like glucose and lipid homeostasis, muscle mass regulation, immune, and brain function (Saxton and Sabatini 2017). Despite these many distinct functions, mTOR operates in one main pathway that dynamically reacts to external stimuli (see **Figure 2**). In neurons, activation of metabolic glutamate receptors (mGluR) and N-methyl-D-aspartic acid receptors (NMDA-R) leads to enhanced activity of the rat sarcoma (Ras) and the phosphoinositide 3-kinase (PI3-K) pathways (Lipton and Sahin 2014). The Ras pathway targets mTOR through activation of the extracellular signal regulated kinase (ERK). This, in turn, inactivates the heterodimer TSC, consisting of Tuberous sclerosis complex 1 (TSC1, also known as harmartin) and TSC2 (also known as tuberin). TSC is a negative regulator of Ras homolog enriched in brain (Rheb), which can only bind and stimulate mTOR in its active guanosine-5'-triphosphate(GTP)-bound form. On the other side, PI3K phosphorylates phosphatidylinositol 4,5-bisphosphate (PIP2) to phosphatidylinositol (3,4,5)-trisphosphate (PIP3), a process that is reversed through phosphatase and tensine homologue (PTEN). PIP3 activates protein kinase B (AKT) through 3-phosphoinositide-dependent protein kinase-1 (PDK1), AKT then targets mTORC1. Furthermore, AKT is directly activated by mTORC2 (Hay and Sonenberg 2004).

The main function of the mTOR downstream pathway is regulation of protein synthesis via two major pathways: the eiF4e binding protein (4EBP) and the ribosomal protein S6 kinase (S6K) pathways (**Figure 2**, bottom). Phosphorylation of 4EBP leads to release of eIF4e that can subsequently bind the 7-methylguanine (7mG) cap of mRNA to promote translation initiation (Hay and Sonenberg 2004; Richter and Sonenberg 2005). Among the two isoforms of S6K, S6K1 and S6K2, S6K1 is the better studied isoform in the mTOR signaling. By phosphorylation of the 40S ribosomal protein S6 (S6) by S6K, producing phosphorylated S6 (pS6), translation is activated (Ma and Blenis 2009; Hay and Sonenberg 2004).

While generally synaptic protein turnover is essential for synaptic function and modulation, it has been shown that activation of protein synthesis increases synaptic activity (Alvarez-Castelao and Schuman 2015). In this context, mTOR pathway has been shown to be an important part of the induction of synaptic protein expression after the stimulation of mGluR (Gong et al. 2006). Regulation of translational activity via the mTOR pathway has been associated with neuronal excitability and disease in many studies, and represents a current approach to understand neuronal physiology and pathology (Swiech et al. 2008; Kepert and Kiebler 2013; Lipton and Sahin 2014). Many components of the mTOR pathway have been directly related to different types of epileptic disorders and are explained in detail below.

1.2.2. The mTOR signaling pathway in epilepsy

mTOR hyperactivation, which is generally measured by pS6 protein expression, has been reported in multiple studies after induction of epileptic seizures through kainate acid or pilocarpine (Buckmaster et al. 2009; Zeng el al. 2009). Excessive protein synthesis through activation of signaling downstream of mTOR is therefore likely to contribute to the observed failure of neuronal homeostasis in epileptogenesis (Sosanya et al. 2015; Niere and Raab-Graham 2017). An example for that is displayed in models of mTOR influencing synaptogenesis: Li *et al.* propose that low doses of ketamine, an anesthetic that functions as a nonselective NMDA receptor antagonist, induced an increase in number and function of synaptic spines in the prefrontal cortex of a rat model for depression in an mTOR dependent manner (Li et al. 2010). Here, mTOR inhibition with rapamycin extinguished the induced expression of postsynaptic density protein 95 (PSD95), mGluR, and synapsin 1 after antagonizing NMDA receptors via ketamine. Similarly, Buckmaster *et al.* described inhibition of mossy fiber and axon sprouting in the dentate gyrus by rapamycin in mouse models of TLE (Buckmaste et al. 2009; Buckmaster and Wen 2011). In particular, in pilocarpine-induced epilepsy, chronic rapamycin infusion (0.01–10mM) leads to reduced mTOR activation and blocks mossy fiber sprouting. Combined, these findings suggest a prominent role of mTOR in epliptogenesis, and especially TLE. As such, mTOR has been proposed as a key contributor to excessive excitability resulting in seizures, both in genetic and acquired epilepsies (Meng et al. 2013). Indeed, in support of this hypothesis, recent studies have documented significant upregulation of both mTOR

protein and activity in TLE patients versus controls (Talos et al. 2018). These findings strongly suggest a pivotal role of mTOR as molecular hub for epileptogenesis.

Also, within the upstream pathway of mTOR activation, two proteins have been directly associated to neurological diseases: the TSC1/2 complex and PTEN (**Figure 2**). In human diseases, decreased expression of TSC1/2 leads to tuberous sclerosis syndrome, a disease, which shows, alongside multiple hamartomas, hypopigmentation and renal carcinoma, an increased predisposition for epilepsy (Curatolo et al. 2018). The TSC1/2 complex inhibits mTOR through inactivation of Ras homolog enriched in brain (Rheb), which is a direct activator of mTOR (Laplante and Sabatini 2009). The epileptic phenotype in TSC is believed to be due to hyperactive mTOR signaling in neurons and structural changes such as formation of tubers in the cortex (Curatolo et al. 2018). Similarly, in PTEN Hamartoma Tumor syndrome, which can lead to neuropsychiatric symptoms, hyperactivation of mTOR activity is believed to be causal for the disease (Krymskaya and Goncharova 2009). PTEN is a phosphatase that influences mTOR signaling through inhibition of the AKT and the ERK signaling pathways, converging with signaling upstream of mTOR (Lipton and Sahin 2014). In fact, many sporadic autism spectrum disorders and cases of macrocephaly, which both correlate with epileptic seizures, exhibit PTEN deletions (Zhou and Parada 2012). Furthermore, several studies have shown that increased neuronal excitability correlates with mTOR upregulation, including in PTEN knock out (KO) mouse models (Pun et al. 2012; Matsushita et al. 2016).

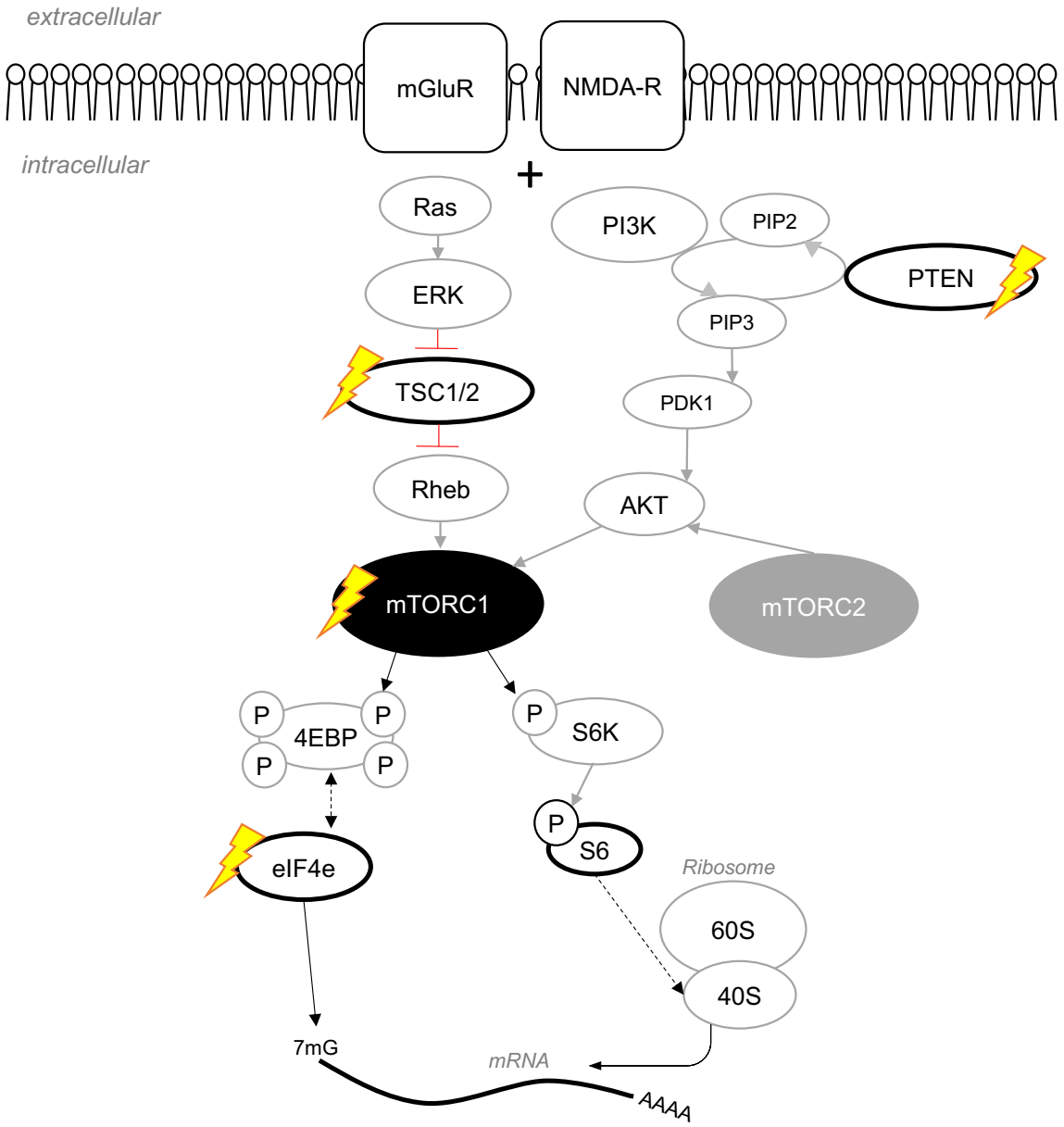

Figure 2: Simplified overview of the mTOR pathway and possible links to epilepsy. Synaptic activation through NMDA or glutamate receptors leads to activation of the Ras-GTP and PI3K pathway. Activation of TSC1/2 via ERK inhibits Rheb, which is necessary for mTOR autophosphorylation and activation. PI3K, antagonized by PTEN, generates PIP3, an activator of the AKT pathway that also targets mTORC1 and can be promoted by mTORC2. Activated mTORC1 phosphorylates 4EBP at four sites, which generates removal of eIF4e from the 7mG cap and initiates translation. Also, S6K is phosphorylated by mTOR, leading to S6 phosphorylation and inclusion into the 40S ribosomal subunit. Black bold circles highlight essential players and flash symbols point to proteins involved in epilepsy (Figure adapted from Lipton et al. 2014).

1.3. RBPs within the mTOR signaling pathway in epilepsy

Having discussed the role of both Pum2 and mTOR in epilepsy, it is now tempting to speculate that both factors might interact, thereby modulating neuronal excitability. The regulation of RBPs by kinases like mTOR represents an exciting mechanism of controlling local protein synthesis in neurons. Interestingly, there is already evidence for such interplay: mTOR and mitogen-activated protein kinase (MAPK) comprise pathways regulating RBPs like ELAV-like protein 4 (HuD), eIF4e, and possibly fragile X mental retardation protein (FMRP) (**Figure 3**, Pernice et al. 2016).

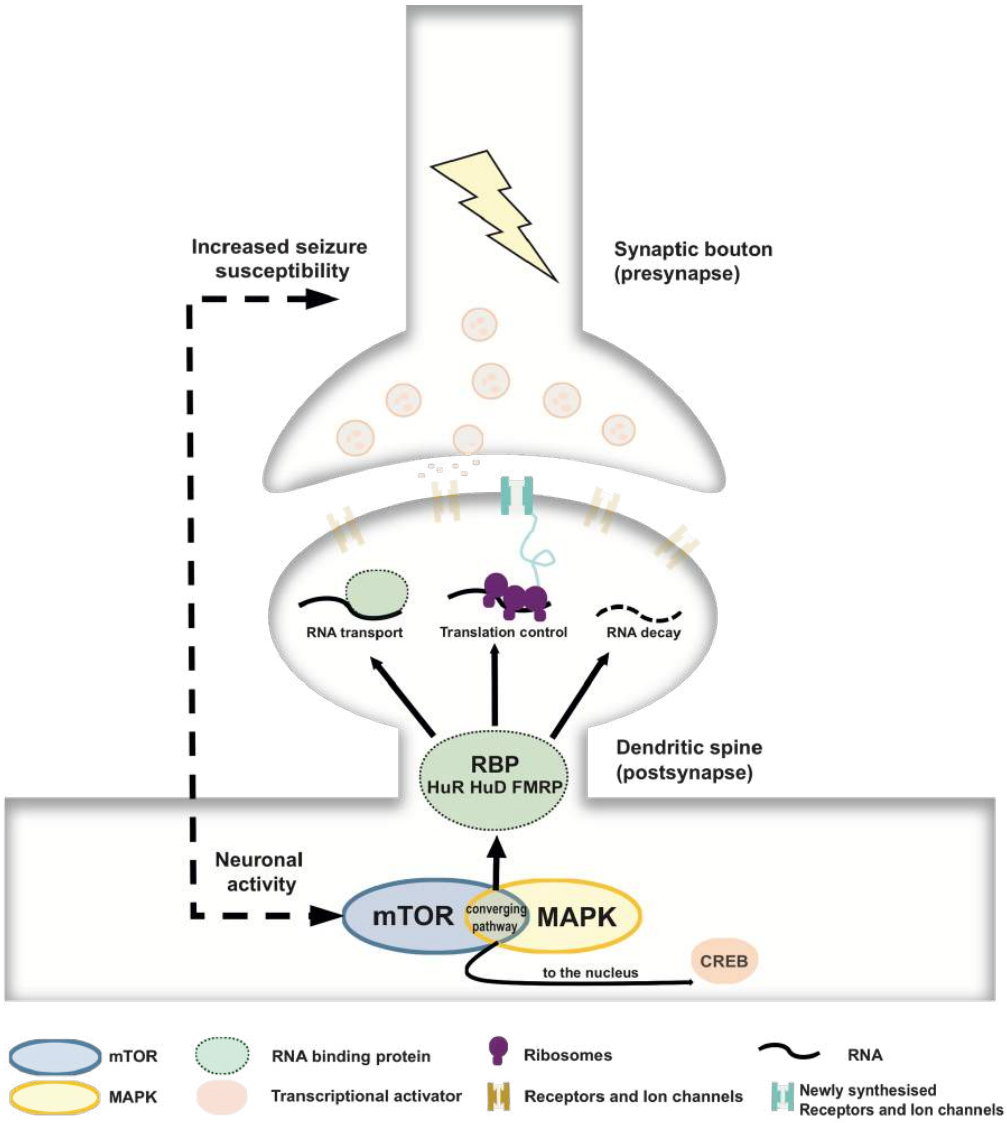

Figure 3: Converging pathways of mTOR and MAPK on RBPs regulating local translation at the synapse. Upon neuronal activation of postsynaptic receptors, mTOR and MAPK both regulate RBPs such as HuR, HuD, FMRP and CREB at dendritic spines. These influence synaptic protein expression via mRNA transport, translational control and mRNA decay, respectively, leading to fine tuning of translation of proteins such as ion channels **(**Figure published in Pernice et al. 2016).

Especially interesting is the interplay between mTOR with HuD and FMRP. The RNA-binding protein HuD is a member of the Hu protein family, which is found to be an important contributor to synaptic plasticity (Deschênes-Furry et al. 2006) and seems to play a role neurological disease such as epilepsy (Perrone-Bizzozero and Bird 2013). The Raab-Graham group has shown that HuD regulates voltage gated potassium channel 1.1 (K_v1.1) expression in hippocampal neurons in a manner antagonistic to mTOR, resulting in downregulation of K_v1.1 protein upon elevated mTOR levels (Sosanya et al. 2013; Raab-Graham et al. 2006). Voltage gated potassium channels are hyperpolarizing channels generally closed at the resting potential (-70mV) and responsible for action potential repolarization (D'Adamo et al. 2013). Mouse models of *KCNA1* knock-out, which encodes K_v1.1, present with epileptic seizures (Smart et al. 1998), and *KCNA1* mutations cause movement disorders such as episodic ataxia type 1 and epilepsy in humans (Paulhus et al. 2020). Recently, mTOR dependent K_v1.1 expression in a mouse model of PTEN deficiency has been reported (Nguyen and Anderson 2018): The PTEN deficient mice exhibit increased mTOR signaling and increased K_v1.1 protein levels, especially in the granular cell layer of the DG of the hippocampus. Another point of convergence between HuD and mTOR potentially is the glycogen synthase kinase 3 (GSK3) pathway (Tiruchinapalli 2008). Interestingly, HuD regulates translation via eIF4e (Fukao et al. 2009) and colocalizes with eIF4e in dendrites and dendritic spine-like protrusions (Tiruchinapalli et al. 2008), pointing out another common target of mTOR and HuD translational control in synaptic plasticity. Furthermore, mTOR possibly regulates FMRP (Narayanan et al. 2008) and plays a role in the neuronal overactivation of Fragile X Syndrome (Sharma et al. 2010). FMRP is a translational regulator of post- and presynaptic proteins, including ion channels like K_v3.1 and K_v4.2, regulating synaptic plasticity locally in the somatodendritic compartment of neurons (Ferron 2016). Mutations in the gene coding for FMRP, *fmr1*, leads to the fragile X syndrome, which often exhibits an epileptic phenotype (Hagerman and Stafstrom 2009). Interestingly, since mTOR is dysregulated in fragile X syndrome, it is a possible interactor of FMRP (Sharma et al. 2010). Another possible common link between FMRP and the mTOR pathway is K_v4.2: K_v4.2 is regulated by FMRP (Gross et al. 2011), and linked to the mTOR pathway through its interaction with ERK (Lugo et al. 2008) and regulation via Neuregulin-1 (Yao et al. 2013).

K_v4.2 channels are A-type voltage-gated potassium channels that are mainly involved in the propagation of action potentials from activated synapses back to the cell body in CA1 pyramidal neurons and associated to epileptogenesis in patients and multiple animal models (D'Adamo et al. 2013). Mutation of the *KCND2* gene, coding for K_v4.2, leads to intractable epilepsy and autism (Lin et al. 2018). Also, *fmr1* KD has been associated to increased K_v4.2 protein levels in the hippocampal CA1 layer (while K_v4.2 mRNA levels did not show any significant changes), suggesting that posttranslationally regulated K_v4.2 contributes to the phenotype of fragile X syndrome (Lee et al. 2011).

In summary, Pum2 is an RBP that functions as a translational repressor, and deficiency leads to an epileptic phenotype in mice, and possibly in humans. mTOR is a serine-threonine kinase involved in metabolic pathways that generally lead to increased protein synthesis and neuronal activity. Evidence suggests that different players of the mTOR pathway can contribute to the pathogenesis of epilepsy. There are several RBPs that are targets of the mTOR signaling pathway and multiple studies have led to the hypothesis that mTOR plays a role in specific RBP-deficiency disorders related to epilepsy. Resulting from these findings, new potential for understanding the epileptogenesis in Pum2 deficiency arises. The aim of this thesis is to explore the role of mTOR in the pathogenesis of the epileptic phenotype of Pum2 deficiency.

2. Statement of purpose

Epilepsy, affecting about 70 million people worldwide, is a disease that is still poorly understood and in many cases lacks therapeutic options (Shakirullah et al. 2014; Löscher et al. 2020). Despite extensive epilepsy research, most genetic causes underlying epilepsy are still unknown today (Scheffer et al. 2017).

In this thesis, I pursue an exciting new direction by using an experimental approach that complements the field's collective efforts to decipher the pathogenesis of genetic epilepsy: the role of the mTOR metabolic pathway in RBP deficiency, by using a Pum2 deficient mouse model. Specifically, I hypothesize that mTOR contributes to epileptogenesis in Pum2 deficient mice. I propose an interplay between the RBP Pum2 and the serine-threonine kinase mTOR in regulating voltage-gated ion channels as key players in epileptogenesis.

To verify and possibly substantiate this hypothesis, I first investigate the effect of Pum2 knock down (KD) by examining mTOR protein expression, its downstream activity, as well as its distribution in the hippocampus in the Pum2 KD model using protein- and immunohistochemistry brain samples of Pum2 deficient mice and hippocampal cell culture. Next, to explore the role of Pum2 KD on known players of epileptogenesis that are regulated directly or indirectly through the mTOR pathway (eIF4e, K_v1.1, and K_v4.2), I perform protein analysis and immunohistochemistry on brain samples of Pum2 deficient mice. Last, I initiate several approaches to test a possible interplay of Pum2 and mTOR protein: With regard to Pum2 function, I consider a possible mechanism of regulation of *mTOR* mRNA by Pum2. On the protein level, I analyze protein colocalization of mTOR and Pum2 and the effect of rapamycin treatment on the expression and colocalization of the two proteins.

By investigating the role of mTOR in the mouse model of Pum2 deficiency, I aim at gaining new insights into the role of mTOR in RBP mediated local translation. I hope to deliver new perspectives on synaptic plasticity, the function of hippocampal localized translational control, and to take another step towards understanding genetic epilepsy.

3. Materials and Methods

3.1. Animals

Pum2 gene-trap ($Pum2^{GT}$) mice (genetic background C57Bl6/J) homozygote for gene trap vector insertion (B6.129P2-$Pum2^{GT(XE772)Byg}$) in the Pum2 locus and wildtype (WT, C57Bl6/J) control animals were used for all mouse experiments. $Pum2^{GT}$ mice were kindly provided by Dr. Eugene Xu (Feinberg School of Medicine, Chicago, USA). Experiments were performed using mice at weaned age (3 weeks old) and adult age (16-20 weeks old). Mice were sacrificed by CO_2 inhalation. Mice that underwent a 4 week lasting behavioral testing battery (3.2.1) in addition to naïve mice at different ages were analyzed to explore how intense behavioral training affects the expression of mTOR.

For neuronal cell culture, pregnant Sprague Dawley rats were purchased from Charles River (Sulzfeld, Germany).

All animal experiments were approved by the German ethics committee and animals were treated according to German animal welfare law. Animals were housed in groups of 2-5 in individually ventilated cages and a 12 h/12 h light/dark cycle and had free access to water and food.

Numbers of individual mice used for experiments for protein quantification in brain lysates using Western blots and for protein quantification in immunohistochemical stainings are shown below.

Table 1: Sample number of mouse brains used for Western blot experiments

Test	weaned (3 weeks)		adult (20 weeks)		Behavioral testing		Figure
	WT	Pum2^{GT}	WT	Pum2^{GT}	WT	Pum2^{GT}	
mTOR	4	4	5	5	3	3	9A, 12A
pmTOR	3	3	3	3	3	3	9B, 12B
S6	3	3	4	4	3	3	9C, 12C
pS6	4	4	5	5	3	3	9D, 12D
eIF4e	4	4	5	5	-	-	13A
K_v1.1	4	4	7	5	-	-	15A
K_v4.2	4	4	5	5	-	-	15B

Table 2: Sample number of mouse brains used for immunohistochemical stainings of the hippocampus (technical replicates per brain: 1-4, 1 section per brain used for final analysis and quantification).

Test	WT (adult = 20 weeks)	Pum2^{GT} (adult = 20 weeks)	Figure
mTOR	3	3	10
eIF4e	3	3	13
K_v1.1	2	2	16B
K_v4.2	2	2	16B

3.2. Mouse experiments and tissue preparation

Mouse brain protein and mRNA expression were analyzed after division into 3 groups:

1. Weaned mice (3 weeks of age).
2. Adult mice (16 weeks of age).
3. Behavioral testing (mice undergoing behavioral tests as described below).

3.2.1. Mouse behavioral and memory training

Adult male mice (16 weeks old) were selected to perform a four week battery of behavioral training. Brain tissue from these mice was used in the “behavioral training” group. The detailed series of behavioral experiments that included open field, novel object recognition, and Barnes maze assays were performed by Bastian Popper and Antonia Demleitner as previously described (Popper et al. 2018).

3.2.2. Mouse dissection and perfusion

The preparation of mouse brain tissue was carried out both for immunohistochemical analysis and for biochemical analysis. The procedure was performed as described previously (Follwaczny et al. 2017). In brief, after sacrifice, mice were sorted into two groups: Immunohistochemical analysis (**Figure 4A**) and biochemical analysis (**Figure 4B**). The procedure for immunohistochemical analysis is described below. For biochemical analysis, brains were dissected shortly after sacrifice and immediately flash frozen in liquid nitrogen and stored at -80°C.

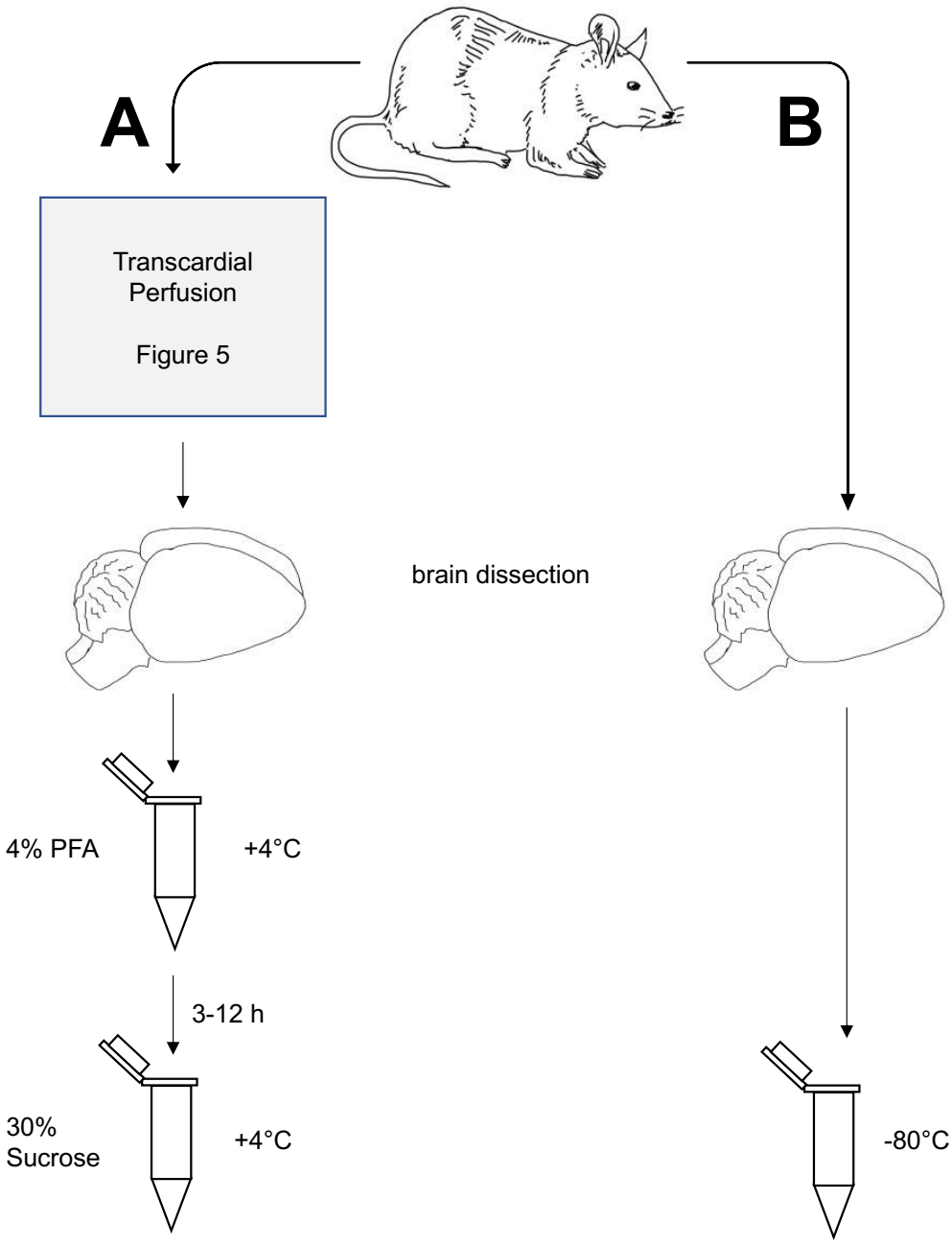

Figure 4: Flowchart of mouse brain dissection. A Mouse brain dissection protocol for immunohistochemical analysis. **B** Mouse brain dissection protocol for biochemical analysis (Graph based on Gage et al. 2012 and Follwaczny et al. 2017).

For immunohistochemical analyses, transcardial perfusion (**Figure 5**) was performed as previously described (Gage et al. 2012): Directly after sacrifice of the mouse, the thorax and abdomen were opened using a Y cut and the heart was accessed. A perfusion needle carrying phosphate buffered saline (PBS, 3.8.4) was placed transapically into the left ventricle, and the vena cava was cut immediately to enable escape of blood from the circulation. After transfusion with PBS at moderate speed for about 7 min until paleness of the liver could be observed, transfusion media was changed to 4% PFA (ROTI®-Histofix 4%, Roth, pH 7.0) for 12 min. Sufficiency of perfusion was tested by checking tail stiffness. PFA-perfused brains were post-fixed in 4% PFA in PBS for 3-12 h at 4°C and dehydrated in 30% sucrose (3.8.4) in ddH_2O at 4°C (for at least 1 week). The brain was dissected and transferred to 4% PFA in PBS.

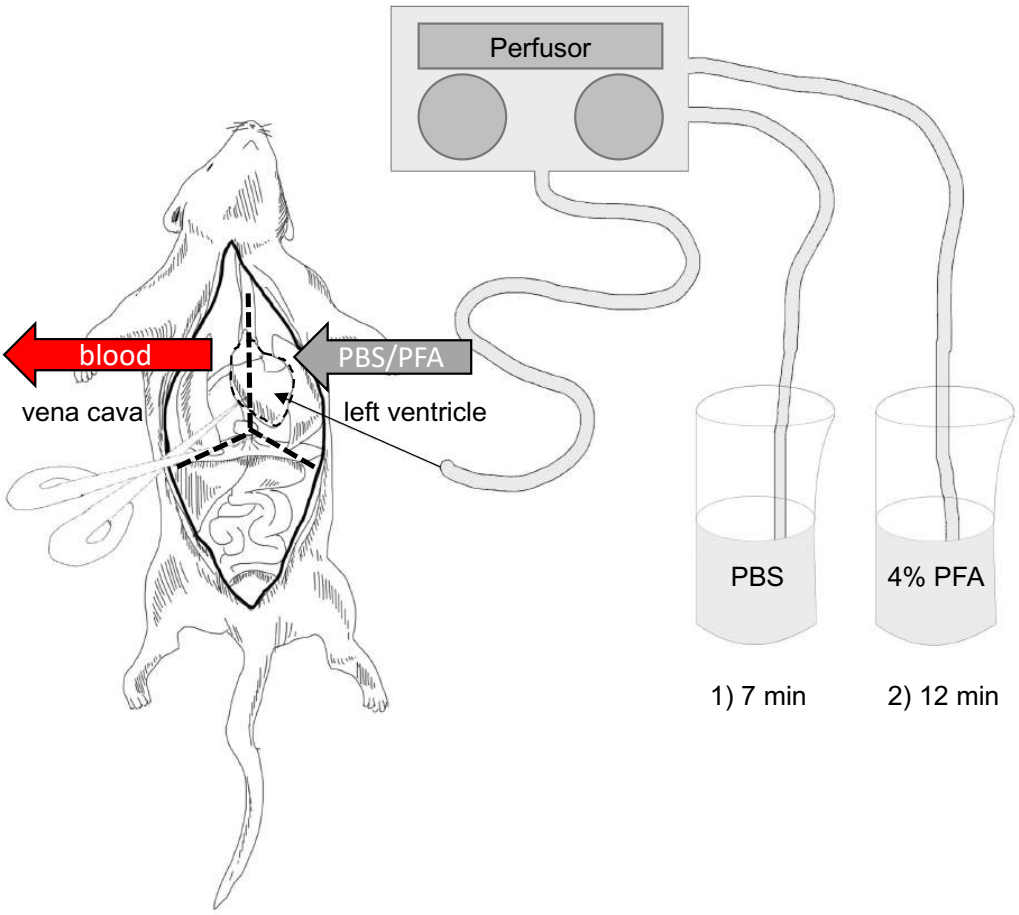

Figure 5: Transcardial perfusion protocol. Opening of the thorax by Y cut to access the heart is indicated by the dashed line. Transcardial perfusion is shown on the right (grey arrow), and cutting of the vena cava is indicated by the scissor, allowing escape of blood from the circulation (red arrow) (Graph based on Gage et al. 2012 and Follwaczny et al. 2017).

3.3. Cell culture

Hippocampal neurons were isolated from E17.5 rat embryos of Sprague Dawley rats as described before (Goetze et al. 2003). Preparation of primary hippocampal cell cultures was kindly performed by Christine Illig and Sabine Thomas. Hippocampal neuroblastoma of embryonic day 10 (HN10e) cell line was generously provided by Prof. Michael Meyer (BMC, LMU Munich).

3.3.1. Culture and transfection of primary hippocampal neurons of the rat

Primary hippocampal neurons were isolated and cultured in Dulbecco's modified Eagle's medium plus horse serum (DMEM+HS medium, see 3.8.1) on poly-L-lysine coated dishes (Goetze et al. 2003). For all experiments, hippocampal neurons at 15 days *in vitro* (DIV 15) were used.

Primary hippocampal neurons were transfected using calcium phosphate precipitation as previously described (Goetze and Kiebler 2006). In brief, 3 µg plasmid DNA, 6 µL 2.5 M calcium chloride and water were mixed in a tube, then 60 µL 2x BES buffered saline (BBS, see Goetze and Kiebler 2006) was added dropwise before mixing gently. Cells were incubated with DNA-calcium precipitates for 1 h at 37°C in Hepes buffered transfection medium, subsequently washed in warm HBSS washing buffer and further cultured in Minimum essential medium plus vitamin B27 supplement (NMEM+B27 medium, see Goetze and Kiebler 2006).

3.3.2. Culture, transfection, differentiation and rapamycin treatment of cell lines

HN10e cells were cultured in DMEM (Invitrogen/GIBCO, Germany) supplemented with 10% FSC at 37°C and 5% CO_2 (Brewer et al. 1993). HN10e cells were passaged maximally 15 times every 2-4 days. HeLa cells were cultured in DMEM with 10% FCS and 2 mM glutamine (Invitrogen/Life Technologies, Germany) as previously described (Macchi et al. 2004).

HN10e and HeLa cells were transfected with Lipofectamine2000 (Invitrogen, Germany) according to the manufacturers' manual.

For differentiation of HN10e cells, different concentrations of retinoic acid (RA) (20, 50 and 100 µM RA) were used as previously described (Weiss et al. 2009; Lee et al. 1990). Every 48 h, medium was exchanged and cells were treated with new RA. HN10e cell treatment with rapamycin (Sigma, Germany) was performed as previously described (Pan et al. 2009). Cells were incubated with 50, 100, and 200 nM rapamycin diluted in dimethyl sulfoxide (DMSO) for 1.5 to 3 h. The short treatment was chosen to minimize indirect effects of rapamycin. Subsequently, cells were lysed and further processed for protein analysis (3.4.3) or washed and fixed for immunocytochemistry (3.4.2).

3.4. Protein expression analysis

3.4.1. Immunohistochemistry, imaging and image analysis of hippocampal brain sections of the mouse

Immunohistochemical stainings were performed as previously described (Follwaczny et al. 2017). In brief, brains were cut in 30 µm sections using a Leica CM3050 S Research Cryostat (Wetzlar, Germany). Free floating sections were blocked in blocking solution for 1 h at room temperature (RT). Then, sections were incubated with primary antibodies overnight at 4°C (see 3.8.8). Sections were washed in PBS 3 times for 10 min at RT and incubated with secondary antibodies (see 3.8.8) diluted in blocking solution for 2 h at RT. Nuclei were counterstained with DAPI, then washed 3 times for 10 min in PBS. Sections were mounted on Superfrost Slides (ThermoScientific, Germany) with Fluoromount (Sigma Aldrich, Germany). The protocol is depicted in **Figure 6**.

Hippocampal sections were imaged using an inverted confocal Leica SP8 microscope with lasers for 405 nm, 488 nm, 552 nm and 638 nm excitation. Pictures were taken using 40x1.4 multi-immersion (IMM) and 68x1.4 IMM objectives; the image pixel size was 80 nm. Images were acquired in four channels with the following filter settings, whereas the individual channels were recorded subsequently:

DAPI: 430 – 470 nm (conventional photomultiplier tube)
AF488: 500 – 550 nm (hybrid photo detector, HyD)
fAF555: 560 – 600 nm (HyD)
AF647: 650 – 700 nm (HyD)

For overview images of the hippocampus, the tile scan function of the Leica imaging software was used. Individual tiles were merged using statistical auto-stitching in slow speed and high definition as previously described (Follwaczny et al. 2017).
For fluorescence intensity analysis of confocal images, Fiji 1.50g (PMID 26153368) was used as previously described (Schindelin et al. 2015; Follwaczny et al. 2017). The fluorescence intensity of the antibody of interest was measured in the following steps:

1. The region of interest (ROI) was selected according to the anatomical borders of the hippocampus.
2. By using a macro (designed by Philipp Follwaczny, see Follwaczny et al. 2017), masks were created to define the dendritic layer outside of the pyramidal layer. An inverted mask allowed to select and measure the intensity in the pyramidal layer.
3. Using the masks, selections could be created in the original channels, thereby enabling to measure the “Mean Gray Value” and of the staining of interest.

The mean of the staining intensity in individual hippocampal areas (*e.g.*, dendritic layer or pyramidal layer) was normalized to the mean intensity of the entire hippocampus.

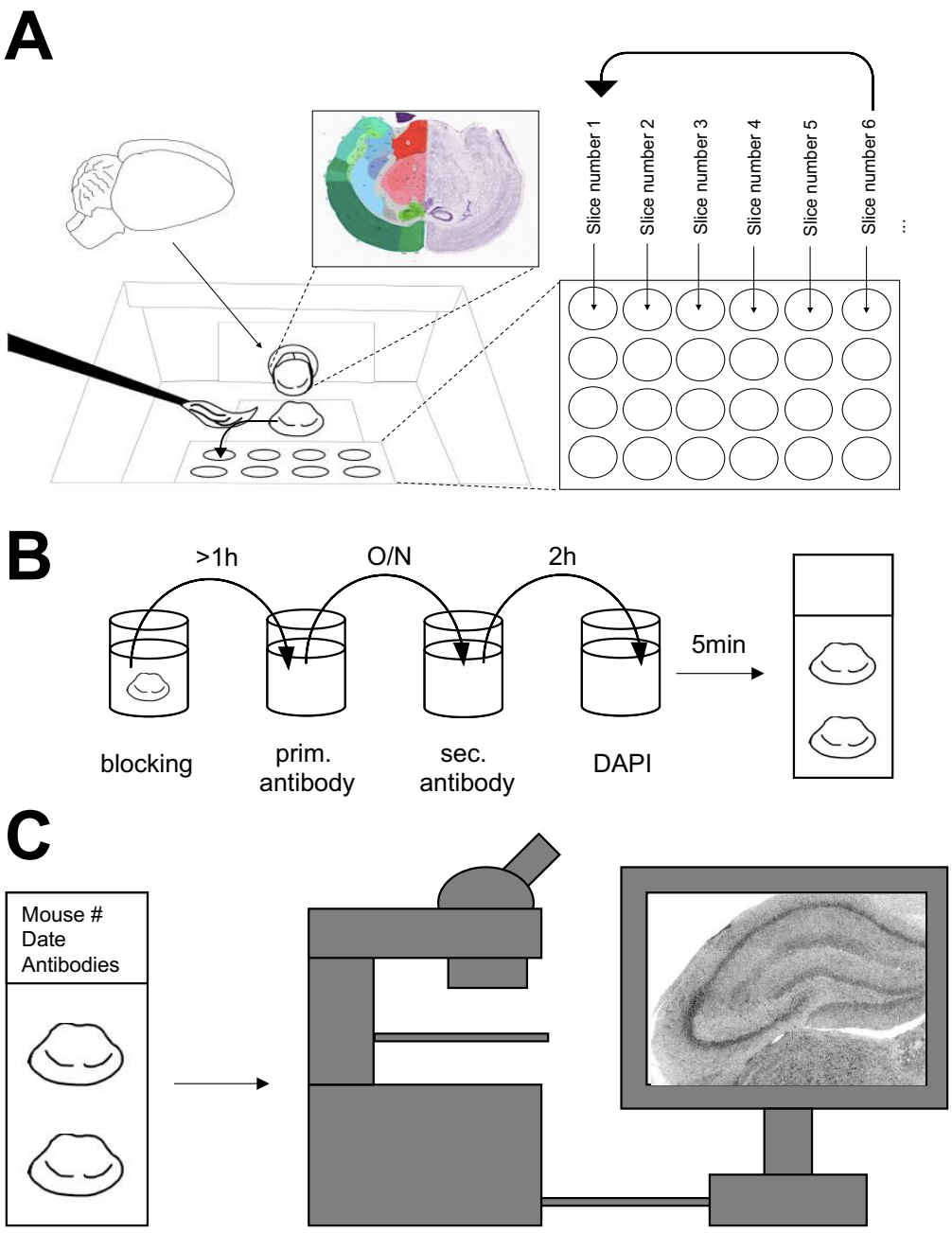

Figure 6: Protocol for immunohistochemical analysis of mouse brain sections. A. Preparation of free floating cryotome sections. **B** Staining procedure of free floating sections. O/N = overnight. **C** Mounting of mouse brain sections on slides, immunohistochemical staining and confocal microscopy.

3.4.2. Immunostaining, imaging and image analysis of cultured cells

Primary hippocampal neurons and HN10e cells were immunostained as described previously (Vessey et al. 2006): Cells were washed in warm Hank's balanced salt solution (HBSS, Thermo Fisher Scientific, Germany) and fixed in warm 4% PFA (16% PFA diluted in HBSS, see 3.8.5). Cells were permeabilized with 0.1% Triton X-100 (Roth, Germany) in HBSS (Thermo Fisher Scientific, Germany), blocked in blocking solution (for immunocytochemistry, see see 3.8.5) and incubated with primary antibodies. Primary antibodies were detected using anti-rabbit or anti-mouse secondary antibodies (see 3.8.8 for primary and secondary antibodies). Coverslips were mounted in fluoromount (Sigma Aldrich, Germany).

For imaging of immunostained primary hippocampal and HN10e cells, a Zeiss Cell Observer Microscope (Plan Apochromat 63x oil Objective; LED-Colibri light source; ZEISS, Germany) was used. Image acquisition was performed in Z-stacks of 50 stacks of 0.26 µm (as recommended by the Zen software) (Sharangdhar et al. 2017). Images were analyzed using the ZEN® (ZEISS, Germany) and Fiji 1.50 g (PMID 26153368) software, respectively. For colocalization analysis, images were deconvolved using default parameters of the ZEN software as described before (Sharangdhar et al. 2017). For quantification of colocalizing puncta per dendrite upon rapamycin treatment (4.3.3), HN10e cells were differentiated for 5 days using 20 µM RA before treatment of cells with 100 nM rapamycin for 1.5 h. Cells were fixed and immunostained against Pum2 and mTOR, respectively (**Figure 24**). Images were deconvoluted, and colocalizing puncta were manually counted in dendrites blind to the condition (Sharangdhar et al. 2017). The number of colocalizing events per µm neurite was quantified.

3.4.3. Western blotting

For protein detection and quantification in mouse brain and cell lysates, Western blotting was performed as described previously (Follwaczny et al. 2017). Brains were lysed in RIPA buffer (3.8.2) supplemented with protease inhibitor cocktail (complete ULTRA tablets, mini, Roche, Germany) and phosphatase inhibitor cocktail (PhosSTOP tablet, Roche, Germany). For homogenizing, a FastPrep-24™ 5G homogenizer was used according to manufacturer's manual (mouse brain program: 6.0 m/s for 40 s, adapter: Quick prep, quantity: 50 mg), then lysates were mixed with 3 mL of SDS lysis buffer (3.8.2) and incubated for 2 h at RT. Cultured cells were first washed with warm

HBSS (Thermo Fisher Scientific, Germany), then put on ice for 5 min. After washing again with cold HBSS, cells were lysed using RIPA buffer and scraped. Both cell and brain lysates were sonicated (three pulses) and spun at 25,000x *g* for 10 min. After adding SDS loading buffer (3.8.2), the supernatant was boiled at 95°C for 5 min. Samples were spun at 25.000x *g* for 10 min before loading. For protein seperation, equal amounts of protein were loaded on SDS polyacrylamide electrophoresis (SDS PAGE), using 8% gels for proteins with a molecular weight larger than 150 kDa, 10% gels for proteins with the molecular weight from 40 to 150 kDa, and 12% gels for proteins smaller than 40 kDa (3.8.2). Proteins were blotted on a nitrocellulose membrane (pore size 0.2 µm) at 100 V for 1 to 1.5 h. Membranes were then blocked in blocking solution for 30 min and incubated with primary antibodies diluted in blocking solution overnight at 4°C (for dilutions see 3.8.8). Membranes were washed with PBS (3.8.4) supplemented with 0.1 % Tween (Sigma, Germany) (PBST) 3 times and incubated with infrared dye labeled secondary antibodies (3.8.8) for 2 h at RT. Membranes were scanned using the Odyssey® CLx Imaging System (*LI-COR*, Germany).

For quantification of optical density of protein Image Studio™ Software (*LI-COR*, Germany) was used. Vinculin, Actin and β-Tubulin III were used as loading control.

3.5. RNA expression analysis

RNA isolation was performed using TRIzol (Sigma, Germany) according to the manufacturer's manual. In brief, brains were homogenized in 1 mL TRIzol using the FastPrep-24™ 5G device (MP Biomedicals, Germany) at 4.0 m/s for 40 s (lysing matrix D, quantity: 100, cycles: 1). Lysate was mixed with 9 mL TRIzol and incubated at RT for 5 min. To digest genomic DNA, the Mini RNeasy Kit (QIAGEN, Germany) was used. Isolated RNA was reverse transcribed using SSIII superscript (Invitrogen, Germany) according to the manufacturer's manual.

3.5.1. quantitative Real-Time PCR (qRT-PCR) and analysis

cDNA Synthesis and qRT-PCR was performed as previously described (Follwaczny et al. 2017). In brief, cDNA was synthesized using Superscript III™ reverse transcriptase (Invitrogen) and random primers according to the manufacturer's instructions. The SYBER Green Master Mix was used for qPCR. For analysis, the LightCycler®96 software (Roche, Germany) was used. All primer pairs were tested using dilution series to have an efficiency of 2.0±0.10.

For mTOR qPCR, the following primers were used:

Fwd: GTG TCC CTT CCT CGA GCT G;

Rev: TTT TTG CGG CCG CTG CTT TTA AAA TTC.

As control, the following 18S primers were used:

Fwd: GAA ACT GCG AAT GGC TCA TTA AA;

Rev: CCA CAG TTA TCC AAG TAG GAG AGG A.

3.6. Luciferase Assay

Luciferase Assay was performed under instruction by Janina Ehses and Sandra Fernandez-Moya as previously described (Sharangdhar et al. 2017). To check whether Pum2 overexpression affects mTOR expression via its 3'-UTR, the mTOR 3'-UTR was amplified from cDNA isolated from mouse brain lysate and cloned downstream of the Renilla luciferase gene into the psiCheck-2 vector (Promega, Germany).

For cloning the 3'-UTR of *mTOR* mRNA, isolated cDNA from a 5 months old WT mouse brain was used. Taq Polymerase (New England Biolabs/ThermoFisher Scientific, 56°C Tm, forward 61°C/reverse 61°C) were used for cloning. The following primers were used for amplification of full length mTOR 3'UTR:

Fwd: GTG TCC CTT CCT CGA GCT G;
Rev: TTT TTG CGG CCG CTG CTT TTA AAA TTC.

PCR was run using the following protocol:

1. 95°C for 5 min
2. 3x
   - 95°C for 10 min
   - 56°C for 30 min
   - 72°C for 60 min
3. 72°C for 10 min
4. 4°C forever

The amplicons were gel purified using a 1.5% agarose gel (expected size 842 bp for mTOR 3'-UTR, TBE see 3.8.7) and the QIAquick® Gel Extraction-kit (Qiagen), following the manufacturer's instructions.
A psiCheck-2 (Promega, Germany) dual luciferase plasmid expressing Renilla and Firefly was chosen. For sequence analysis and plasmid mapping, A Plasmid Editor (ApE, version 2.0.47 by Wayne Davis) was used (**Figure 7**). The plasmid and the purified mTOR 3'-UTR DNA (insert) were cut using the restriction enzymes Xho1 and Not1 (New England Biolabs). Ligation of plasmid and insert DNA was performed using T4 DNA Ligase (New England Biolabs) and a 2:1 ratio of insert to plasmid following the manufacturer's instructions. Ligations were performed at 16°C overnight.

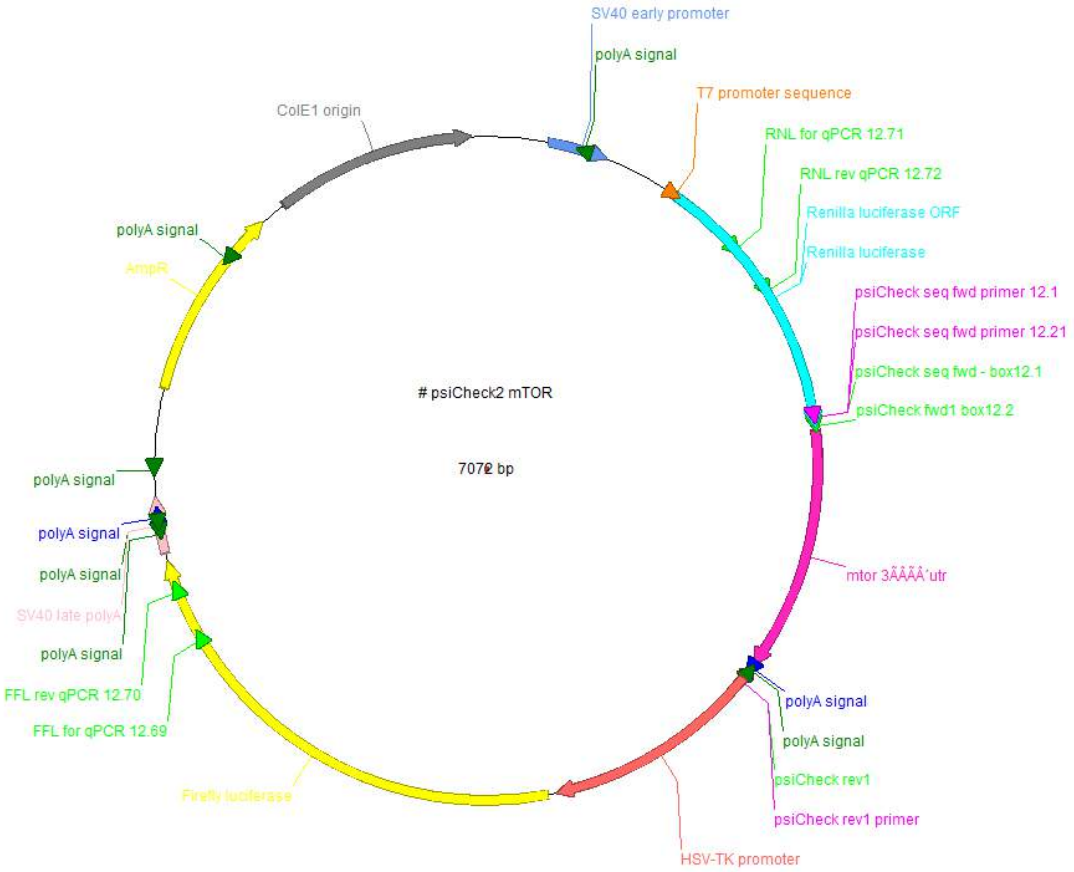

Figure 7: psiCheck-2 plasmid map for Luciferase assays. (Plasmid map generated using ApE – A plasmid Editor by M. Wayne Davis, USA, Utah).

The ligated plasmid was transformed in chemically competent TOP10 *E.coli* cells using a heat shock at 42°C for 50 s. Cells were plated on an agar plate containing ampicillin and stored at 37°C overnight. Plasmids were isolated from the bacterial cultures using GenElute^{TM} Plasmid Mini-Prep kit (SIGMA-Aldrich). For test digestion, the isolated DNA was cut using Xbal (New England BioLabs). The ligation product showed no point mutation and was therefore used for all following experiments.

HeLa cells were used for luciferase assay experiments as described before (Sharangdhar et al. 2017). Cells were transfected using Lipofectamine 2000 (Invitrogen, Germany) according to manufacturers' manual in a 24-well plate. 3 technical replicates were transfected for each condition: TagRFP Pum2, TagRFP control, empty vector, and mTOR 3'-UTR vector. Plasmids used for shRNA constructs against Pum2 and control have described earlier (Vessey et al. 2006). Transfection

efficiency was checked 24 h post transfection and the luciferase assay was performed 3 days after transfection.

Expression of Renilla and Firefly luciferase was detected using a homemade detection solution (3.8.7). Solutions were prepared with 10 µL lysate per well and the Dual-Glow Luciferase Assay System (Promega, Germany) was used as instructed by the manufacturer. Photon emission was measured using a Centro XS^3LB960 Luminometer (Berthold Technologies, Germany). Raw data was saved and normalized to controls (YFP-NTC and empty luciferase reporter). The ratio of Renilla and Firefly luciferase photon emission was calculated and normalized to yellow fluorescent protein (YFP) non-treated control (NTC), and empty luciferase reporter. The procedure is depicted in **Figure 8**.

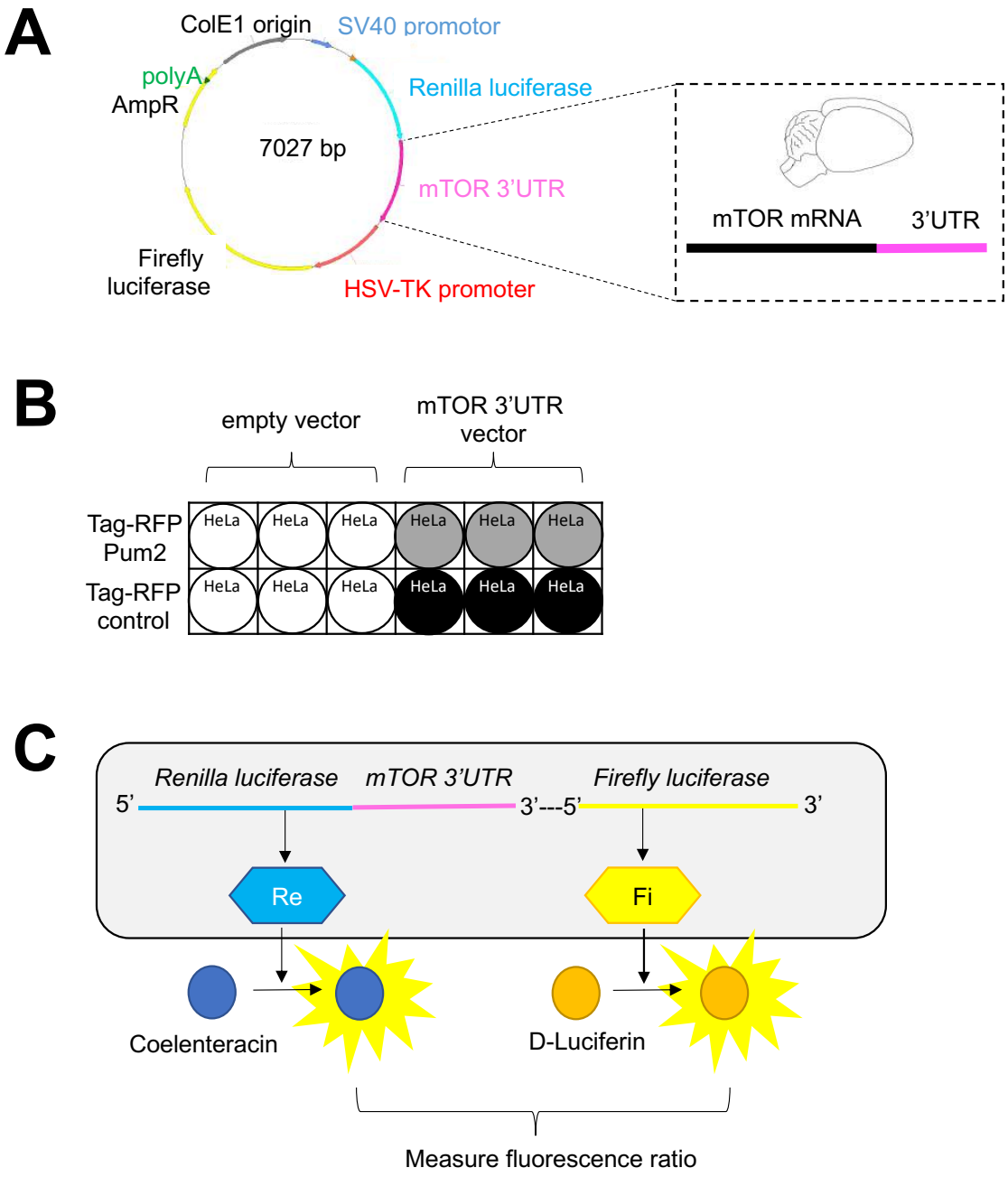

Figure 8: Overview for luciferase assay. Luciferase assay of mTOR 3'-UTR in HeLa cells overexpressing Pum2 vs tag-RFP control. **A** Plasmid map of Luciferase plasmid of the mTOR 3'-UTR in a psiCheck-2 (ColE1) dual luciferase plasmid expressing Renilla and Firefly luciferase. **B** Transfection scheme for HeLa cells. **C** Scheme for luciferase assay. Renilla and Firefly proteins were detected by adding specific luciferins. For each condition, ratios of Renilla and Firefly luciferin fluorescence were measured to determine enzyme activity, correlating to translation under the given conditions.

3.7. Statistical Analysis

All statistical analysis was performed using Prism Graph-Software (Version 5; GraphPad, San Diego, CA, USA). All graphs depict mean +SEM. P-values were determined using unpaired t-test for normally distributed sample groups and Mann-Whitney U-test not normally distributed sample groups. Outliers were detected by Grubb's test. Significant outcome was determined by $p<0.05$ (*), $p<0.01$ (**), or $p<0.001$ (***).

3.8. Buffers, solutions and media

3.8.1. Cell Culture Media

Media for culture and transfection of cells were kindly provided by Christine Illig and Sabine Thomas.

Table 3: DMEM+HS Medium

Name	Amount	Manufacturer
DMEM	1 L	Invitrogen
HS	10% (v/v)	Invitrogen
Sodium pyruvate	1 mM	Sigma
L-Glutamine	100 mM	Sigma

Table 4. Trypsin-EDTA

Name	Amount	Manufacturer
10x Trypsin-EDTA-solution	100 mL	Biochrom
2-(4-(2-Hydroxyethyl)-piperazinyl-ethanosulfonic acid (Hepes) 1M	10 mL	Sigma
Penicillin/Streptomycin (if necessary)	10 mL	Biochrom
In ddH_2O, store at -20°C	Up to 1 L	EMD Millipore

3.8.2. Buffers and gels for SDS PAGE

Table 5: RIPA Buffer

Name	Amount	Manufacturer
NaCl	150 mM	Merck
NP-40 Surfactant	10% (v/v)	Thermo Fisher Scientific
Sodium deoxycholate	0.5% (w/v)	Sigma
alpha-Dodecylsulfate (SDS)	0.1% (w/v)	Roth
Tris-HCl pH 8.0	50 mM	Roth
Protease Inhibitor Cocktail	1 Tablet	Roche
In ddH_2O	Up to 10 mL	EMD Millipore

Table 6. SDS lysis buffer (8 mL)

Name	Amount	Manufacturer
Tris pH 7.4	50 mM	Roth
NaCl	500 mM	Merck
SDS	0.4% (v/v)	Roth
EDTA	5 mM	Biochrom
1,4–Dithiothreitol (DTT)	1 mM	Applichem
Protease Inhibitor Cocktail	0.04% (v/v)	Roche
In ddH_2O	Up to 8 mL	EMD Millipore

Table 7. SDS loading and running buffer

3x SDS loading buffer		
Name	Amount	Manufacturer
Tris/HCl pH 6.8	65 mM	Roth
Glycerol	10% (v/v)	Roth
SDS	2.3% (w/v)	Roth
Mercaptoethanol	5 % (v/v)	Sigma
10x SDS running buffer		
Name	Amount	Manufacturer
Tris pH 7.4	0.25 M	Roth
Glycerol	1.92 M	Roth
SDS	1% (w/v)	Roth

Table 8. Acrylamide gels – separation gel (for 2 gels)

Name		Amount	Manufacturer
Lower Stock		2.5 mL	
	Tris	1.5 M	Roth
	SDS	0.4% (w/v)	Roth
Acrylamide 30:0.8		8/10/12%	Roth
Ammonium persulfate (APS)		100 µL	Roth
N,N,N',N-Tetramethylethylenediamine (TEMED)		10 µL	Roth
In ddH_2O		Up to 5 mL	EMD Millipore

Table 9. Acrylamide gels – collection gel (for 2 gels)

Name		Amount	Manufacturer
Upper Stock		2.5 mL	
	Tris	0.5 M	Roth
	SDS	0.4% (w/v)	Roth
Acrylamide 30:0.8		1.3 mL	Roth
ddH_2O		6.2 mL	EMD Millipore
Ammonium persulfate (APS)		100 µL	Roth
TEMED		10 µL	Roth

3.8.3. Buffers for Western Blots

Table 10. 1x Blotting Buffer

Name		Amount	Manufacturer
10x Blotting Buffer		10% (v/v)	
	Tris	25 mM	Roth
	Glycine	190 mM	Roth
	SDS	0.02% (w/v)	Roth
Methanol		20% (v/v)	Roth
In ddH_2O		Up to 1 L	EMD Millipore

Table 11. Western Blot Blocking Solution

Name		Amount	Manufacturer
Bovine serum albumin (BSA)		2% (w/v)	Roth
Tween 20		0.1% (v/v)	Sigma
In tris buffered saline (TBS) pH 7.6			
	Tris	15 mM	Roth
	NaCl	150 mM	Merck
	In ddH_2O	Up to 1 L	EMD Millipore

3.8.4. Solutions for Immunohistochemistry

Table 12. Phosphate buffered saline (PBS), also for Western blot

Name	Amount	Manufacturer
NaCl	137 mM	Merck
KCl	2.7 mM	Sigma
Na_2HPO_4	8.1 mM	Roth
KH_2PO_4	1.5 mM	Roth
In ddH_2O, pH 7,4	Up to 1 L	EMD Millipore

Table 13: 30% Sucrose Solution (for storage of mouse brains)

Name	Amount	Manufacturer
Succrose	30% (v/v)	Roth
In ddH_2O	1 L	EMD Millipore

Table 14. IHC Glycerol Solution (for slice storage longer than 2 weeks)

Name		Amount	Manufacturer
Phosphate buffer, pH 7.3		10% (v/v)	
	Sodium hydroxide (NaOH)	0.9 mM	Merck
	NaH_2PO_4	1.2 mM	Roth
	ddH_2O	Up to 400 mL, pH 7.2 – 7.4	EMD Millipore
Glycerol		30% (v/v)	Roth
Ethyleneglycol		30% (v/v)	Fluka
In ddH_2O, pH 7.4		150 ml (up to 500 ml)	EMD Millipore

Table 15. IHC Blocking Solution

Name	Amount	Manufacturer
Triton X100	0.5% (v/v)	Roth
BSA fraction V pH7	1% (w/v)	PAA
In PBS	Up to 40 mL	Sigma

3.8.5. Solutions for Immunocytochemistry

Table 16. 16% PFA (cell fixation)

Name	Amount	Manufacturer
PFA	16 % (w/v)	Sigma
ddH_2O (stir while heating up to 60°C)	Up to 70 ml	EMD Millipore
NaOH (cool down, then heat up again to 60°C)	1 - 2 pellets	Sigma
10x PBS	10 % (v/v)	Sigma
In ddH_2O, pH7.4 (store at -20°C)	Up to 100 mL	EMD Millipore

Table 17: Blocking solution for immunocytochemistry

Name	Amount	Manufacturer
FCS	2% (w/v)	ThermoFisher Scientific
BSA	2% (w/v)	Roth
Fish Gelatine in H_2O	0.2% (w/v)	Sigma
10x PBS	10% (v/v)	Sigma
In ddH_2O (store at -20°C)	Up to 100 mL	EMD Millipore

3.8.6. Solutions for RNA analysis

Table 18: cDNA Synthesis Mix (for 1 µl RNA per mix; RNA concentration example: 0.9 µg/µL, for 13 µL volume)

Name	Amount	Amount	Manufacturer
	(+) Reverse transcriptase mix	**(-) Reverse transcriptase mix**	-
RNA (0.9 µg/µL)	1.1 µL	1.1 µL	selfmade
ddH_2O	9.4 µL	9.4 µL	Sigma
Ribolock (40 U/µL)	0.5 µL (on ice)	0.5 µL (on ice)	Thermo Scientific
Random Primer N6 (60 mM)	1 µL	1 µL	Biolabs
dNTPs (10 mM)	1 µL	1 µL	Biolabs
keep 5 min. at 65°C, then 5 at min. 4°C			
First Strand buffer 5x	4 µL	4 µL	Invitrogen
DTT (0.1 mM)	1 µL	1 µL	Invitrogen
ddH_2O	1 µL	2 µL	Sigma
SuperScript III™ reverse transcriptase (200 U/µL)	1 µL	-	Invitrogen

Table 19. CYBER Green Master Mix

Name	Amount	Manufacturer
1x Standard Taq Buffer	200 µL	New England Biolabs
BSA	20 µg/mL	New England Biolabs
Betaine	1 M	Sigma
Desoxynucleoside triphosphates (dNTPs)	16 µM	New England Biolabs
Hot-Start Taq DNA polymerase	0.6 U per reaction	New England Biolabs
SYBR Green 1:100	1 µL/mL	Lumiprobe
In ddH_2O	Up to 1 mL	EMD Millipore

3.8.7. Buffers for Luciferase Assay

Table 20. Tris-Borate-EDTA Buffer (TBE, 10x), pH 8.0, for agarose gels

Name	Amount	Manufacturer
Tris base	890 mM	Roth
Boric acid	890 mM	Sigma
EDTA	20 mM	Sigma

Table 21. Master Mix

Name	Amount	Manufacturer
cDNA (WT mouse brain 190-15) (1µg/µL)	1 µL	selfmade
dNTPs (1µg/µL)	1 µL	New England Biolabs
Forward primer (1:10) = 10 µM	2 µL	Eurofins
Reverse primer (1:10) = 10 µM	2 µL	Eurofins
Taq buffer or 4 µL Phusion buffer	2 µL	New England Biolabs
Enzyme (Taq Polymerase/Phusion), added last	0.5 µL	New England Biolabs/ThermoFisher Scientific
In ddH_2O	Up to 20 µL	EMD Millipore

Table 22. LB media

Name	Amount	Manufacturer
Peptone	10 g	Sigma-Aldrich
Yeast Extract	5 g	Thermo Fisher Scientific
NaCl	10 g	Roth
In ddH_2O	Up to 1 L	EMD Millipore

Table 23. SOC-media (in LB media)

Name	Amount	Manufacturer
KCl	2.5 mM	Roth
$MgCl_2$	10 mM	Roth
Glucose	20 mM	Merck
In LB-media	Up to 1 L	

Table 24: Homemade Luciferase Assay Detection Solution (for 10 µL lysate/well, 36 samples, 50µL injection volume)

Name		Amount	Manufacturer
Firefly			
5x Firefly Buffer		560 µL	
	Tricine	20 mM	Sigma
	$MgSO_4$ x $7H_2O$	2.67 mM	Roth
	EDTA	0.1 mM	Sigma
DTT (1 M)		93 µL	Sigma
ATP (100 mM)		15 µL	PJK Biotech
Coenzyme A (100 mM)		8 µL	PJK Biotech
D-Luciferin in methanol (10 mM)		132 µL	PJK Biotech
In ddH_2O		Up tp 2800 µL	EMD Millipore
Stop and Renilla			
2x Renilla Buffer		1400 µL	
	Na_2EDTA	2.2 mM	Sigma
	KH_2PO_4	220 mM	Merck
	NaCl	1.1 M	Sigma
	NaN_3	1.3 mM	Sigma
BSA (10 mg/mL)		123 µL	Sigma
Coelenterazin (1 mM)		37 µL	PJK Biotech
ddH_2O		Up to 2800 µL	EMD Millipore

3.8.8. Antibodies

Primary and secondary antibodies, respectively, are depicted in the following tables. For counterstaining of nuclei, 4′,6-diamidino-2-phenylindole (DAPI, ThermoFisher Scientific), diluted to a final concentration of 300 nM, was used.

Table 25. Primary antibodies

Antibody	Species	Dilution WB	Dilution IHC	Dilution IF	Company	Reference
Anti-NeuN	chicken polyclonal	--	2:500	--	Millipore (#ABN91)	(Follwaczny et al. 2017)
Anti-mTOR (Ser2481)	rabbit	1:1000	1:200	1:500	Cell Signaling	(Wahl et al. 2018), (Rodriguez et al. 2018)
Anti-phospho-mTOR (Ser2448)	rabbit polyclonal	1:1000	1:200	1:500	Cell Signaling	(Yang et al. 2018)
Anti S6 ribosomal protein	mouse monoclonal	1:2000	1:400	--	Cell Signaling	(Urbanska et al. 2018)
Anti-phospho-S6	rabbit polyclonal	1:1000	1:400	1:100	Cell Signaling	(Urbanska et al. 2018)
Anti-Pum2	goat polyclonal	--	1:200	1:500	Abcam	--
Anti-Pum2	rabbit polycolial	1:1000	1:200	1:500	Abcam	(Follwaczny et al. 2017)
Anti-Kv4.2	rabbit polyclonal	1:1000	1:200	1:500	Alomone Labs	(Wolff et al. 2016), (Hall et al. 2015)
Anti-Kv1.1	rabbit polyclonal	1:1000	1:100	1:200	Alomone Labs	(Bagchi et al. 2014), (Jang et al. 2015)
Anti-eIF4E	rabbit polyclonal	1:1000	1:200	1:100	Abcam	(Stoll et al. 2013)
Anti-Homer1	Mouse monoclonal	--	--	1:100	Synaptic Systems	(Tao-Cheng et al. 2014)
Anti-Vinculin	goat polyclonal	1:200	--	--	Santa Cruz Biotechnology, Inc.	(Xiong et al. 2019)
Anti-Tubulin beta	mouse monoclonal	1:1000	--	--	Sigma-Aldrich	(Zhang et al. 2016)

Table 26. Secondary antibodies

Secondary Antibody	Storage	Company	Dil. IF/IHC	Dil. WB	Dye
Donkey Anti-Rabbit IgG	-20°C	Life technologies	1/1000	--	Alexa Fluor 488
Donkey Anti-Mouse IgG	4°C	LI-COR	--	1/10 000	IRDye 680RD
Donkey Anti-Rabbit	-20°C	Dianova	1/500	--	Cy5
Calf Anti-Goat	-20°C	Life Technologies	1/1000	--	Alexa Fluor 488
Calf Anti-Goat	-20°C	Dianova	1/1000	--	Cy3
Donkey anti mouse	-20°C	Life Technologies	1/1000	--	Alexa 555
Donkey anti mouse	-20°C	Molecular Probes (LifeTechnologies)	1/500	--	Alexa 647
Donkey Anti-Goat IgG	4°C	LI-COR	--	1/10 000	IRDye 680RD
Donkey Anti-Rabbit	4°C	LI-COR	--	1/10 000	IRDye 800CW
Donkey Anti-Rabbit	-20°C	Life Technologies	1/500	--	Alexa 647
Donkey Anti-Rabbit	-20°C	Molecular Probes (LifeTechnologies)	1/1000	--	Alexa 555
Goat Anti-Chicken IgY	-20°C	Life Technologies	1/500	--	Alexa 647

4. Results

4.1. Pum2 effects on mTOR protein and activity

Adult Pumilio2 gene trap ($Pum2^{GT}$) mice exhibit a strong epileptic phenotype. Seizures occur spontaneously, as witnessed in daily procedures such as feeding of the mice. There have been several studies that already reported the epileptic phenotype of the $Pum2^{GT}$ mouse line (Siemen et al. 2011; Follwaczny et al. 2017). Furthermore, a Pum2 deficiency has been reported in patients with idiopathic epilepsy (Wu et al. 2015). At the same time, several studies have linked the kinase mechanistic target of rapamycin (mTOR) with epilepsy (Meng et al. 2013). To investigate a possible role of mTOR in the $Pum2^{GT}$ phenotype, I analyzed the mRNA and protein expression of mTOR, as well as the phosphorylation levels of either mTOR or its downstream target ribosomal protein S6 in $Pum2^{GT}$ brains.

4.1.1. $Pum2^{GT}$ mice exhibit changes in mTOR protein expression

Since an epileptic phenotype has been detected in adult $Pum2^{GT}$ mice, I tested for changes in mTOR protein levels in $Pum2^{GT}$ mice compared to wild type (WT) controls. To test for an effect of the age of mice, I also analyzed mTOR protein levels in weaned $Pum2^{GT}$ mice, that do not yet show seizures, compared to age-matched WT mice. I analyzed lysates of whole brains of adult mice for protein analysis using Western blot (**Figure 9A**). There was a significant drop of mTOR protein expression in brains of weaned $Pum2^{GT}$ mice (0.90 ± 0.02, normalized to WT = 1.00 ± 0.02). Adult mice, however, showed large variation among individuals, and despite an apparent upward trend did not show a significant difference between $Pum2^{GT}$ and WT (0.44 ± 0.02 in Pum2 vs. 1.00 ± 0.40 in WT). In contrast, qRT-PCR experiments did not show any significant change of *mTOR* mRNA expression at either age of the mice (not shown). Thus, I focused on the protein levels and investigated the downstream phosphorylation activity of mTOR in order to analyze a possible change in kinase activity in $Pum2^{GT}$ vs. WT mice. I aimed at measuring the phosphorylation levels of mTOR protein at the chosen time points during mouse development (**Figure 9B**).

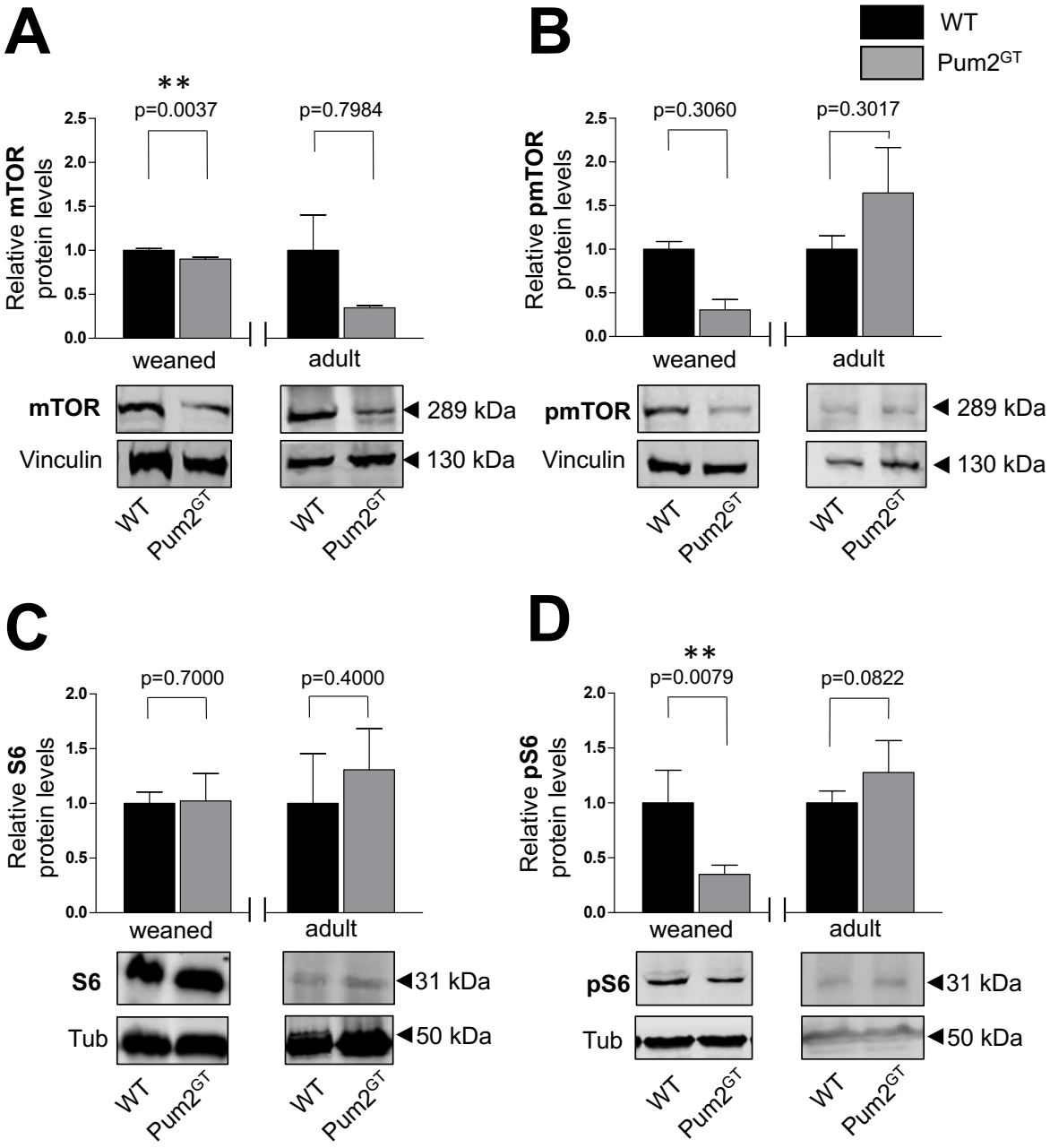

Figure 9: Weaned Pum2^{GT} mice show decreased mTOR protein and phosphorylation levels of S6. Western blot and quantification of **A** mTOR protein and **B** phospho-mTOR (pmTOR) protein normalized to vinculin, **C** phospho-S6 ribosomal protein (pS6) protein, and **D** S6 ribosomal protein (S6) normalized to tubulin in brain lysates of Pumilio2 gene-trap (Pum2^{GT}) mice compared to age-matched WT controls. Statistics: Mann-Whitney U-test, n = 4, mean + SEM.

Pum2^{GT} mice showed a trend suggesting decreased protein expression of phosphorylated mTOR (pmTOR) in weaned mice (normalized values: 0.30±0.12 in Pum2^{GT} mice vs. 1.00±0.09 in WT), while adult mice demonstrated slightly elevated levels of pmTOR protein (1.64±0.52 in Pum2^{GT} vs. 1.00±0.15 in WT), although the difference was not (yet) statistically significant. Additionally, mTOR kinase activity is

commonly measured by quantifying the phosphorylation of downstream targets, *e.g.*, ribosomal protein S6 (S6) protein (Zeng et al. 2009). Analysis of S6 protein (**Figure 9C**) and phosphorylated S6 (pS6) protein (**Figure 9D**) was performed using Western blot using phospho-specific antibodies. Weaned $Pum2^{GT}$ mice showed a significant reduction of pS6 protein (0.35±0.03 in $Pum2^{GT}$ vs. 1.00±0.29 in WT), while adult $Pum2^{GT}$ mice showed a non-significant increase compared to WT (1.28±0.29 vs. 1.00±0.11 in WT). S6 protein levels remained stable at both ages of $Pum2^{GT}$ mice compared to control (weaned 1.02±0.25 in $Pum2^{GT}$ vs. 1.00±0.10 in WT; adult 1.31±0.38 in $Pum2^{GT}$ vs. 1.00±0.46 in WT).

In summary, mTOR, pmTOR, and pS6 protein levels were reduced in weaned $Pum2^{GT}$ mice, while adult mice showed no significant differences compared to WT.

4.1.2. mTOR protein is localized in dendrites of hippocampal pyramidal neurons in the mouse brain

The hippocampus is a brain region that is known to be involved in epileptogenesis (Sendrowski and Sobaniec 2013). Pum2 is furthermore known to have an impact on hippocampal dendrite morphogenesis and excitability (Vessey et al. 2006, 2010; Driscoll et al. 2013), and has been associated with temporal lobe epilepsy (Wu et al. 2015). I therefore investigated mTOR expression and localization in the hippocampus of adult mice, the age in which epileptic seizures routinely occur (Follwaczny et al. 2017). I performed immunohistochemical stainings against mTOR on perfusion-fixed, cryopreserved, 30 µm thick frontal sections of the dorsal hippocampus of adult mice. As depicted in **Figure 10A**, overall intensity of mTOR staining was reduced in the $Pum2^{GT}$ mouse's hippocampus compared to WT. mTOR staining was prominent in the cell layer and in the stratum lacunosum moleculare (SLM) in WT and $Pum2^{GT}$ mice, respectively. Since the cornu ammonis (CA)1 and CA3 regions were relevant in epileptogenesis (El-Hassar et al. 2017; Alexander et al. 2016; Navidhamidi et al. 2017), and have been related to Pum2 localization and function (Follwaczny et al. 2017), I specifically investigated the dendritic localization of mTOR in these regions. Dendritic localization of mTOR protein that could be assigned to single neurons could be detected in the stratum radiatum (SR) of CA1 (**Figure 10B**, top).

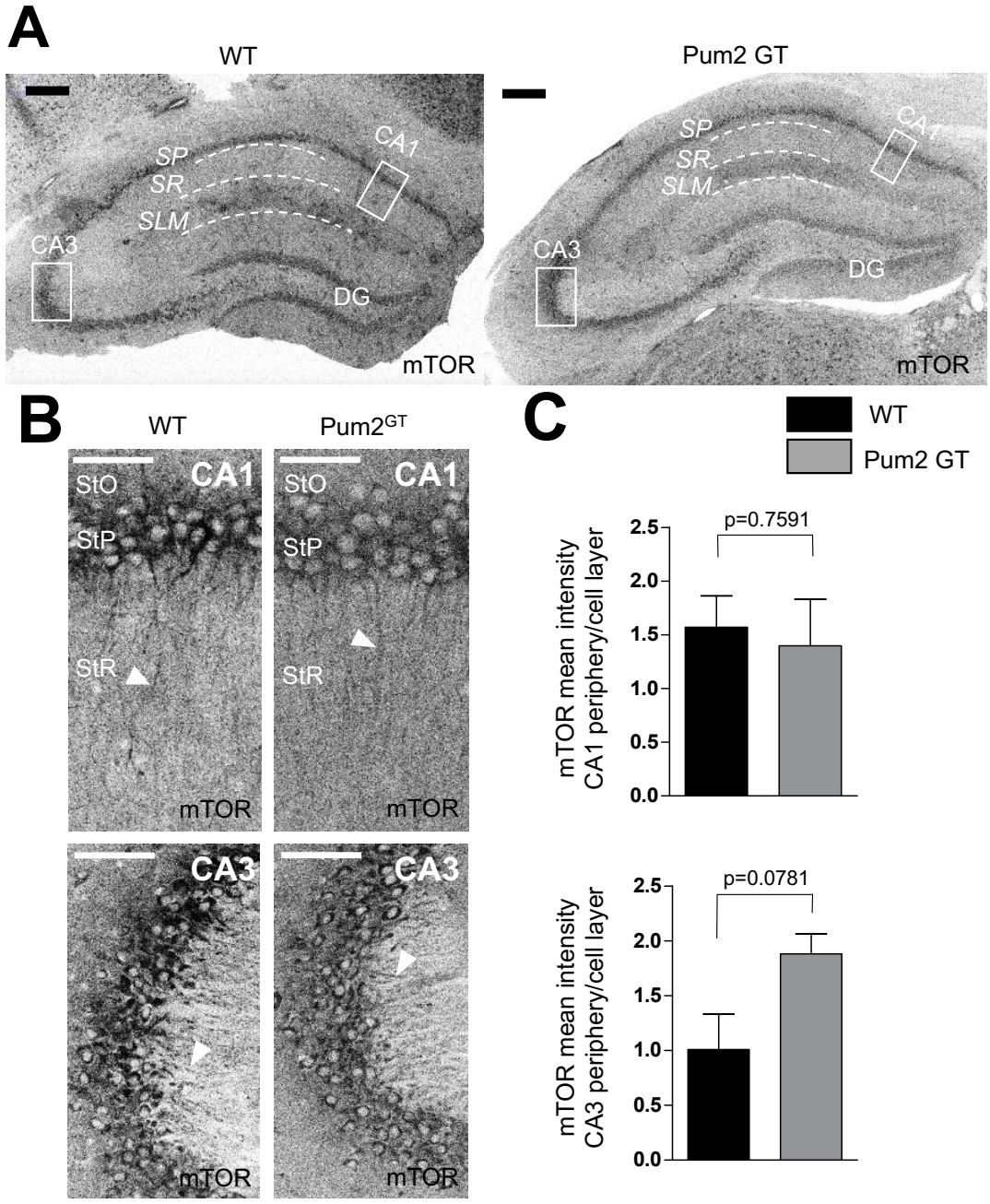

Figure 10: mTOR protein localization in dendrites of pyramidal cells of mouse hippocampus. A Immunohistochemical staining of mTOR protein in the dorsal hippocampus of adult WT and Pum2^{GT} mice. 20x magnification, scale bar = 200 µm. **B** Inset of CA1 (top) and CA3 (bottom) cell layers. mTOR protein localization in dendrites of pyramidal cells in CA1 and CA3 is shown by white arrowheads. Scale bar = 20 µm. **C** Quantification of mean mTOR intensity in periphery of the CA1 and CA3 cell layers, representing dendritic mTOR protein, relative to mTOR intensity in cell layers. Statistics: Unpaired t-test, n = 3, mean + SEM. StO, stratum oriens; StP, statum pyramidale; StR, stratum radiatum; SLM, stratum lacunosum moleculare; CA, cornu ammonis; DG, dentate gyrus.

In CA3, mTOR protein was more prominent in cell bodies, but localization of mTOR was also visible in proximal dendrites (**Figure 10B**, bottom).

In order to analyze the intensity of mTOR immunostaining in dendrites compared to the cell layer, I quantified the mean staining intensity of the corresponding cell layers (**Figure 10C**). No significant difference of staining intensity in the periphery of CA1 or CA3 region between WT and $Pum2^{GT}$ was detectable. In CA3 pyramidal neurons, a shift of mTOR protein could be seen from StP to StR in $Pum2^{GT}$ mice, although quantification showed no statistical significance (1.88±0.18 in $Pum2^{GT}$ vs. 1.00±0.32 in WT).

In summary, immunohistochemical stainings showed decreased overall staining intensity of mTOR protein in $Pum2^{GT}$ mouse hippocampus compared to WT. Dendritic distribution of mTOR protein could be seen in CA1 and CA3 regions in $Pum2^{GT}$ and WT mice.

4.1.3. mTOR protein localization at synapses in primary hippocampal neurons

The RBP Pum2 is localized close to dendritic spines and believed to influence synaptic connectivity and stability through localized translational regulation at dendritic spines upon synaptic activation (Vessey et al. 2006). Cultured rat primary hippocampal neurons were used for further analysis of mTOR localization. Cells were stained against mTOR and the synaptic marker Homer 1, and the possible overlap of the respective stainings was investigated. Homer is a marker for postsynaptic sites or so-called “postsynaptic densities”, which defines the protein-rich area at the synaptic membrane (Tao-Cheng et al. 2014), and has been shown to couple to the mTOR activator PI3 Kinase (Rong et al. 2003). **Figure 11** depicts representative images generated using confocal microscopy of co-immunostained neurons (mTOR/Homer) at DIV15. Localization in the cell body and dendrites could be seen for both stainings. Colocalization was best visible in distal dendrites as depicted in the insets of **Figure 11** (bottom).

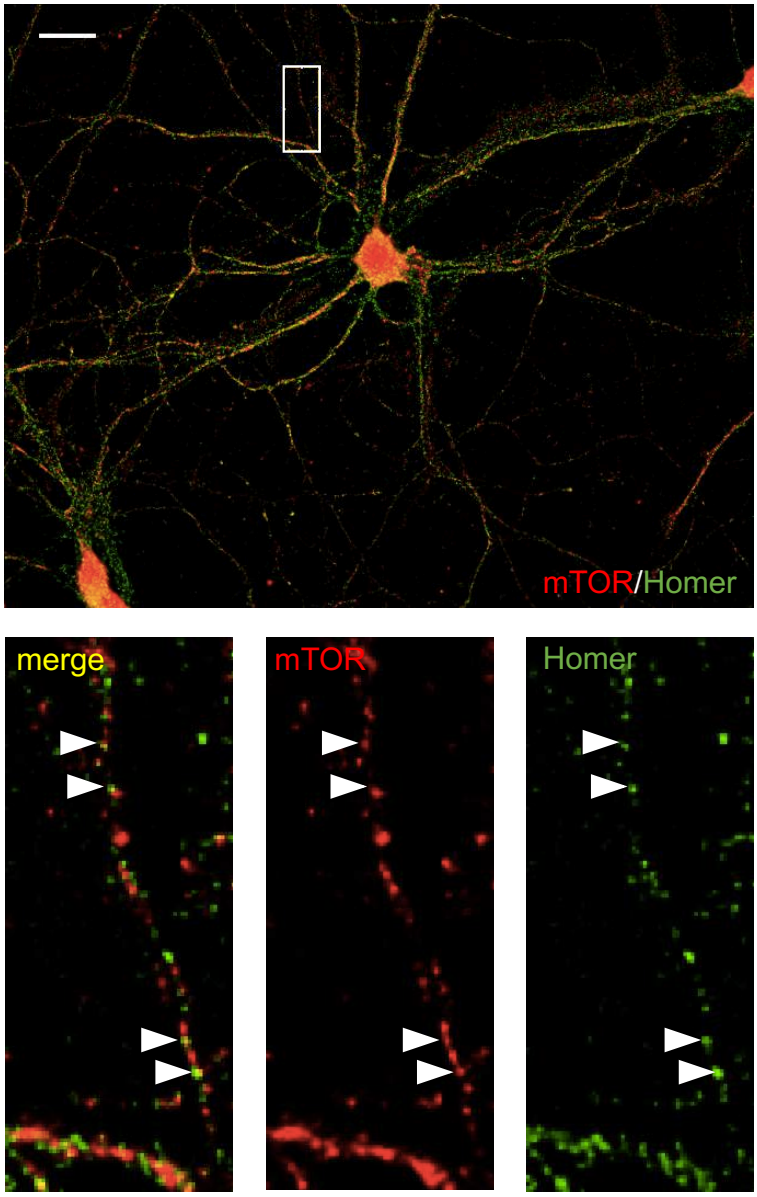

Figure 11: mTOR is partially localized at synapses. Representative images of an mTOR/Homer co-immunostained rat hippocampal neuron (DIV 15). Colocalizing proteins (yellow) of mTOR (red) and Homer (green) are indicated by arrowheads. 63x magnification. Scale bar = 20 µm.

4.1.4. Behavioral and memory training of mice leads to increased mTOR expression

Along with its role in the pathogenesis of the epileptic phenotype, Pum2 regulates synaptic plasticity (Dong et al. 2018). Also mTOR is known to be involved in neuronal activation that underlies synaptic plasticity and learning (Lipton and Sahin 2014). Therefore, we tested for changes in mTOR, pmTOR and S6, pS6 protein levels in adult $Pum2^{GT}$ and WT mice that underwent a 4 week battery of behavioral and memory training (Popper et al. 2018). Graphs showing mTOR, pmTOR and S6, pS6 protein levels are depicted in **Figure 12**. Whole brain lysates were used for Western blot analysis of adult mice ("naïve" group) and mice after behavioral training ("training" group). $Pum2^{GT}$ mice exhibited an up to five-fold increase in mTOR protein expression after training (5.05±0.48) compared to WT mice (1.00±0.13; **Figure 12A**). Likewise, pmTOR protein was elevated about 8-fold in the mutant mice (8.19±3.22 in $Pum2^{GT}$ vs. 1.00±0.26 in WT), and pS6 protein also increased 4.5-fold compared to WT protein expression (4.52±73 in $Pum2^{GT}$ vs. 1.00±0.09 in WT). In contrast, S6 levels did not differ between WT and $Pum2^{GT}$ (1.02±0.25 $Pum2^{G}$ in vs. 1.00±0.13 in WT; **Figure 12B-D**).

In summary, neuronal activation through memory and behavioral training showed an increase of mTOR protein, phosphorylation, and phosphorylated S6 protein.

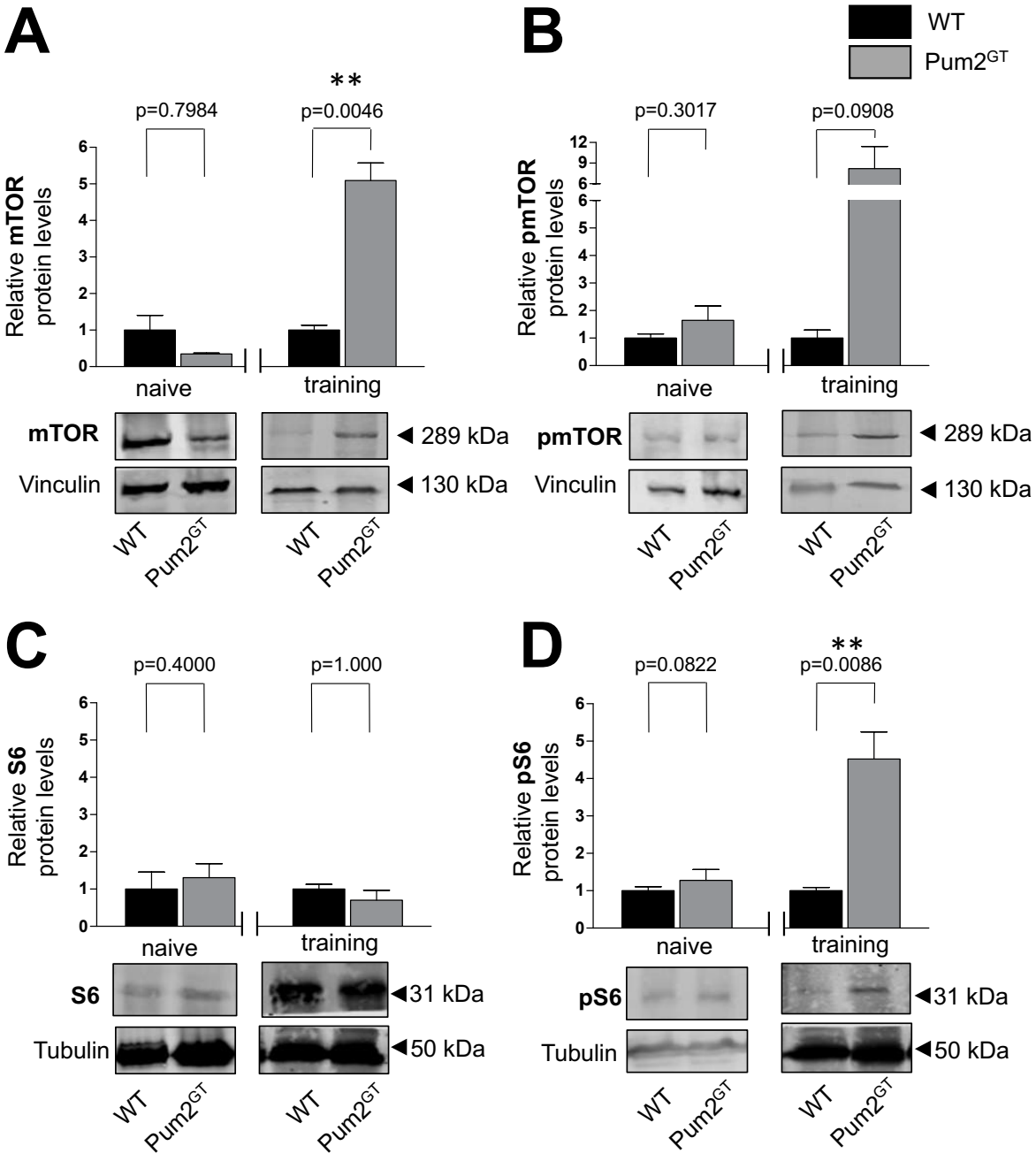

Figure 12: Pum2^{GT} mice show increased mTOR protein and S6 phosphorylation levels upon behavioral training. Western blot of **A** mTOR protein and **B** phospho-mTOR (pmTOR) protein normalized to vinculin, **C** phospho-S6 ribosomal protein (pS6) protein, and **D** S6 ribosomal protein (S6) normalized to tubulin in brain lysates of Pum2^{GT} mice compared to age-matched WT controls before (naïve) or after training (training). Statistics: Mann-Whitney U-test, n = 3, mean + SEM.

4.2. Pum2 KD effects on possible epilepsy targets

Specific target proteins such as gamma-aminobutyric acid A receptors ($GABA_AR$) (Follwaczny et al. 2017) and voltage-gated sodium channel 1.6 ($Na_v1.6$) (Driscoll et al. 2013) are known players in epileptogenesis in Pum2 deficient mice. Since a Pum2 KD showed effects on mTOR expression, I tested for other targets associated with epilepsy that have previously been shown to be (indirectly) regulated by the mTOR pathway: eukaryotic initiation factor 4e (eIF4e) (Hay and Sonenberg 2004), voltage-gated potassium channels (K_v) 1.1 (Raab-Graham et al. 2006; Sosanya et al. 2013) and $K_v4.2$ (Yao et al. 2013; Lugo et al. 2008). Experiments were performed to test for change in protein expression upon Pum2 KD that could point to a possible involvement of Pum2 in the mTOR pathway and a joint regulation of targets by the RBP and the mTOR kinase.

4.2.1. Downregulation of Pum2 does not change protein expression levels of eukaryotic initiation factor 4e (eIF4e) in mouse brains

There have been several studies linking Pum2 with translational repression through translational control of eIF4e (Menon et al. 2004; Vessey et al. 2010). Additionally, eIF4e is a known target of the mTOR pathway (Laplante and Sabatini 2012). As multiple studies have associated eIF4e with neuropsychiatric disease (Amorim et al. 2018), an involvement of this protein in epileptogenesis of $Pum2^{GT}$ mice is likely. Therefore, I decided to test for eIF4e protein concentration in lysates of dissected and snap-frozen brains of weaned and adult mice using Western blot analysis (**Figure 13A**). eIF4e protein levels did not significantly differ between mutant and WT in either age group (0.82 ± 0.07 in weaned $Pum2^{GT}$ vs. 1.00 ± 0.07 in weaned WT; 2.34 ± 1.01 in adult $Pum2^{GT}$ vs. 1.00 ± 0.08 in adult WT). In order to check for possible differences in eIF4e protein expression that might occur in different parts of the brain, I analyzed hippocampal sections of adult $Pum2^{GT}$ and WT mice for eIF4e distribution using immunohistochemical staining (**Figure 13B**). Though quantification of eIF4e protein intensity in the whole hippocampus, cell layer, and periphery did not show any significant differences between $Pum2^{GT}$ and WT (**Figure 13**), microscopical analysis of the sections revealed noticeably more dendrites that showed eIF4e staining in

Pum2^{GT} mice (arrowheads in insets in **Figure 13B**). In order to confirm the observations, the experiment was repeated in cultured hippocampal neurons.

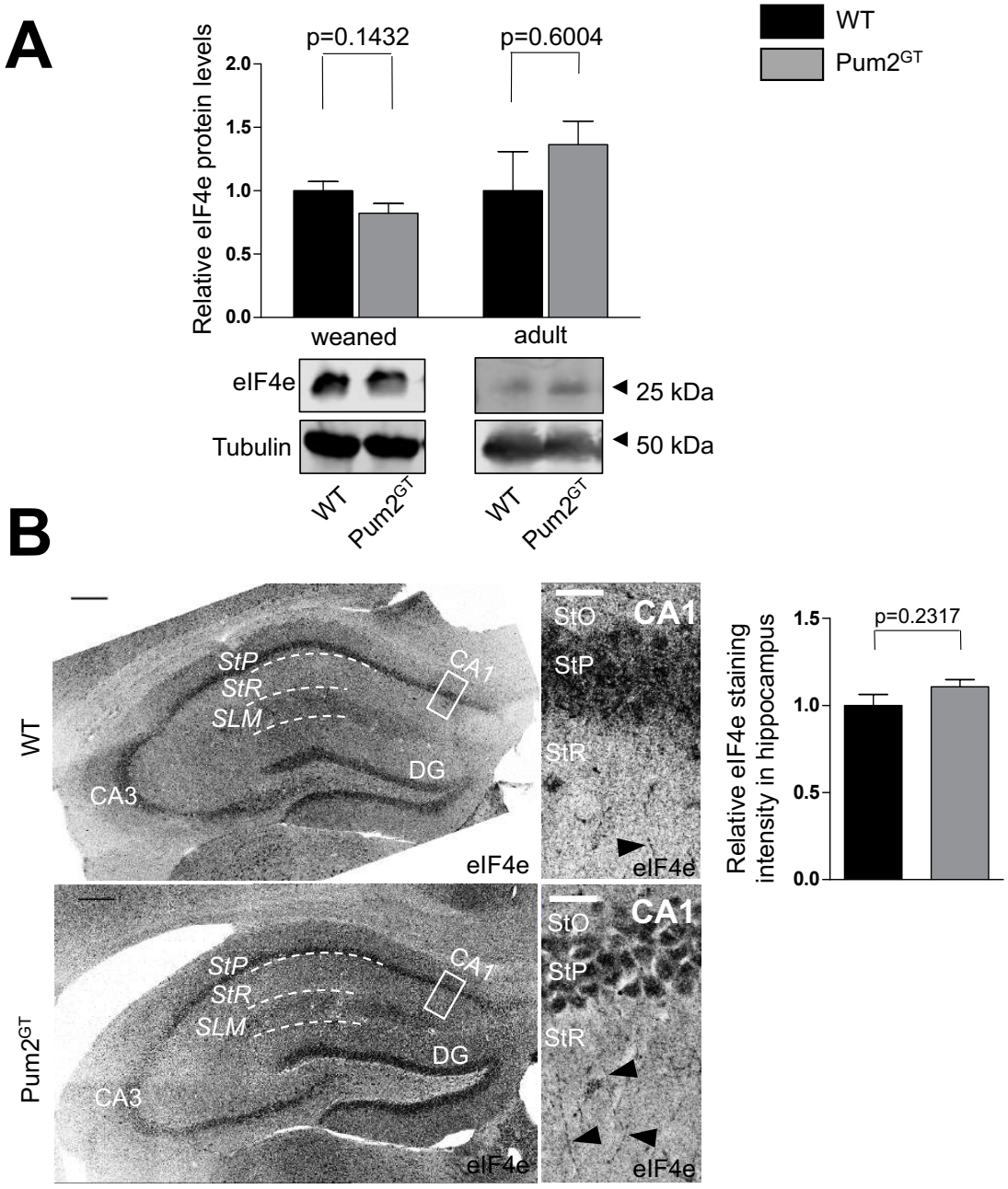

Figure 13: Comparable expression levels of eIF4e protein in Pum2^{GT} and WT mice and similar dendritic localization patterns in both groups. **A** Western blot analysis of eIF4e protein in brain lysates of weaned and adult Pum2^{GT} mice compared to age matched WT controls. There is no significant difference in protein expression in brain lysates between Pum2^{GT} mice and WT controls. Statistics: Mann-Whitney-test, n = 4-5; mean + SEM. **B** Immunohistochemical staining and quantification of eIF4e protein in sections of adult Pum2^{GT} and WT mouse hippocampus. Immunostaining in dendrites of CA1 neurons is pointed out by arrowheads in insets. Scale bar overview = 200 µm, scale bar inset = 20 µm. StO, stratum oriens; StP, statum pyramidale; StR, stratum radiatum; SLM, stratum lacunosum moleculare; CA, cornu ammonis; DG, dentate gyrus.

4.2.2. eIF4e protein is localized in synapses of primary hippocampal neurons

Cultured rat hippocampal neurons were transfected with either shRNA construct directed against Pum2 (shPum2) or for non-targeting control (shNTC) and immunostained against eIF4e. Since hippocampal sections of mice showed dendritic localization of eIF4e protein and eIF4e mRNA has been reported to be located at synapses (Moon et al. 2009), I asked the question whether eIF4e protein is located at synapses in hippocampal neurons upon Pum2 KD. To test this, I co-immunostained shPum2 and shNTC-expressing cells against eIF4e and the synaptic marker Homer 1 which revealed partial colocalization of both proteins as shown in **Figure 14**. There was no prominent difference in observed colocalizing puncta between the shPum2 and the shNTC group.

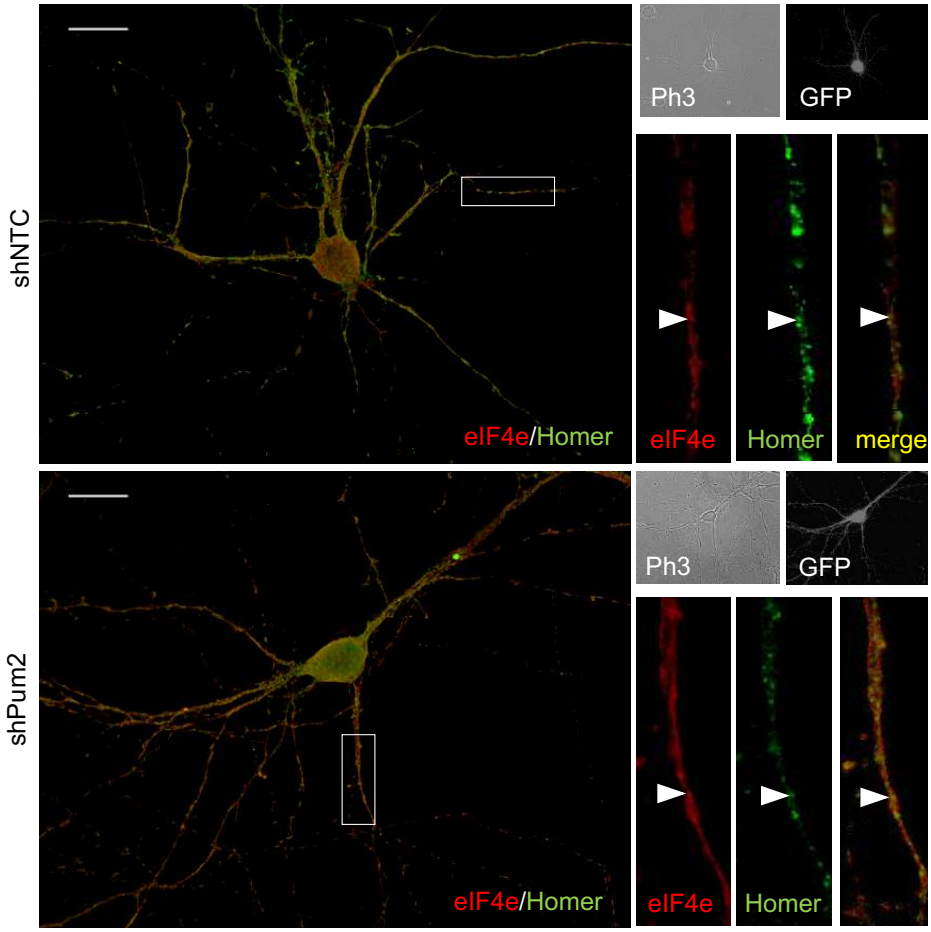

Figure 14: Immunocytochemistry of eIF4e and the synaptic marker Homer show partial colocalization in either shPum2- or shNTC-expressing rat hippocampal dendrites. Cultured rat hippocampal neurons (DIV 15) were transfected with shPum2 or shNTC, respectively, and co-immunostained with eIF4e and Homer antibodies. Merged images of the whole cell (left), phase contrast (Ph3), and GFP channel, as well as eIF4e and Homer single immunostainings of representative dendrites are depicted. Scale bar = 20 µm.

4.2.3. Downregulation of Pum2 changes K_v1.1 and K_v4.2 protein expression in mouse brains

In genetic epilepsy, disturbed homeostasis of synaptic function leads to hyperexcitability and abnormal synchronization of neuronal circuits (Jarero-Basulto et al. 2018). Likewise, Pum2^{GT} mice show a misbalance of voltage-gated sodium channel and $GABA_AR$, which is believed to contribute to their epileptic phenotype (Follwaczny et al. 2017). Also, potassium channels have been linked to epilepsy: Especially voltage-gated potassium channels K_v1.1 and K_v4.2 have been linked to mTOR or its pathway in epileptogenesis (Nguyen and Anderson 2018; Yao et al. 2013). I first tested the K_v1.1 protein expression levels in both weaned and adult Pum2^{GT} mice compared to age matched WT controls using Western blot analysis of whole brain lysates (**Figure 15**). K_v1.1 protein levels in weaned Pum2^{GT} mice showed a significant decrease of about 10% compared to WT (0.90±0.02 in Pum2^{GT} vs. 1.00±2.23 in WT, **Figure 15A**). Adult Pum2^{GT} mice showed a 1.90±0.32 fold increase relative to WT (1.00±0.21, **Figure 15B**). K_v4.2 protein levels were significantly changed only in weaned mice; here Pum2^{GT} exhibited a 1.87±0.27 fold increase compared to WT (1.00±0.15). In adult mice, K_v4.2 tended to be reduced in Pum2^{GT}, although this reduction was not statistically significant (0.55±0.11 in Pum2^{GT} vs. 1.00±0.42 in WT).

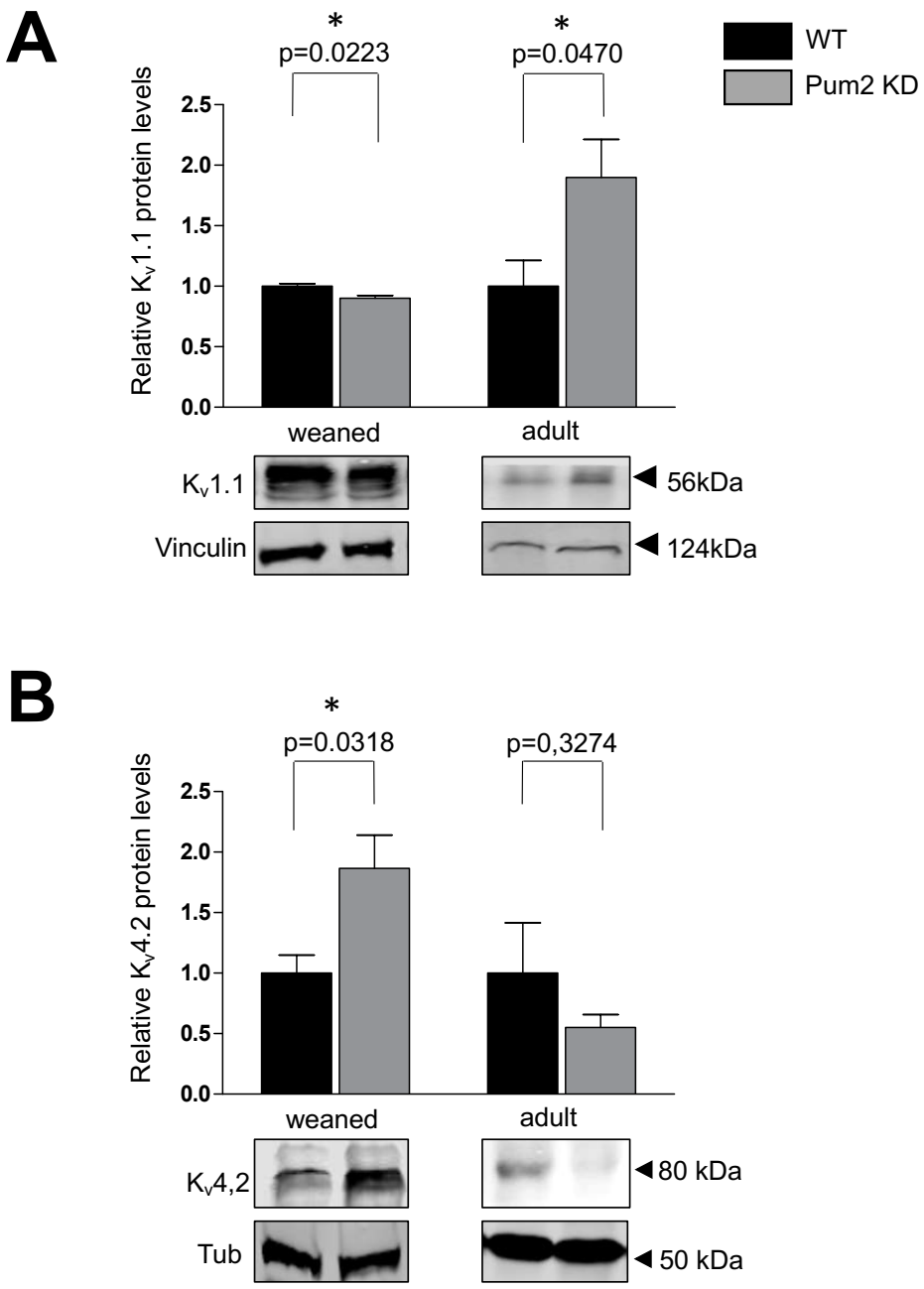

Figure 15: Voltage-gated potassium channels K_v1.1 and K_v4.2 are misregulated in Pum2^{GT} mice. Western blot analysis of K_v1.1 (**A**) and K_v4.2 (**B**) protein in brain lysates of weaned (3 weeks old) and adult (20 weeks old) Pum2^{GT} mice and age matched WT controls. Statistics: Unpaired t-test, n = 4-5, mean + SEM.

4.2.4. K_v1.1, but not K_v4.2 is expressed in dendritic layers of mouse hippocampus

Expression of voltage-gated potassium channel protein was affected by Pum2 downregulation whole brain lysates compared to WT (**Figure 15**). To further analyze the expression and localization of these channels in the hippocampus of adult, epileptic mice, I tested for localization of K_v1.1 and K_v4.2 using immunohistochemical stainings (**Figure 16**). K_v1.1 staining (**Figure 16A**) was visible in the CA and the SLM, but more prominent in the hilus of the DG than in the granular layer of the DG. In comparison to WT, K_v1.1 staining intensity appeared to be stronger in Pum2^{GT} hippocampus by visual inspection, however, quantification of replicates did not show significant differences between mutant and WT (**Figure 16A**, right). Closer analysis of the CA1 layer showed staining in pyramidal cell dendrites in both WT and Pum2^{GT} mouse hippocampus (arrowheads in insets, **Figure 16A**).

K_v4.2 staining was prominent almost exclusively in the pyramidal cell layer of the CA band and the granular layer of the DG (**Figure 16B**). Magnification of the CA did not reveal localization in dendrites, as representative insets of the CA1 region demonstrate. Although staining intensities were much stronger in WT compared to Pum2^{GT} hippocampus especially in the dendritic area, quantification of staining intensities did not lead to significant differences (**Figure 16B**, right).

In summary, eIF4e protein did not significantly change in brains of Pum2^{GT} mice compared to WT controls but showed synaptic localization in cultures of hippocampal neurons of the rat. Protein levels of K_v1.1 channels were significantly reduced in brains of weaned, and a significantly increased in brains of adult Pum2^{GT} mice compared to WT. K_v4.2 protein expression was significantly increased only in brains of weaned but not in adult Pum2^{GT} mice compared to WT. Dendritic localization in hippocampal slices was only seen for K_v1.1., not for K_v4.2.

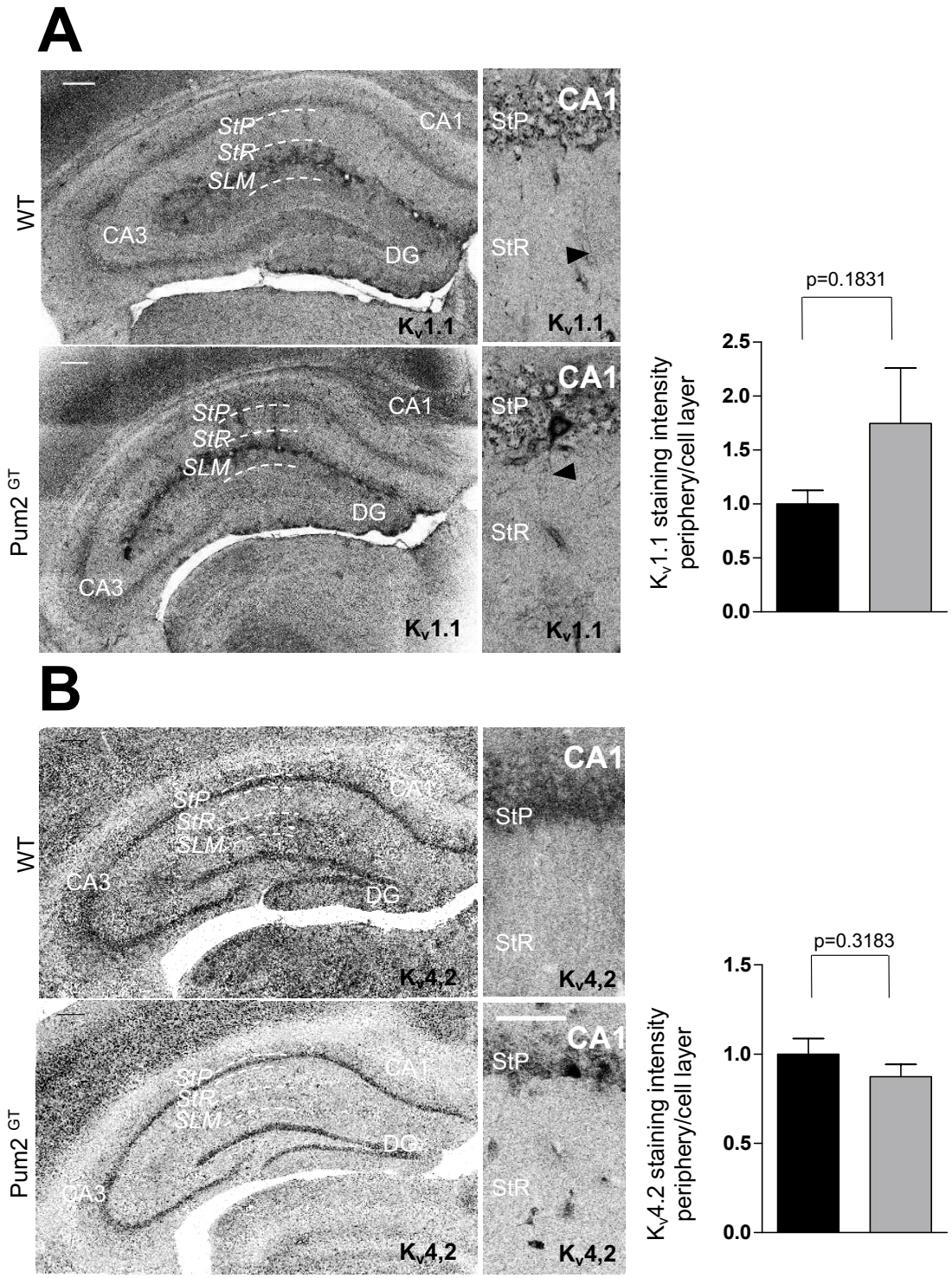

Figure 16: Voltage-gated potassium channels K_v1.1 and K_v4.2 show different localization in brains of adult mice. Immunohistochemical staining of K_v1.1 protein (**A**) and K_v4.2 protein (**B**), respectively, in the hippocampus of adult Pum2^{GT} and WT mice. Quantification of staining intensity in the dendritic compartment (periphery) in relation to cell layer is shown on the right. Magnification 20x, scale bar overview = 200 µm, scale bar inset = 20 µm. StO, stratum oriens; StP, stratum pyramidale; StR, stratum radiatum; SLM, stratum lacunosum moleculare; CA, cornu ammonis; DG, dentate gyrus.

4.3. Investigation of a possible Pum2 and mTOR interaction

Pum2^{GT} mice showed changes in mTOR protein expression (4.1.1) and target proteins such as K_v channels (4.2.4). mTOR has already been discussed to be involved in RBP-mediated local translation regulation (Pernice et al. 2016). In order to investigate such an interplay between Pum2 and mTOR in the regulation of the mentioned target proteins in the Pum2^{GT} mouse, I analyzed a possible interaction of Pum2 and mTOR.

4.3.1. Pum2 overexpression has no effect on mTOR 3'-UTR dependent translation

mTOR mRNA location via binding of 3'UTR has been shown before (Terenzio et al. 2018). Since Pum2 is also involved in location regulation and binds the 3'UTR of its targets (Martínez et al. 2019), I first investigated whether the RBP Pum2 regulates the translation of mTOR via its 3'-UTR. This approach was chosen, because mTOR was localized in dendrites and its expression suggested to be dependent of Pum2 expression (4.1). Therefore, we performed luciferase assays (**Figure 17**). For this, we cloned the 3'-UTR of *mTOR* mRNA into a dual luciferase reporter plasmid. Subsequently, HeLa cells were co-transfected with the mTOR 3'-UTR containing plasmid or control, and with a red fluorescent protein (tagRFP) construct to overexpress tagRFP-Pum2 or tagRFP only. In the luciferase experiment, the impact of Pum2 overexpression on translation of the luciferase gene containing the mTOR 3'-UTR was measured by adding luciferin and quantifying fluorescence compared to the empty vector control (no Pum2 overexpression). As depicted in **Figure 17B** (bottom), there was no difference between translation of the gene containing mTOR 3'-UTR when Pum2 is overexpressed compared to NTC: 0.95±0.18 fold change of the YFP-Pum2 group compared to YFP only (normalized to 1). Therefore, in the following experiments I concentrated on a possible protein-protein interaction between Pum2 and mTOR.

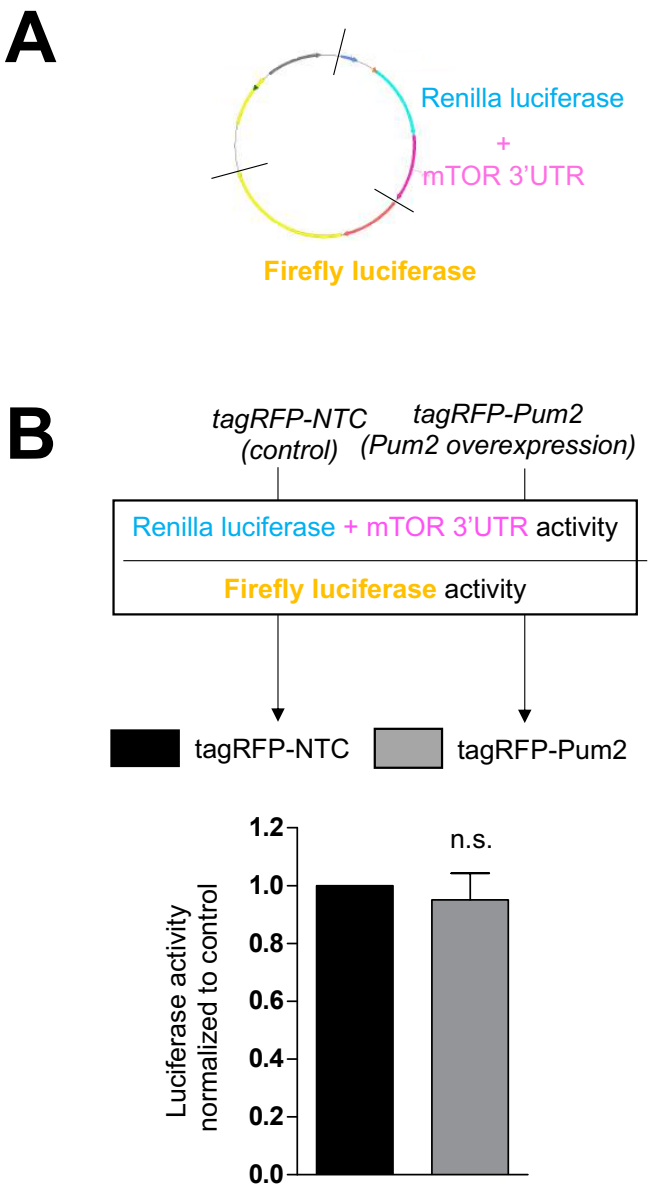

Figure 17: Pum2 overexpression has no effect on mTOR 3'-UTR dependent translation. The dual luciferase plasmid containing the mTOR 3'-UTR is shown in **A**. The graph in **B** depicts total luciferase activit. Statistics: Unpaired t-test, n (replicates) = 3, n (independent cultures) = 4, mean + SEM.

4.3.2. mTOR and Pum2 protein partially colocalize in the mouse hippocampus and in synapses of rat hippocampal neurons

Previous unpublished work by Rico Schieweck in the Kiebler group has shown phosphorylation of Pum2 through Phostag gels, which specifically trap phosphorylated proteins. Furthermore, phosphoproteome analysis of mouse brain tissue indicates Pum2 phosphorylation. To check for (transient) protein-protein interactions possibly allowing enzymatic interaction such as phosphorylation of Pum2 by mTOR, I investigated colocalization of the two proteins (Kohnhorst et al. 2016). First, hippocampal tissue of adult WT mice was co-immunostained against mTOR and Pum2, respectively (**Figure 18**). In the overview, there was colocalization visible, particularly in the CA1 cell layer. Using a higher magnification of this inset, colocalizing puncta were visible in cell bodies and to a lesser extent in dendrites of pyramidal neurons. Images of these sections only showed colocalization events in cell bodies as pointed out by arrowheads (**Figure 18**). For a more precise analysis of a possible colocalization, rat hippocampal neurons were used for immunostaining against Pum2 and mTOR (**Figure 19**). Here, I additionally co-immunostained with Homer 1 to check for possible synaptic localization of both proteins. Partial colocalization of Pum2 and Homer puncta (**Figure 19**, top), as well as mTOR and Homer puncta (**Figure 19**, middle) could be seen in the widefield images. Last, co-immunostainings for Pum2 and mTOR were merged and showed overlap in the same Homer-labeled puncta, indicating synaptic localization (arrowheads in **Figure 19**, bottom). Additional colocalization events that did not clearly relate to Homer-positive synapses are pointed out by arrows.

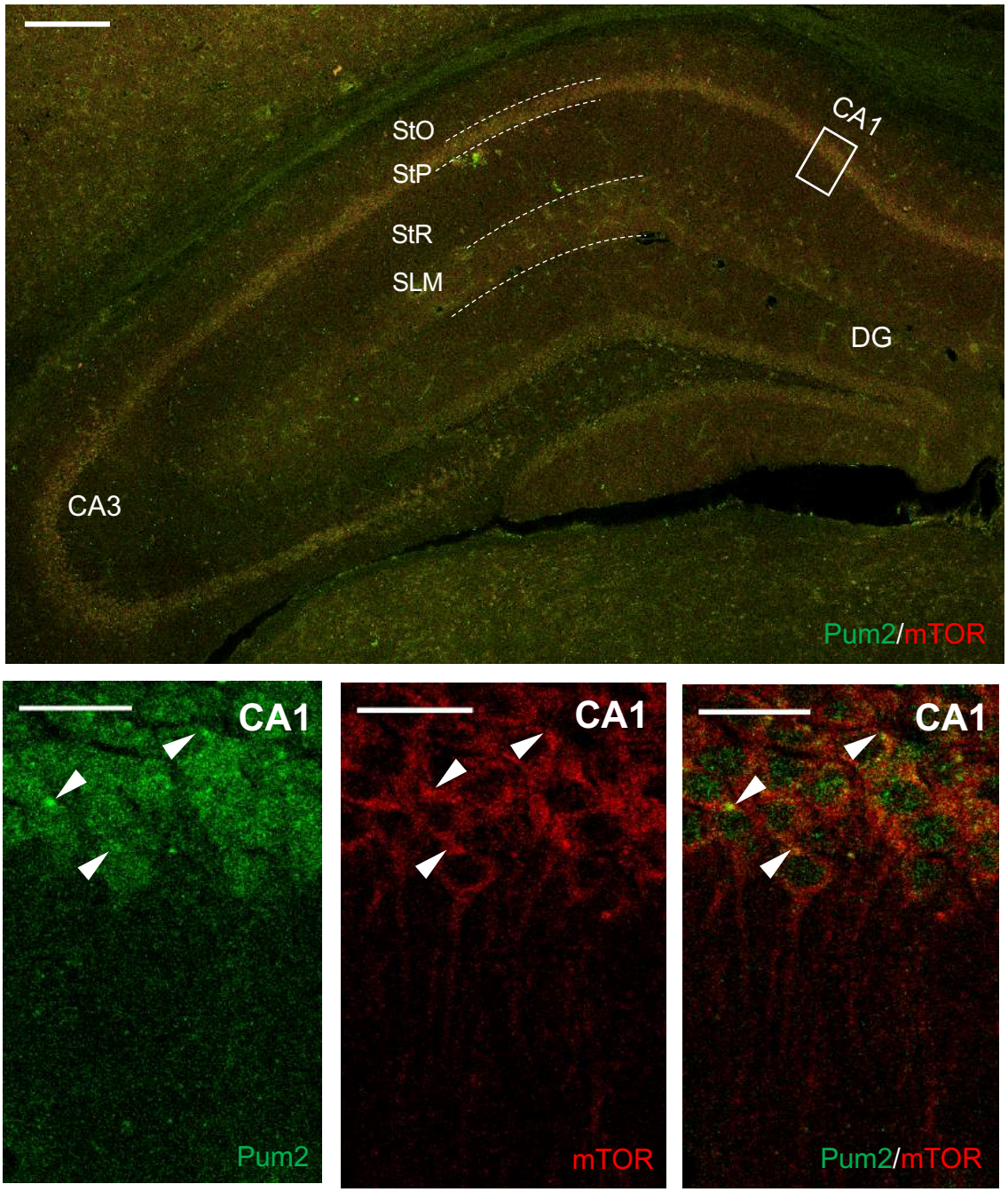

Figure 18: Pum2 and mTOR protein partially colocalize in the hippocampus. Immunohistochemical staining of hippocampal sections of 5 months old WT mice. Pum2 and mTOR colocalization is prominent in the CA1 and CA2 region, as well as in the SLM. White arrowheads point to colocalizing puncta of mTOR and Pum2 protein, respectively in cell bodies of pyramidal neurons, in magnifications of the CA1 cell layer. Magnification 20x, scale bar: Overview 200 µm, inset 20 µm. StO, stratum oriens; StP, statum pyramidale; StR, stratum radiatum; SLM, stratum lacunosum moleculare; CA, cornu ammonis; DG, dentate gyrus.

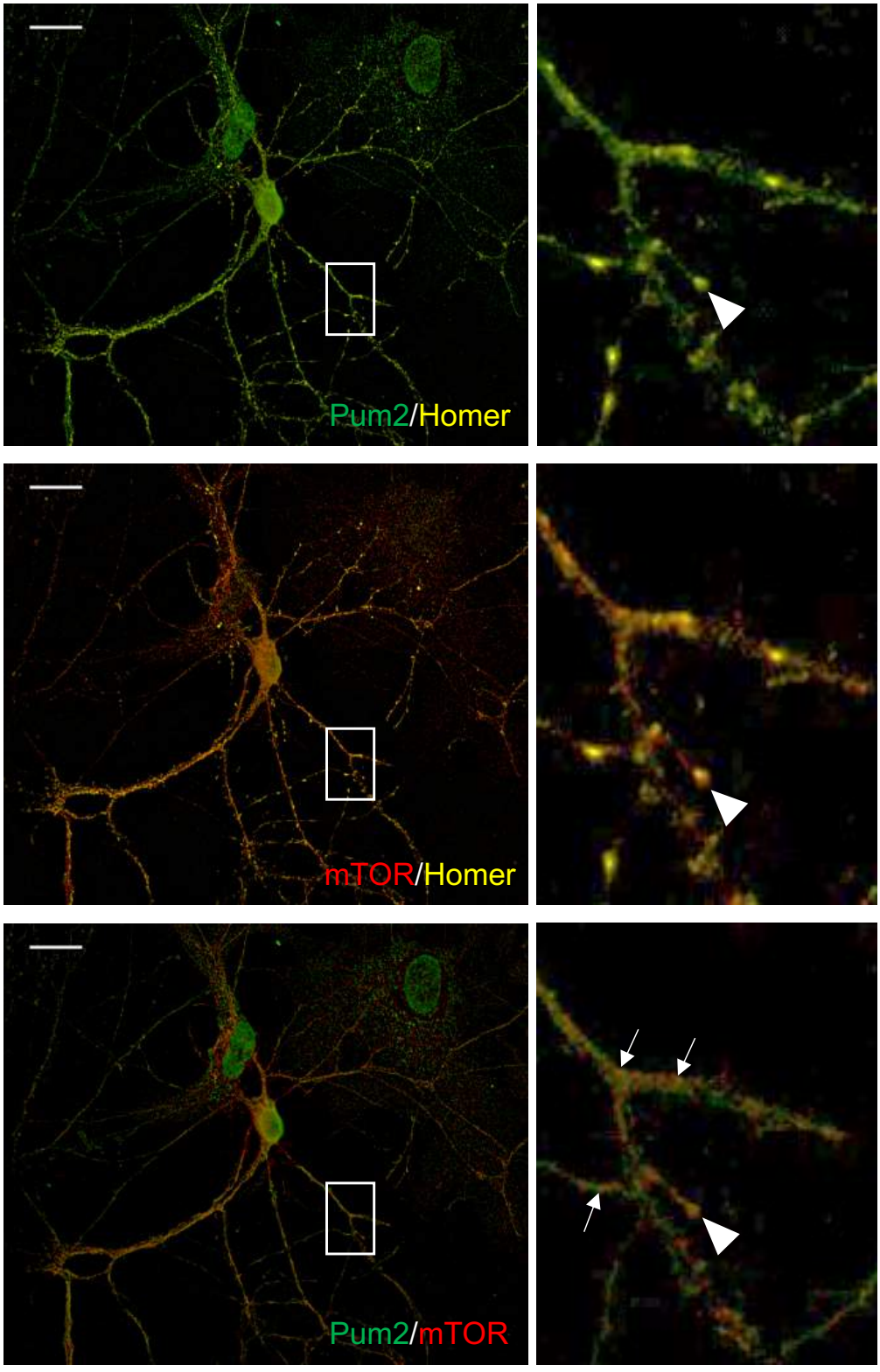

Figure 19: Pum2 and mTOR protein partially colocalize at synapses. Cultured rat hippocampal neurons (DIV 15) were immunostained with anti-Pum2, anti-mTOR and anti-Homer antibodies, respectively. Representative deconvoluted images are depicted. mTOR (top) and Pum2 (middle) partial association with Homer positive puncta, representing synapses, is indicated by arrowheads. Additional mTOR and Pum2 colocalization independent of Homer is indicated by arrows (bottom). Magnification 63x, scale bar = 20 µm.

4.3.3. Rapamycin treatment of HN10e cells inhibits mTOR and S6 phosphorylation and reduces colocalization of Pum2 and mTOR

Previous experiments suggested a partial colocalization of mTOR and Pum2 in sections of the mouse hippocampus as well as in rat hippocampal neurons (4.3.2). As effects of Pum2 downregulation had already shown to impact protein expression of common targets of Pum2 and mTOR, I now asked the question which effect mTOR inhibition might play on Pum2 and on the possible interaction between Pum2 and mTOR. In order to perform these experiments without the need of animal sacrifice, I established an immortalized cell line. Using the hippocampal neuroblastoma cell line from embryonic day 10 (HN10e) as a reproducible model (Lee et al. 1990), the effect of rapamycin (Rapa) treatment was tested. For this, undifferentiated HN10e cells were treated with 100 µM rapamycin or left untreated (control) for 1.5 h. Cell lysates were then used for Western blot analysis for mTOR, pmTOR and pS6, respectively as depicted in **Figure 20**. To determine the concentration achieving the best inhibition of mTOR, three different concentrations of rapamycin, 50 nM, 100 nM, and 200 nM, were tested. Also, DMSO alone was applied to one experimental group to rule out effects through the solvent alone. mTOR protein did not show any prominent change, while pmTOR showed slightly weaker bands with increasing rapamycin concentration. A pronounced reduction of pS6 protein was visible with increasing rapamycin concentration.

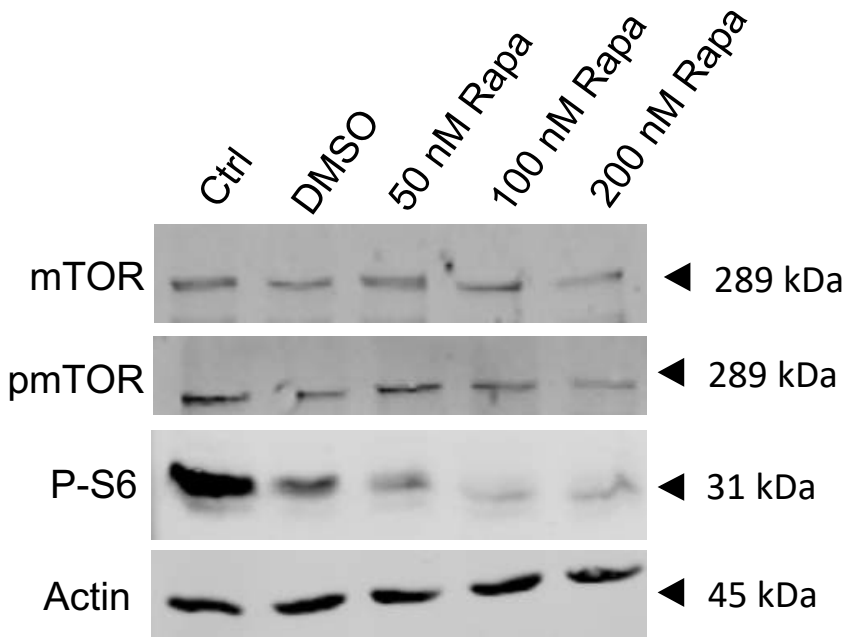

Figure 20: Rapamycin treatment reduces pS6 protein levels in HN10e cell line. Western blot analysis of HN10e cell line treated with final concentrations of 50, 100, and 200 nM rapamycin (Rapa).

To further investigate the colocalization of Pum2 and mTOR, I differentiated HN10e cells (Weiss et al. 2009; Lee et al. 1990). For this, I tested for the ideal concentration of retinolic acid (RA) to induce growth of neurites allowing survival of cells, using 20, 50, and 100 µM RA compared to no treatment (**Figure 21**). As a criteria for differentiation, development of more than 3 neurites was chosen. Here, concentrations of 20 and 50 µM RA showed the best survival of HN10e cells developing more than 3 neurites. Cells treated with 100 µM RA as well as controls died, although death through other reasons than RA toxicity could not be excluded, because also the untreated control culture did not survive beyond day 3 of the experiment. Therefore, further experiments also included 100 µM as a test concentration evaluating the effect of different RA concentrations on HN10e cells.

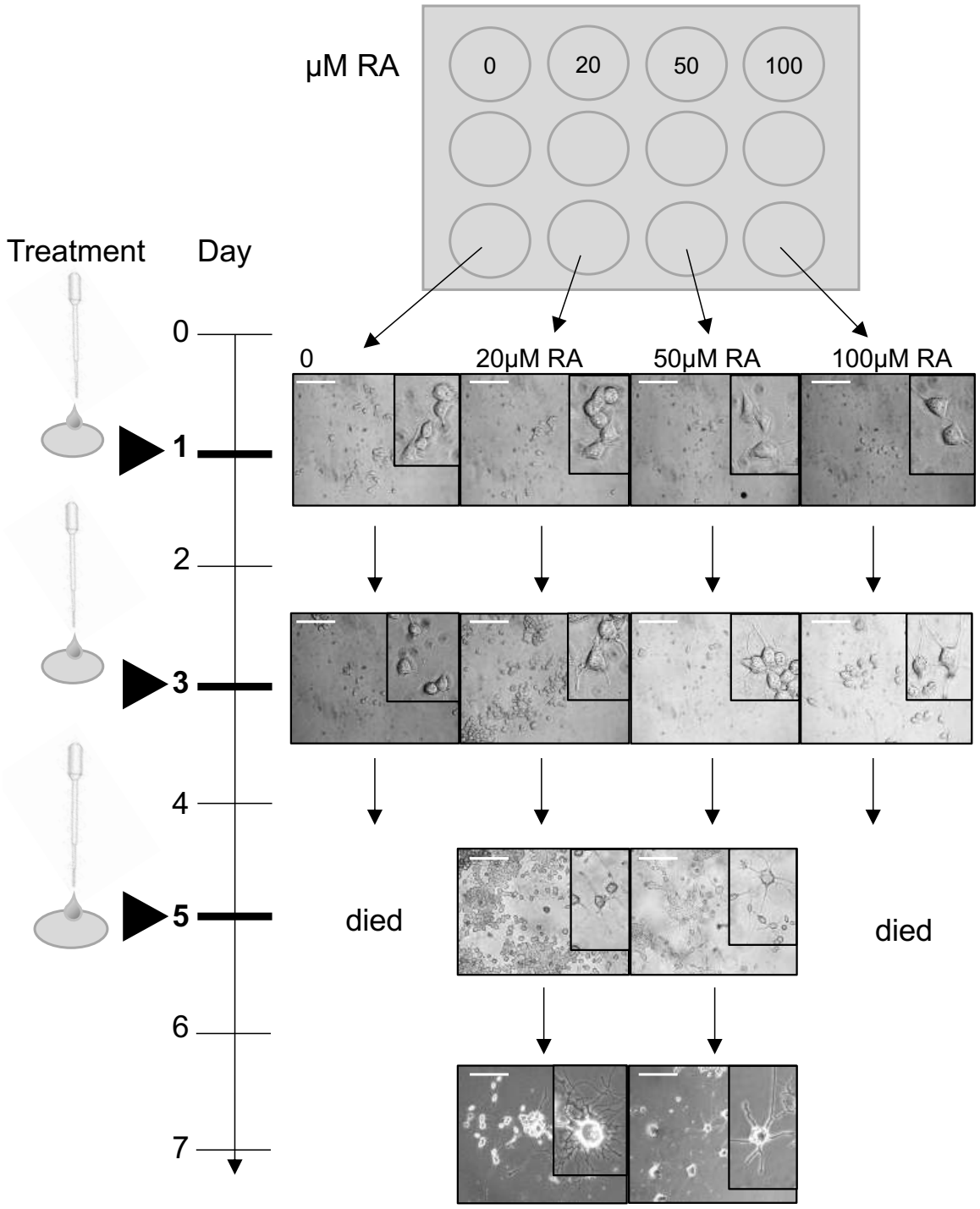

Figure 21: Differentiation of hippocampal neuroblastoma cell line of embryonic day 10 (HN10e) by retinoic acid (RA). HN10e neurons were cultured in FCS DMEM media in 12-well plates and subsequently treated with RA diluted in DMSO. Concentrations of 20 µM, 50 µM and 100 µM were chosen to test for differentiation and survival of the cells. Cells were treated and imaged every second day until day 7 after initial treatment. Magnification 10x. Scale bar = 20 µm.

In order to find the concentration of FCS in culture media and the concentration of RA allowing cell growth and survival under additional treatment with shRNA constructs or rapamycin, I tested different concentrations of DMEM FCS media, transfection efficiency and the effect of rapamycin on differentiated HN10e cells (**Figure 22**). Since previously published studies showed culture of HN10e cells in both DMEM medium supplied with both 1% FCS (Lee et al. 1990) and 10% FCS (Weiss et al. 2009) for culture of HN10e, I tested for differences in growth and survival of cells depending on FCS complementation to find the optimal concentration for following experiments. Growth of undifferentiated HN10e cells was observed up to 7 days and cell death was determined by detachment of cells from the dish. Culture of cells for 7 days showed a comparable growth and survival of cells in 1% and 10% DMEM FCS media (**Figure 22A**). Because there were no signs of a toxic effect (cell death) and nutrient availability was higher in 10% DMEM FCS availability, following experiments with differentiated HN10e cells were performed in 10% DMEM FCS media. To check for transfection efficiency, an shPum2 construct containing GFP was chosen. The purpose of using this plasmid was to simultaneously test for cell death or change in cell morphology in RA-treated cells in combination with Pum2 KD. After transfection of equally grown HN10e cells treated with 0, 10, 50, and 100 µM RA, the number of fluorescent cells was observed by imaging. Here, 20 µM RA showed most transfected cells (**Figure 22B**). Therefore, 20 µM RA was used for HN10e differentiation in further experiments. Inhibition of mTOR has important effects on cell metabolism (Saxton and Sabatini 2017). Therefore, the effect of rapamycin on cell morphology and survival of HN10e cells treated with 20 µM RA was tested. Here, no obvious difference in morphology was seen in cell survival and morphology.

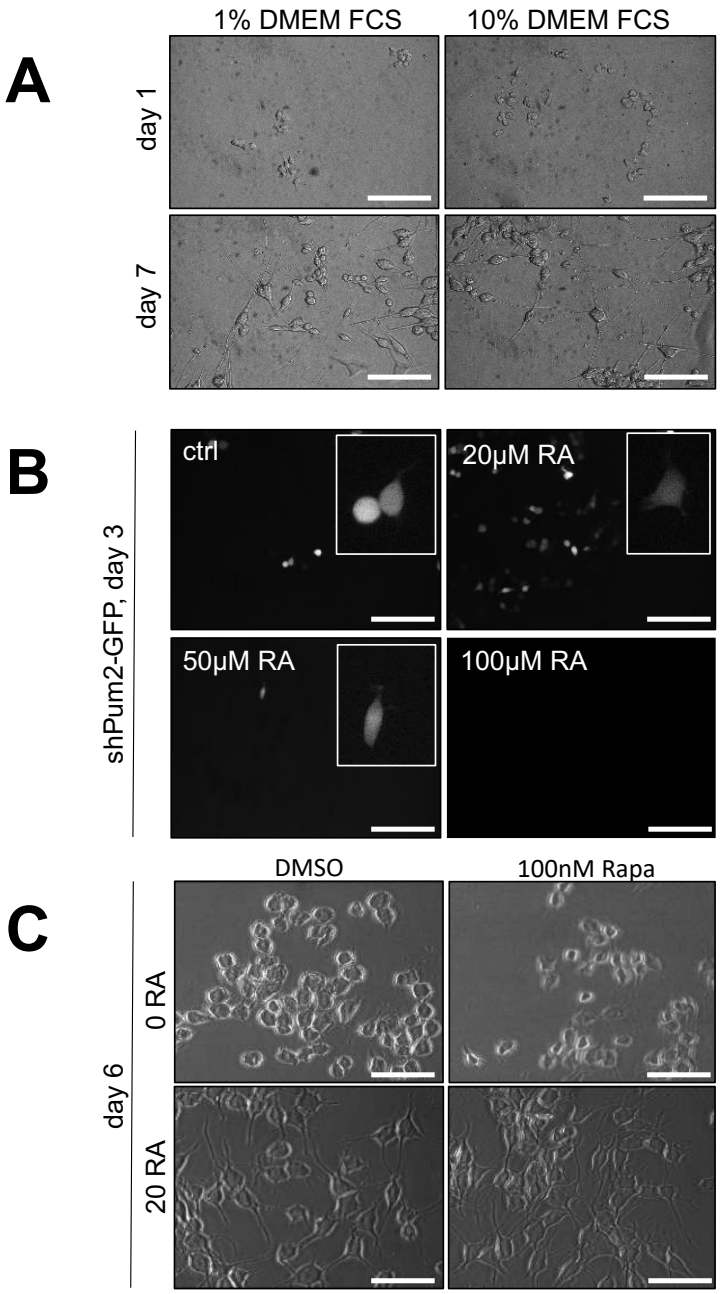

Figure 22: Cultured HN10e cells in different DMEM media concentrations, transfected and treated with rapamycin. **A** HN10e cells were cultured in FCS media containing either 1% (left) or 10% DMEM (right). **B** GFP fluorescence of HN10e cells transfected with shPum2-GFP for 3 days in culture treated with either no, 20, 50, or 100 μM RA for 3 days is shown. **C** HN10e cells were treated with RA for 6 days and 100 nM rapamycin (Rapa) for 1.5 h on day 6 of differentiation. Magnification 10x. Scale bar = 100 μm.

Differentiated HN10e cells were immunostained against Pum2 and mTOR to check for colocalization and to compare staining patterns to cultured primary hippocampal neurons. After 3 days of differentiation, HN10e cells were fixed and immunostained, as depicted in **Figure 23**. Individual Pum2 and mTOR puncta were visible (pointed out with green colored arrowheads for Pum2 and red arrowheads for mTOR). Also, numerous colocalizing puncta were detectable in neurites of differentiated HN10e cells (white arrowheads).

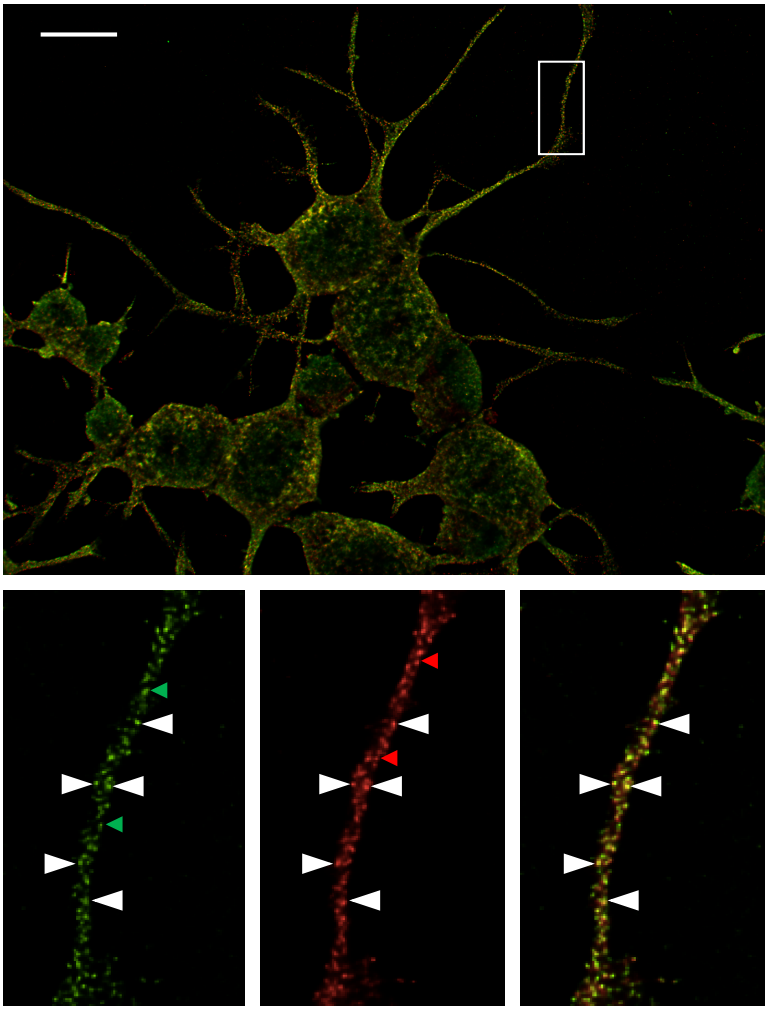

Figure 23: Pum2 and mTOR partially colocalize in HN10e differentiated neurons. Representative image of HN10e neurons that were cultured and differentiated using RA for 6 days, then fixed, washed and co-immunostained with anti-Pum2 (green) and anti-mTOR (red) antibodies, respectively. White arrowheads in the magnification of a representative neurite show colocalizing puncta. Red arrowheads show mTOR only puncta, green arrowheads point to Pum2 only puncta. Magnification 63x, scale bar = 20 µm.

Compared to hippocampal neurons (**Figure 19**), HN10e cells displayed less branches of neurites and a higher cell body to neurite ratio. The staining pattern was less intense in the cell body of HN10e cells compared to hippocampal neurons. However, clear similarities in cell morphology seen were seen here and in previous studies, which also described comparable electrophysiological features between HN10e and primary hippocampal cells (Lee et al. 1990). Because of the effective reduction of S6 and mTOR phosphorylation by rapamycin treatment on HN10e cells (see **Figure 20**), I decided to use HN10e cells to perform pilot experiments on the effect of rapamycin treatment on Pum2 and mTOR staining patterns.

In the next experiment, I therefore quantified colocalization events of Pum2- and mTOR-positive puncta in differentiated HN10e cells that were treated with 100 nM rapamycin compared to the DMSO-treated control. Colocalization events were quantified per micrometer neurite length. The graph depicted in **Figure 24** shows a reduction from 0.18±0.03 colocalizing puncta per µm neurite length in DMSO vs. only 0.08±0.02 colocalizing puncta per µm neurite length in the rapamycin group.

In summary, rapamycin treatment on HN10e cells led to reduced protein expression of pmTOR and pS6 compared to DMSO-treated control. In primary hippocampal neurons of the rat, where immunostaining of Pum2 and mTOR showed multiple colocalizing puncta in neurites, rapamycin reduced the amount of colocalizing puncta significantly.

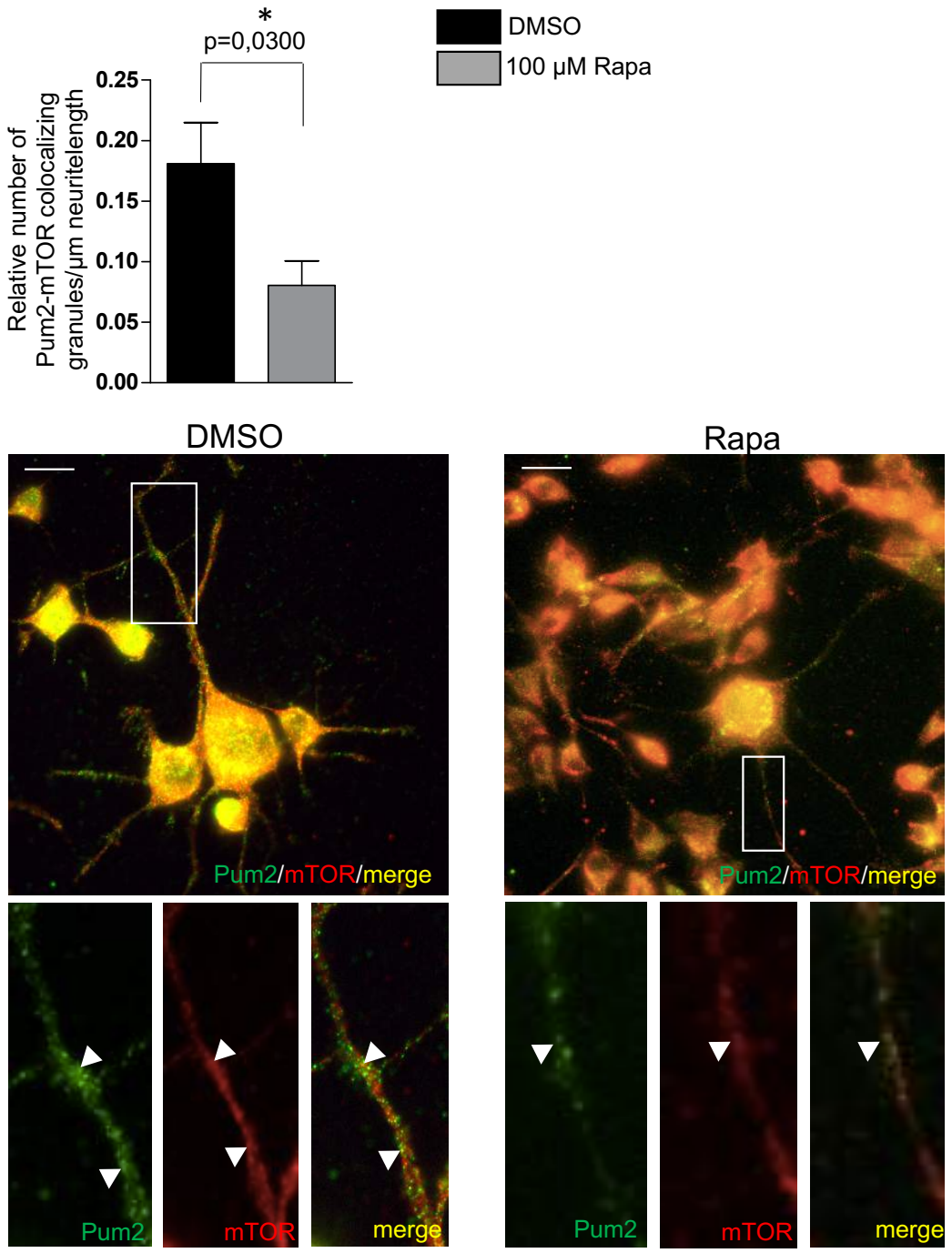

Figure 24: Rapamycin treatment reduces mTOR and Pum2 colocalization in differentiated HN10e neurons. HN10e neurons were differentiated for 5 days using 20µM RA and treated with 100nM rapamycin (right) or DMSO control (left) for 1.5h. Cells were then fixed, washed and immunostained with anti-Pum2 and anti-mTOR antibodies, respectively. Colocalizing puncta were counted in 17 neurites (DMSO) vs 12 neurites (Rapa) from 15 cells each of one neuronal culture. Statistics: Unpaired t-test. Magnification 63x, scale bar = 20 µm.

Rapamycin led to a reduction of the colocalization events and therefore on a potential interaction of Pum2 and mTOR. The aim of the next experiment was to mimic rapamycin treatment of a Pum2 KD and to explore possible changes in protein expression and phosphorylation of mTOR and S6. Therefore, I tested for the effects of simultaneous mTOR inhibition and Pum2 KD on mTOR expression, the underlying mTOR pathway, and Pum2 protein. Undifferentiated cells at passage 6 were transfected with shPum2 or shNTC. After two days of transfection, a fraction of either group was treated with DMSO or rapamycin for 1.5 h. Western blot for analysis of mTOR, pmTOR, S6, pS6 and Pum2 protein levels was performed (**Figure 25**). mTOR protein was mildly increased upon Pum2 KD, but was unaffected under any other condition. pmTOR band intensities were similar to mTOR. S6 protein did not show apparent differences, while the pS6 band was very pronounced in Pum2 KD cells and almost undetectable in all conditions that involved rapamycin application, including combination of Pum2 KD and mTOR inhibition. Pum2 band intensities were strongly reduced in Pum2 KD and rapamycin treatment alone but not when the two conditions are combined.

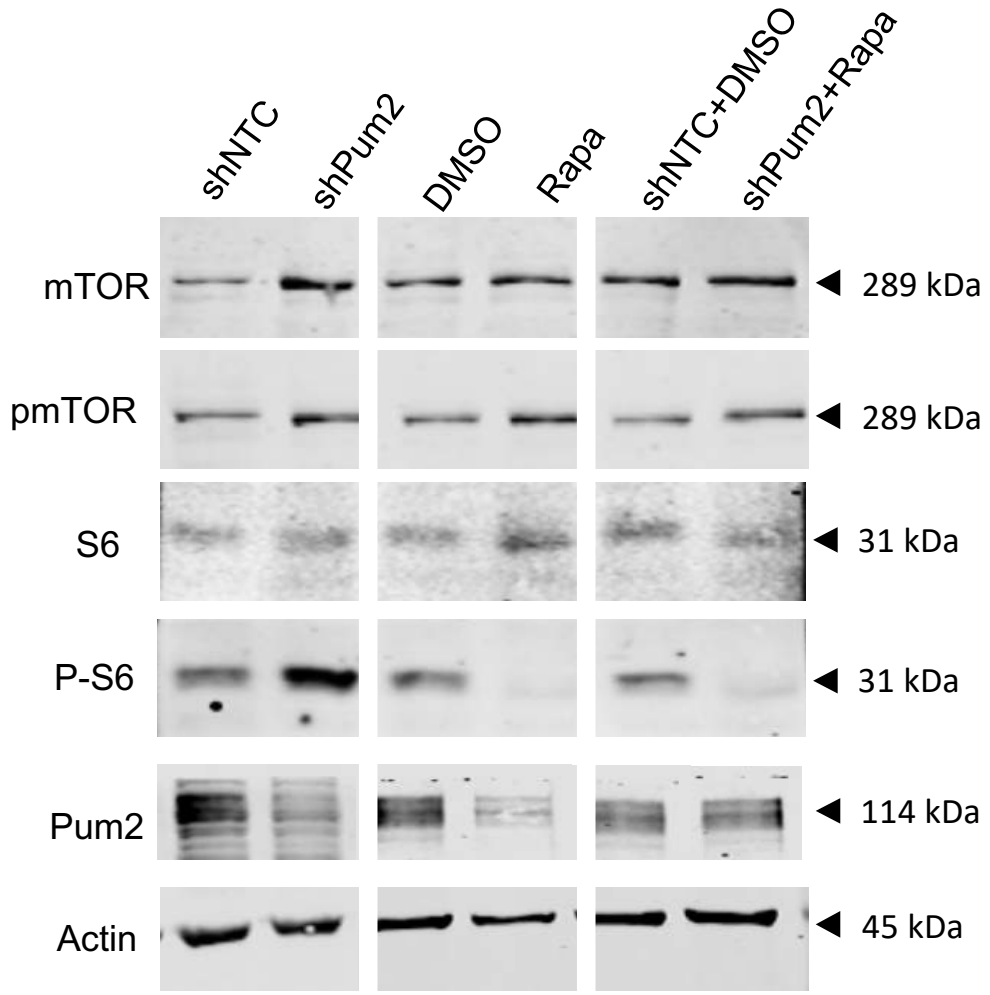

Figure 25: Effect of shPum2 and rapamycin treatment on mTOR and S6 phosphorylation and Pum2 protein expression in HN10e. Western blot analysis of protein in HN10e cells under different conditions. Undifferentiated HN10e cells were transfected with shNTC or shPum2 for 24 h (left) or treated with DMSO or Rapa for 1.5 h (middle), then both conditions were combined (right). Rapamycin treatment shows strong effects on pS6 and Pum2 protein levels, but not on mTOR, pmTOR or S6.

4.4. Summary of results

The role of mTOR for epileptogenesis in a mouse model of Pumilio2 deficiency by (1) testing for changes in mTOR expression in $Pum2^{GT}$ mice, (2) analyzing expression of relevant targets in $Pum2^{GT}$ mice, and (3) investigating a possible interplay of Pum2 and mTOR was analyzed here.

Weaned, pre-symptomatic $Pum2^{GT}$ mice show decreased mTOR protein levels. Adult, epileptic $Pum2^{GT}$ mice, in contrast, do not show any significant difference compared to WT. Upon memory training and stress, mTOR levels increase five-fold in $Pum2^{GT}$ mice. Immunochemical stainings of the mouse hippocampus and primary hippocampal neurons of the rat show that mTOR localizes dendritically and partially in synapses.

The translational regulator eIF4e shows no difference between $Pum2^{GT}$ and WT mice but increasingly localizes to synapses upon Pum2 KD. The voltage-gated potassium channel $K_v1.1$ is significantly decreased in weaned $Pum2^{GT}$ mice and increased in adult $Pum2^{GT}$ animals compared to WT and localizes in hippocampal dendrites. $K_v4.2$ is significantly upregulated in weaned $Pum2^{GT}$ mice but shows no difference to WT in adult animals and does not localize in dendrites.

A luciferase assay showed that translation of the 3'-UTR of mTOR is Pum2 independent. Costaining of Pum2 and mTOR in slices of the mouse hippocampus, primary hippocampal neurons of the rat, and differentiated HN10e cells showed partial colocalization of the two proteins in neurites. Rapamycin treatment of HN10e cells decreased the number of colocalizating puncta.

These findings suggest a dynamic role of mTOR and potassium channel expression in the aging brain of $Pum2^{GT}$ mice. The resulting potential mechanisms of epileptogenesis and the consequence of a possible relationship between Pum2 and mTOR will be discussed below.

5. Discussion

5.1. A possible role for mTOR in the epileptogenesis of Pum2^{GT} mice

In juvenile, 3 weeks old Pumilio2 gene trap (Pum2^{GT}) mice, we detected a significant downregulation of mechanistic target of rapamycin (mTOR) and phosphorylated ribosomal protein S6 (pS6) protein indicating reduced activity of the mTOR pathway. Interestingly, adult mice (5 months old) exhibited no effect on mTOR expression or S6 phosphorylation. At this same age, Pum2^{GT} mice experience epileptic seizures (Follwaczny et al. 2017; Siemen et al. 2011). Strikingly, Pum2^{GT} mice that underwent cognitive behavior testings such as novel object recognition/localization and Barnes maze testing – all paradigms that depend on hippocampus-dependent and independent spatial memory and novelty response – showed significantly higher mTOR protein and activity levels compared to WT animals that underwent the same procedure. I hypothesize that the balance between Pum2- and mTOR-mediated regulation of synaptic homeostasis contributes to synaptic plasticity in this model of genetic epilepsy (**Figure 26**). Absence of Pum2 has shown an increase in dendritic expression of proteins contributing to neuronal excitability, such as the metabolic glutamate receptor (mGluR) (Dong et al. 2018). Therefore, my model proposes that in the WT hippocampus (**Figure 26A**), Pum2 contributes to repression of dendritic protein expression, and acts against hyperexcitability. At the same time, mTOR in its role as an activator of translation, contributes to excitability in response to stimuli (Takei and Nawa 2014; Swiech et al. 2008). In the WT mouse, mTOR acts as an activator of neuronal activity, and, in balance with Pum2 as a suppressor, supports neuronal homeostasis. Earlier studies described that reduction of mTOR signaling reduces seizures (McDaniel and Wong 2011). Upon deficiency of Pum2, my findings indicate that downregulation of mTOR during epileptogenesis in juvenile animals is compensatory, preventing epileptic seizures at this age (5.1.1). I conclude that the downregulation of mTOR as a central regulator of versatile cellular functions including translation and synaptic transmission (Saxton and Sabatini 2017) compensates the higher network activity observed in juvenile Pum2^{GT} mice (Follwaczny et al. 2017), therefore suppressing epileptic seizures in weaned mice (**Figure 26B**). Secondly (5.1.2), I propose that the relative increase of mTOR protein in adult (compared to weaned), seizure-prone Pum2^{GT} mice fails to balance increased excitability, which is

supposedly generated by the decreased paired-pulse inhibition in adult Pum2^{GT} mice (Follwaczny et al. 2017), and, in turn, contributes to network hyperexcitability (**Figure 26C**). Finally (5.1.3), our behavior testings strongly suggest that neuronal activation during cognition boosts mTOR expression (**Figure 26C**, bottom). To dissect the role of mTOR in Pum2 depleted neurons, I focused on important aspects of the mTOR pathway such as synaptic localization and effects on eIF4e and K_v1.1. and K_v4.2. proteins, which are potentially targets of this kinase (Pernice et al. 2016).

5.1.1. mTOR downregulation as an antiepileptic factor in weaned Pum2^{GT} mice

A disruption of synaptic homeostasis through changed expression of potassium channels Na_v1.1, Na_v1.2 and Na_v1.6 are contributors to epileptogenesis (Lerche et al. 2013; Driscoll et al. 2013), and, as Follwaczny et al. reported, especially juvenile mice are likely to establish this changed expression of Na_vs and present with seizures at an older age (Follwaczny et al. 2017). mTOR, in general, is believed to be a central positive regulator of protein synthesis, leading to a higher level of cellular activity and excitability (Saxton and Sabatini 2017). In several studies, it has been shown that not only increased mTOR activity promotes epilepsy, but also inhibition of the mTOR pathway decreases neuronal activity and seizure frequency (McDaniel and Wong 2011) in different mouse models (Ljungberg et al. 2009; Tang et al. 2012) as well as in pharmaceutical trials in humans (French et al. 2016). Since I was able to detect a significant downregulation of mTOR as well as pS6 protein in Pum2^{GT} mice compared to WT, it allows me to assume that the low mTOR levels and activity might compensate the increasing excitability possibly induced by or Na_v channel misregulation (Follwaczny et al. 2017), therefore preventing the onset of epilepsy in weaned mice (**Figure 26B**).

5.1.2. mTOR as a contributor to hyperexcitability in adult Pum2^{GT} mice

In adult Pum2^{GT} mice, however, mTOR protein is no longer downregulated compared to WT, which raises the possibility that mTOR might contribute to epilepsy in adult Pum2^{GT} mice. At 5 months of age, Pum2^{GT} mice develop epileptic seizures (Follwaczny et al. 2017). According to the hypothesis that downregulated mTOR in

weaned Pum2^{GT} mice balances excitability and prevents epilepsy, the rising mTOR levels in adult Pum2^{GT} mice might lead to hyperexcitability (**Figure 26C**). Other studies have already shown that mTOR is an essential local regulator of synaptic transmission (Niere and Raab-Graham 2017). In pyramidal neurons of the CA1 hippocampal cell layer, NMDA dependent late long term potentiation (LTP) is rapamycin sensitive (Vickers et al. 2005). Furthermore, in CA3-CA1 pyramidal neurons, the mTOR pathway is activated by the extracellular signal regulated kinase (ERK) upon high frequency stimulation (Tsokas et al. 2007). Therefore, I asked whether mTOR is increasingly localized in dendrites of Pum2^{GT} mouse hippocampi, contributing to epileptogenesis in this model. My immunohistochemical stainings of adult Pum2^{GT} and WT mouse hippocampus show dominant signal intensity of mTOR in dendrites of CA3 pyramidal neurons that is slightly stronger in Pum2^{GT} mice, though in the quantification of staining intensity of the periphery compared to the cell layer the difference is not (yet) significant. This supports the hypothesis of a selective localization of mTOR in Pum2^{GT} mouse hippocampus, and might point to an increase of mTOR signaling at the postsynaptic side of connections between mossy fibers and CA3 pyramidal dendrites. Several studies have reported reduced mossy fiber sprouting upon mTOR inhibition, proposing that mTOR plays a role in the increase in the connection between dentate gyrus (DG) cells and the CA pyramidal cells, which contribute to the pathogenesis of TLE (Buckmaster and Lew 2011; Yamawaki et al. 2015; Godale and Danzer 2018). Additionally, mossy fiber sprouting likely plays a role in epileptogenesis in Pum2^{GT} mice as well, for Pum2 KD leads to increased dendritic growth (Vessey et al. 2010) and also increased axon growth through Pum2 KD has been shown (Martínez et al. 2019). The prominent mTOR staining in CA3 dendrites in Pum2^{GT} mice might contribute to this process.

In order to confirm my results showing dendritic mTOR localization in immunohistochemistry of mouse brain sections, I performed immunocytochemistry on rat primary hippocampal neurons, where mTOR and Homer partially colocalize at synapses. Consistent with this, previous studies have linked mTOR signaling to synapses: Rong *et al*. reported that the synaptic marker Homer 1 couples the metabolic glutamate receptor 1 (mGluR1) to PI3K/mTOR pathway (Rong et al. 2003). Therefore, synaptic stimulation through mGluR1 via the mTOR pathway could also be a contributor to increased synaptic activity in Pum2^{GT} mice.

5.1.3. mTOR as a marker for failed synaptic homeostasis in adult Pum2^{GT} mice after behavioral training

Interestingly, Western blot experiments in Pum2^{GT} mice that were subject to behavioral training suggest that mTOR levels and activity shoots up upon neuronal stimulation through learning in Pum2^{GT} mice, but not in WT littermates. This suggests that in Pum2^{GT} mice, mTOR fails to balance synaptic activity upon increased firing. Previous studies have suggested the importance of the mTOR pathway in memory and learning: Inhibition of mTOR by rapamycin strongly inhibits LTP in mice (Stoica et al. 2011) and rats (Tang et al. 2002); furthermore, mTOR signaling is required for mGluR dependent long-term depression in mice (Hou and Klann 2004). Compatible with prior studies suggesting mTOR activation to be crucial for memory and learning (Graber et al. 2013), the uprising mTOR levels in Pum2^{GT} mice after behavioral training provide further support for this hypothesis. I suggest that the observed excessive mTOR signaling after the exposition to stimulating situations and memory induction in Pum2^{GT} mice is due to a generally increased susceptibility of the mTOR pathway, leading to higher neuronal excitability in epileptic Pum2^{GT} mice (**Figure 26C**, bottom). Whether the observed increased tendency of mTOR expression upon synaptic stimulation is caused by Pum2 directly, by a greater induction of mGluR-mediated signals or by other indirect factors is yet to be determined.

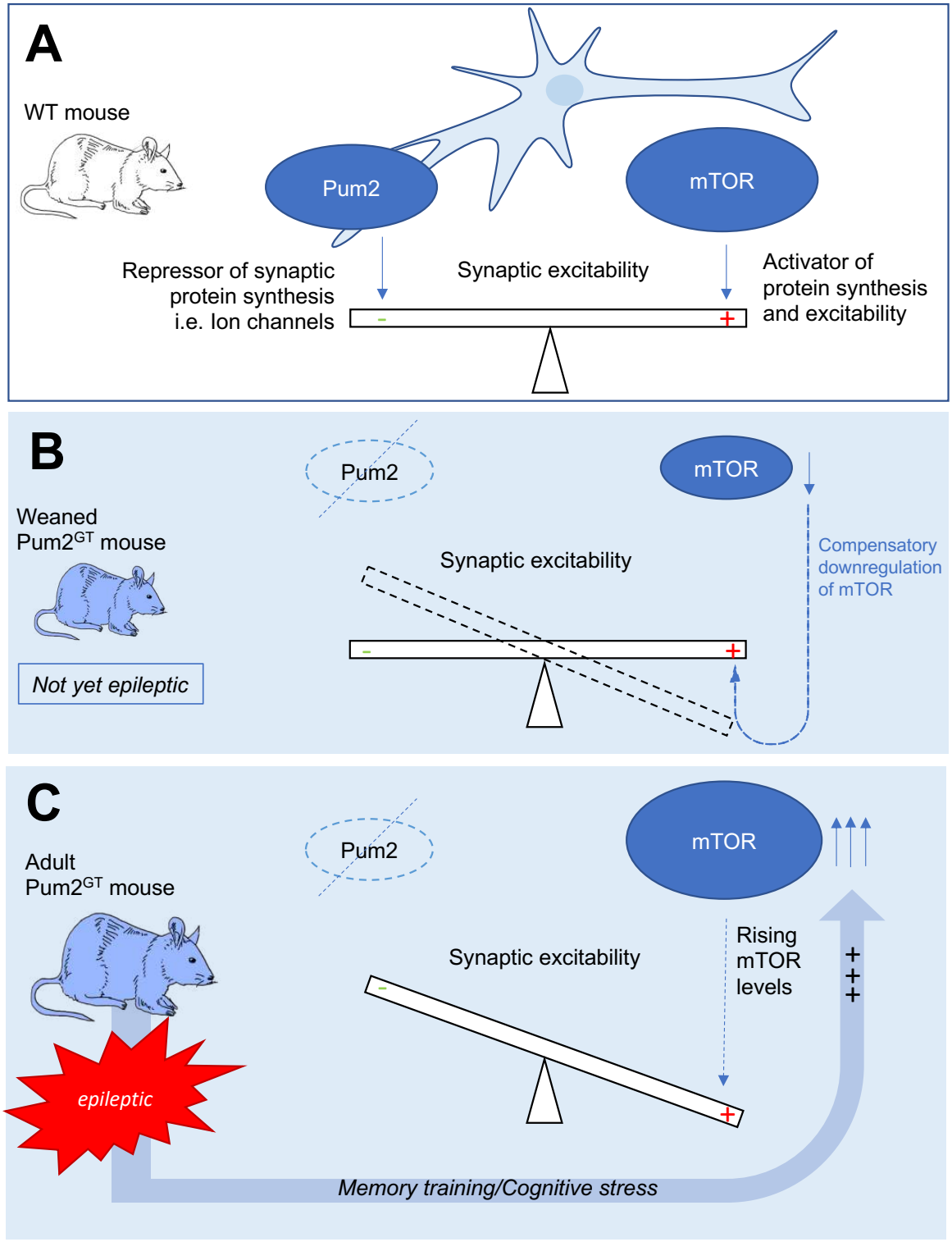

Figure 26: Model for the potential role of mTOR in epileptogenesis in Pum2^{GT} mice. A. Model of Pum2 and mTOR interaction in WT mice. Pum2 is dendritically localized and stabilizes excitability by repression of local protein synthesis. mTOR increases excitability through increased protein synthesis. **B** Weaned Pum2^{GT} mice exhibit increased excitability. Excitability is balanced by downregulation of mTOR. **C** In adult Pum2^{GT} mice, mTOR is no longer downregulated and increased excitability overweighs and results in seizures. Additionally, memory and behavioral training or cognitive stress lead to elevation of mTOR protein levels (own graph).

5.2. Voltage-gated potassium channels are potentially regulated by mTOR and may contribute to epileptogenesis in adult Pum2^{GT} mice

In Pum2^{GT} mice, channelopathies have been suggested to largely contribute to the epileptic phenotype (Follwaczny et al. 2017). Also, K_v1.1 has been linked to mTOR signaling and epilepsy in multiple previous studies, including models of cultured hippocampal neurons (Raab-Graham et al. 2006; Sosanya et al. 2013), kainate induced status epilepticus in rats (Sosanya et al. 2015), and PTEN KO mouse models (Nguyen and Anderson 2018). Since Pum2^{GT} mice showed disturbed mTOR signaling, I investigated a possible effect on K_v1.1 protein expression in Pum2^{GT} mice. Interestingly, weaned mice show a significantly decreased level of K_v1.1 protein, while K_v1.1 protein expression is elevated in adult Pum2^{GT} mouse brains. A genetic deficit of K_v1.1 has shown to cause an epileptic phenotype (reviewed in D'Adamo *et al.*, 2013). Since Pum2^{GT} mice are likely to develop epilepsy in the juvenile age, the reported lack of K_v1.1 protein could be a factor contributing to the pathogenesis of the epileptic phenotype. Kirchheim *et. al* on the other hand found an increase of *K_v1.1* mRNA and protein in the kainate injected mouse hippocampus (Kirchheim et al. 2013). Here, besides the potassium channel protein levels, also action potential response delays were measured by gramicidin-perforated patch-clamp recordings in kainate-treated dentate granule cells, resulting in a highly increased response delays in treated cells compared to control. The authors interpret the elevation of K_v1.1 as a compensatory effect, since K_v channels usually promote the hyperpolarizing current leading to reduced excitability (Kirchheim et al. 2013). A similar effect could be seen in whole brain lysates of adult (20 weeks old) Pum2^{GT} mice, the age at which the epileptic phenotype is believed to be already established (Follwaczny et al. 2017). K_v1.1 might therefore contribute to epileptogenesis in weaned Pum2^{GT} mice, and could be upregulated as a compensatory reaction to the hyperexcitability in adult Pum2^{GT} mice. Could the changing protein expression levels of K_v1.1 be influenced by mTOR? Previous studies have shown increased staining intensity of K_v1.1 in the dendritic compartment of pyramidal neurons of the CA1 hippocampal subregion upon mTOR inhibition (Raab-Graham et al. 2006). Also, the immunohistochemical staining patterns of both Pum2^{GT} and WT adult mice hippocampus show prominent dendritic staining patterns in the CA1 region. This matches previously published immunostainings (Vacher et al. 2008; Rhodes et al. 1997; Veh et al. 1995; Monaghan et al. 2001).

However, Pum2^{GT} hippocampus only show slightly stronger K_v1.1 staining intensities in quantification, making future studies necessary to further evaluate a significant effect. Nevertheless, many studies have pointed towards an interaction between mTOR and K_v1.1 (Raab-Graham et al. 2006; Sosanya et al. 2013; Sosanya et al. 2015; Nguyen and Anderson 2018). Recently, Nguyen and Anderson showed that higher mTOR levels correlate with higher K_v1.1 levels in an epileptic PTEN KO mouse model, in which both mTOR and K_v1.1 overexpression could be reversed by rapamycin treatment (Nguyen and Anderson 2018). Similar parallel expression changes are seen in Pum2^{GT} mice: In weaned Pum2^{GT} mice, both mTOR and K_v1.1 protein levels were reduced compared to WT. In adult mice, both protein levels relatively increase. Other studies show an upregulation of K_v1.1 protein levels when mTOR is decreased (Sosanya et al. 2015; Raab-Graham et al. 2006; Sosanya et al. 2013). In these studies, local protein synthesis of K_v1.1 in dendrites was observed upon inhibition of mTOR or the N-methyl-D-aspartate receptor (NMDAR), indicating that increased synaptic excitation and increased mTOR signaling reduces local K_v1.1 synthesis (Niere and Raab-Graham 2017; Nguyen and Anderson 2018). However, these results originate drug induced epilepsy and cell culture models, while a in genetic epilepsy such as modeled by the Pum2^{GT} mouse, mTOR and K_v1.1 expression are likely influenced by an interplay of many more factors.

In contrast to elevated K_v1.1, K_v4.2 protein is reduced in weaned Pum2^{GT} mice brains compared to WT controls, while adult Pum2^{GT} mice show normal K_v4.2 protein levels. As reduced K_v4.2 expression levels lead to increased seizure susceptibility (Barnwell et al. 2009), upregulation of K_v4.2 protein in Pum2^{GT} mice could be, like mTOR downregulation, a compensatory effect to the beginning hyperexcitability in weaned mice. In the literature, changed expression levels of K_v4.2 have been reported to contribute to disruption of synaptic homeostasis in various epilepsy models, including mouse (Barnwell et al. 2009), rat (Su et al. 2008; Lugo et al. 2008), hippocampal cell culture (Kim et al. 2007), and *Xenopus laevis* oocyte models (Lin et al. 2018), as well as tissue of patients with hippocampal sclerosis (Aronica et al. 2009). Due to these data, I suggest that the low K_v4.2 levels could be mediated by mTOR, which also shows low protein levels in weaned Pum2^{GT} mice. In various epilepsy models, an increased excitability through ERK mediated phosphorylation of K_v4.2 was proposed (Aronica et al. 2009; Lugo et al. 2008). Since ERK and mTOR act on several common epilepsy targets (Pernice et al. 2016), a similar influence of mTOR on K_v4.2 in Pum2^{GT} is

possible. Also, regulation of K_v4.2 by FMRP, which has been associated with mTOR in several studies (Sharma et al. 2010; Narayanan et al. 2008; Hoeffer et al. 2012), has been reported, providing another possible interaction mechanism between the mTOR pathway and K_v4.2 (Lee et al. 2011; Gross et al. 2011). Other than K_v1.1 though, K_v4.2 protein showed dendritic localization in neither Pum2^{GT} mice, nor in WT. In epilepsy associated focal lesions of human brains, including hippocampal sclerosis, focal cortical dysplasia, cortical tubers of patients with tuberous sclerosis, and ganglioglioma, a reduction of K_v4.2 immunoreactivity in the neuropil and prominent staining in the cell body has been reported (Aronica et al. 2009). This data is compatible with the immunohistochemistry performed on adult Pum2^{GT} and WT mouse hippocampus, although a difference between mutant and WT is not obvious. In conclusion, the increase of K_v4.2 protein in weaned Pum2^{GT} mice brains is more likely to be a compensatory mechanism than an effect of disturbed local translation control in weaned mice.

Other than K_v1.1 and K_v4.2, eIF4e levels do not change significantly in the developing Pum2^{GT} mouse brain. As a central downstream indirect target of mTOR, the eIF4e is central for (local) translation (Graber et al. 2013). The effect of Pum2 on eIF4e mRNA is commonly accepted in the literature; several studies have provided data implying direct binding and suppression of *eIF4e* mRNA by Pum2 in mouse (Vessey et al. 2010), *Drosophila* (Menon et al. 2004), and *Saccharomyces cerevisiae* models (Blewett and Goldstrohm 2012). Furthermore, in glia cells within the hippocampus of patients with TLE as well as of a kainate acid induced epilepsy mouse model, increased levels of eIF4e binding protein 1 (4EBP1), the upstream activator of eIF4e, could be observed (Shuyan et al. 2019). Even though in Pum2^{GT} and WT mouse brains, eIF4e can be seen in CA1 dendrites, which play an important part in epileptogenesis (El-Hassar et al. 2017), a significant difference between WT and mutant could not be seen here. It is more likely that the changing mTOR levels in the Pum2^{GT} mouse influence epileptogenesis through large scale changes in ion channel expression, while eIF4e expression changes might be more local or independent mechanisms.

5.3. Outlook: Possible Pum2-mTOR interaction and therapeutic significance

mTOR protein levels change significantly during development and upon stimulation in $Pum2^{GT}$ mice. Furthermore, mTOR shows dendritic localization. As mTOR and several potential mTOR targets are misregulated in $Pum2^{GT}$ mice, I conducted pilot experiments on a possible interplay between the Pum2 and mTOR pathways. Because mTOR has been reported to be transported and locally translated by RBPs depending on its 3'-UTR in axons of dorsal root ganglion (DRG) neurons (Terenzio et al. 2018), I performed luciferase assays to investigate a possible regulation of the mTOR 3'-UTR by Pum2. There was no difference in luciferase activity in HeLa cells overexpressing Pum2 versus control, indicating that either mTOR expression is Pum2 independent, a different region of the *mTOR* mRNA is recognized by Pum2, or entirely different mechanisms for translational control, such as coding or non-coding sequences, are responsible (Jung et al. 2014). Interestingly, it has already been shown that Pum2 binds to the 3'-UTRs of mRNAs coding for both mitogen-activated protein kinase 1 (MAPK1) and p38α MAPK (Lee et al. 2007), which do not only have similar functions, but also overlap with the mTOR pathway (Pernice et al. 2016). Therefore, the observed changes of protein expression of target proteins like $K_v1.1$ and $K_v4.2$ in $Pum2^{GT}$ mice might underlie a more complex or multistep regulation involving Pum2 and mTOR. Another possible mechanism is regulation of RBPs by mTOR through phosphorylation, which has been proposed before (Venigalla and Turner 2012). Also, a local function of mTOR at the synapse in regulating mRNAs has been previously discussed (Niere and Raab-Graham 2017). Since Pum2 acts as a local dendritic translational regulator, a joint regulation of common targets appears to be possible. Therefore, I investigated colocalization of Pum2 and mTOR, and found partial colocalization in immunohistochemical stainings of adult mouse hippocampus, as well as in immunostaining of cultured rat primary hippocampal neurons. In the latter, partial overlap of mTOR and Pum2 at Homer-marked synapses could be seen, suggesting synaptic localization. Assuming a protein-protein interaction, the most likely mechanism is phosphorylation of Pum2 by mTOR. Unpublished data previously established by the Kiebler group shows Pum2 phosphorylation using Phostag gels (Schieweck, unpublished). As a serine/threonine kinase, mTOR targets sites match those detected in Pum2. Furthermore, a phosphoproteome analysis of the mouse brain

performed in cooperation with Rico Schieweck (unpublished data) shows rapamycin dependent Pum2 phosphorylation. I tested differentiated cells of the hippocampal neuroblastoma cell line of embryonic day 10 (HN10e), in which colocalization of Pum2 and mTOR was prominent. Rapamycin is the best known drug for mTOR inhibition, and is also effectively used in a phase 3 study treating drug refractory epilepsy in TCS (French et al. 2016). In HN10e cells, rapamycin treatment reduced the number of Pum2 puncta colocalizing with mTOR significantly. This might point to a reduced interaction between the two proteins. Western blot analysis of Pum2 protein expression in HN10e cells upon rapamycin treatment showed reduction of Pum2, while Pum2 KD increased mTOR expression. My pilot experiments therefore suggest that Pum2 and mTOR might interact, further studies, however, will be necessary to substantiate this interaction in more detail.

In summary, my results suggest that mTOR is a likely contributor to epileptogenesis in adult $Pum2^{GT}$ mice, effecting downstream targets like voltage-gated potassium channels that influence synaptic excitability. A direct interaction of Pum2 and mTOR, however, can only be assumed. In the future, it will be of great interest to investigate the role of mTOR in genetic epilepsies such as those caused by RBP deficiencies. Already, mTOR inhibitors are successfully used in treatment of epilepsies caused by TSC (French et al. 2016). Furthermore, promising results have been shown in animal models, suggesting that the antiepileptic effect of ketogenic diets largely functions through inhibition of the mTOR pathway (McDaniel and Wong 2011). Interestingly, the concept of mTOR inhibition as a therapeutic option does not only account for genetic epilepsies that are believed to be directly caused by mTOR misregulation, but also in different kinds of genetic and acquired epilepsies (Citraro et al. 2016). On the other hand, further knowledge about the interplay of the mTOR pathway with RBPs could provide a new perspective on diagnosing intractable genetic epilepsy: Pum2 could play a role in yet unknown types of epilepsy, and other RBPs than FMRP, HuD and Pum2 may be controlled by mTOR. In the future, screenings for RBP deficiencies in patients suffering from unknown genetic epilepsies could provide valuable hints for seizure prevention and treatment, maybe even through pharmaceutical mTOR inhibition.

References

Alexander, A, M Maroso, and I Soltesz. 2016. “Organization and Control of Epileptic Circuits in Temporal Lobe Epilepsy.” *Progress in Brain Research* 226: 127–54. https://doi.org/10.1016/bs.pbr.2016.04.007.

Alvarez-Castelao, B, and E M Schuman. 2015. “The Regulation of Synaptic Protein Turnover.” *The Journal of Biological Chemistry* 290 (48): 28623–28630. https://doi.org/10.1074/jbc.R115.657130.

Amorim, I S, G Lach, and C G Gkogkas. 2018. “The Role of the Eukaryotic Translation Initiation Factor 4E (EIF4E) in Neuropsychiatric Disorders.” *Frontiers in Genetics* 9 (561): 1–9. https://doi.org/10.3389/fgene.2018.00561.

Aronica, E, K Boer, K J Doorn, E Zurolo, W G M Spliet, P C van Rijen, J C Baayen, J A Gorter, and A Jeromin. 2009. “Expression and Localization of Voltage Dependent Potassium Channel Kv4.2 in Epilepsy Associated Focal Lesions.” *Neurobiology of Disease* 36 (1): 81–95. https://doi.org/10.1016/j.nbd.2009.06.016.

Bagchi, B, A Al-Sabi, S Kaza, D Scholz, V B O’Leary, J O Dolly, and S V Ovsepian. 2014. “Disruption of Myelin Leads to Ectopic Expression of KV1.1 Channels with Abnormal Conductivity of Optic Nerve Axons in a Cuprizone-Induced Model of Demyelination.” *PLoS ONE* 9 (2): e87736. https://doi.org/10.1371/journal.pone.0087736.

Barnwell, L F S, J N Lugo, W L Lee, S E Willis, S J Gertz, R A Hrachovy, and A E Anderson. 2009. “Kv4.2 Knockout Mice Demonstrate Increased Susceptibility to Convulsant Stimulation.” *Epilepsia* 50 (7): 1741–51. https://doi.org/10.1111/j.1528-1167.2009.02086.x.

Biever, A, P G Donlin-Asp, and E M Schuman. 2019. “Local Translation in Neuronal Processes.” *Current Opinion in Neurobiology* 57: 141–48. https://doi.org/10.1016/j.conb.2019.02.008.

Blewett, N H, and A C Goldstrohm. 2012. “A Eukaryotic Translation Initiation Factor 4E-Binding Protein Promotes MRNA Decapping and Is Required for PUF Repression.” *Molecular and Cellular Biology* 32 (20): 4181–94. https://doi.org/10.1128/MCB.00483-12.

Blobel, G. 1980. “Intracellular Protein Topogenesis.” *Proceedings of the National Academy of Sciences* 77 (3): 1496–1500. https://doi.org/10.1073/pnas.77.3.1496.

Bohn, J A, J L Van Etten, T L Schagat, B M Bowman, R C McEachin, P L Freddolino, and A C Goldstrohm. 2018. “Identification of Diverse Target RNAs That Are Functionally Regulated by Human Pumilio Proteins.” *Nucleic Acids Research* 46 (1): 362–86. https://doi.org/10.1093/nar/gkx1120.

Brewer, GJ J, JR R Torricelli, E K Evege, and P J Price. 1993. “Optimized Survival of Hippocampal Neurons in B27-Supplemented Neurobasal?, A New Serum-Free Medium Combination.” *The Journal of Neuroscience Research* 35 (5): 567–76. https://doi.org/10.1002/jnr.490350513.

Buckmaster, P S, E A Ingram, and X Wen. 2009. “Inhibition of the Mammalian Target of Rapamycin Signaling Pathway Suppresses Dentate Granule Cell Axon Sprouting in a Rodent Model of Temporal Lobe Epilepsy.” *The Journal of Neuroscience* 29 (25): 8259–69. https://doi.org/10.1523/JNEUROSCI.4179-08.2009.

Buckmaster, P S, and F H Lew. 2011. “Rapamycin Suppresses Mossy Fiber Sprouting but Not Seizure Frequency in a Mouse Model of Temporal Lobe Epilepsy.” *The Journal of Neuroscience* 31 (6): 2337–47. https://doi.org/10.1523/JNEUROSCI.4852-10.2011.

Buckmaster, P S, and X Wen. 2011. “Rapamycin Suppresses Axon Sprouting by Somatostatin Interneurons in a Mouse Model of Temporal Lobe Epilepsy.” *Epilepsia* 52 (11): 2057–64. https://doi.org/10.1111/j.1528-1167.2011.03253.x.

Cao, Q, K Padmanabhan, and J D Richter. 2010. “Pumilio 2 Controls Translation by Competing with EIF4E for 7-Methyl Guanosine Cap Recognition.” *RNA (New York, N.Y.)* 16 (1): 221–27. https://doi.org/10.1261/rna.1884610.

Citraro, R, A Leo, A Constanti, E Russo, and G De Sarro. 2016. “MTOR Pathway Inhibition as a New Therapeutic Strategy in Epilepsy and Epileptogenesis.” *Pharmacological Research* 107: 333–43. https://doi.org/10.1016/j.phrs.2016.03.039.

Collart, M A. 2016. “The Ccr4-Not Complex Is a Key Regulator of Eukaryotic Gene Expression.” *Wiley Interdisciplinary Reviews: RNA* 7 (4): 438–54. https://doi.org/10.1002/wrna.1332.

Curatolo, P, R Moavero, J van Scheppingen, and E Aronica. 2018. “MTOR Dysregulation and Tuberous Sclerosis- Related Epilepsy.” *Expert Review of Neurotherapeutics* 18 (3): 185–201. https://doi.org/10.1080/14737175.2018.1428562.

D'Adamo, M C, L Catacuzzeno, G Di Giovanni, F Franciolini, and M Pessia. 2013. "K+ Channelepsy: Progress in the Neurobiology of Potassium Channels and Epilepsy." *Frontiers in Cellular Neuroscience* 7 (134): 1–21. https://doi.org/10.3389/fncel.2013.00134.

Dahm, R, and M A Kiebler. 2005. "Cell Biology: Silenced RNA on the Move." *Nature* 438 (7067): 432–35. https://doi.org/10.1038/438432a.

Deschênes-Furry, J, N Perrone-Bizzozero, and B J Jasmin. 2006. "The RNA-Binding Protein HuD: A Regulator of Neuronal Differentiation, Maintenance and Plasticity." *BioEssays* 28 (8): 822-833. https://doi.org/10.1002/bies.20449.

Dhiman, V. 2017. "Molecular Genetics of Epilepsy: A Clinician's Perspective." *Annals of Indian Academy of Neurology* 20 (2): 96–102. https://doi.org/10.4103/aian.AIAN_447_16.

Dong, H, M Zhu, L Meng, Y Ding, D Yang, S Zhang, W Qiang, D W Fisher, and E Y Xu. 2018. "Pumilio2 Regulates Synaptic Plasticity via Translational Repression of Synaptic Receptors in Mice." *Oncotarget* 9 (63): 32134–48. https://doi.org/10.18632/oncotarget.24345.

Doyle, M, and M A Kiebler. 2011. "Mechanisms of Dendritic MRNA Transport and Its Role in Synaptic Tagging." *The EMBO Journal* 30 (17): 3540–52. https://doi.org/10.1038/emboj.2011.278.

Driscoll, H E, N I Muraro, M He, and R A Baines. 2013. "Pumilio-2 Regulates Translation of Nav1.6 to Mediate Homeostasis of Membrane Excitability." *The Journal of Neuroscience* 33 (23): 9644–54. https://doi.org/10.1523/JNEUROSCI.0921-13.2013.

El-Hassar, L, M Esclapez, and C Bernard. 2017. "Hyperexcitability of the CA1 Hippocampal Region during Epileptogenesis." *Epilepsia* 48 (S5): 131–139. https://doi.org/10.1111/j.1528-1167.2007.01301.x.

Etten, J Van, T L Schagat, J Hrit, C A Weidmann, J Brumbaugh, J J Coon, and A C Goldstrohm. 2012. "Human Pumilio Proteins Recruit Multiple Deadenylases to Efficiently Repress Messenger RNAs." *The Journal of Biological Chemistry* 287 (43): 36370–83. https://doi.org/10.1074/jbc.M112.373522.

Ferron, L. 2016. "Fragile X Mental Retardation Protein Controls Ion Channel Expression and Activity." *The Journal of Physiology* 594 (20): 5861–67. https://doi.org/10.1113/JP270675.

Follwaczny, P, R Schieweck, T Riedemann, A Demleitner, T Straub, A H Klemm, M

Bilban, B Sutor, B Popper, and M A Kiebler. 2017. “Pumilio2-Deficient Mice Show a Predisposition for Epilepsy.” *Disease Models & Mechanisms* 10 (11): 1333–42. https://doi.org/10.1242/dmm.029678.

French, J A, J A Lawson, Z Yapici, H Ikeda, T Polster, R Nabbout, P Curatolo, et al. 2016. “Adjunctive Everolimus Therapy for Treatment-Resistant Focal-Onset Seizures Associated with Tuberous Sclerosis (EXIST-3): A Phase 3, Randomised, Double-Blind, Placebo-Controlled Study.” *The Lancet* 388 (10056): 2153–63. https://doi.org/10.1016/S0140-6736(16)31419-2.

Fukao, A, Y Sasano, H Imataka, K Inoue, H Sakamoto, N Sonenberg, C Thoma, and T Fujiwara. 2009. “The ELAV Protein HuD Stimulates Cap-Dependent Translation in a Poly(A)- and EIF4A-Dependent Manner.” *Molecular Cell* 36 (6): 1007–17. https://doi.org/10.1016/j.molcel.2009.11.013.

Gage, G J, D R Kipke, and W Shain. 2012. “Whole Animal Perfusion Fixation for Rodents.” *Journal of Visualized Experiments* 30 (65): 3564. https://doi.org/10.3791/3564.

Gehman, L T, P Stoilov, J Maguire, A Damianov, C H Lin, L Shiue, M Ares, I Mody, and D L Black. 2011. “The Splicing Regulator Rbfox1 (A2BP1) Controls Neuronal Excitation in the Mammalian Brain.” *Nature Genetics* 43 (7): 706–11. https://doi.org/10.1038/ng.841.

Godale, C M, and S C Danzer. 2018. “Signaling Pathways and Cellular Mechanisms Regulating Mossy Fiber Sprouting in the Development of Epilepsy.” *Frontiers in Neurology* 9 (298): 1–7. https://doi.org/10.3389/fneur.2018.00298.

Goetze, B, B Grunewald, M A Kiebler, and P Macchi. 2003. “Coupling the Iron-Responsive Element to GFP--an Inducible System to Study Translation in a Single Living Cell.” *Science’s STKE : Signal Transduction Knowledge Environment* 2003 (204): 1–15. https://doi.org/10.1126/stke.2003.204.pl12.

Goetze, B, and M A Kiebler. 2006. “Transfection of Hippocampal Neurons with Plasmid DNA Using Calcium Phosphate Coprecipitation.” In *Cold Spring Harbor Protocols*, 405–9. Vienna. https://doi.org/10.1101/pdb.prot4445.

Goldstrohm, A C, T M T Hall, and K M McKenney. 2018. “Post-Transcriptional Regulatory Functions of Mammalian Pumilio Proteins.” *Trends in Genetics* 34 (12): 972–90. https://doi.org/10.1016/j.tig.2018.09.006.

Goldstrohm, A C, B A Hook, D J Seay, and M Wickens. 2006. “PUF Proteins Bind Pop2p to Regulate Messenger RNAs.” *Nature Structural and Molecular Biology*

13 (6): 533–39. https://doi.org/10.1038/nsmb1100.

Goldstrohm, A C, and M Wickens. 2008. “Multifunctional Deadenylase Complexes Diversify MRNA Control.” *Nature Reviews Molecular Cell Biology* 9 (4): 337–44. https://doi.org/10.1038/nrm2370.

Gong, R, C S Park, N R Abbassi, and SJ Tang. 2006. “Roles of Glutamate Receptors and the Mammalian Target of Rapamycin (MTOR) Signaling Pathway in Activity-Dependent Dendritic Protein Synthesis in Hippocampal Neurons.” *The Journal of Biological Chemistry* 281 (27): 18802–15. https://doi.org/10.1074/jbc.M512524200.

Graber, T E, Pa McCamphill, and W S Sossin. 2013. “A Recollection of MTOR Signaling in Learning and Memory.” *Learning & Memory (Cold Spring Harbor, N.Y.)* 20 (10): 518–30. https://doi.org/10.1101/lm.027664.112.

Gross, C, X Yao, D L Pong, A Jeromin, and G J Bassell. 2011. “Fragile X Mental Retardation Protein Regulates Protein Expression and MRNA Translation of the Potassium Channel Kv4.2.” *The Journal of Neuroscience* 31 (15): 5693–98. https://doi.org/10.1523/JNEUROSCI.6661-10.2011.

Hagerman, P J, and C E Stafstrom. 2009. “Origins of Epilepsy in Fragile X Syndrome.” *Epilepsy Currents* 9 (4): 108–12. https://doi.org/10.1111/j.1535-7511.2009.01309.x.

Hall, A M, B T Throesch, S C Buckingham, S J Markwardt, Y Peng, Q Wang, D A Hoffman, and E D Roberson. 2015. “Tau-Dependent Kv4.2 Depletion and Dendritic Hyperexcitability in a Mouse Model of Alzheimer’s Disease.” *The Journal of Neuroscience* 35 (15): 6221–30. https://doi.org/10.1523/JNEUROSCI.2552-14.2015.

Hargus, N J, A Nigam, E H Bertram, and M K Patel. 2013. “Evidence for a Role of Nav1.6 in Facilitating Increases in Neuronal Hyperexcitability during Epileptogenesis.” *Journal of Neurophysiology* 110 (5): 1144–57. https://doi.org/10.1152/jn.00383.2013.

Hay, N, and N Sonenberg. 2004. “Upstream and Downstream of MTOR.” *Genes and Development* 18 (16): 1926–45. https://doi.org/10.1101/gad.1212704.

Hildebrand, M S, H H M Dahl, J A Damiano, R J H Smith, I E Scheffer, and S F Berkovic. 2013. “Recent Advances in the Molecular Genetics of Epilepsy.” *Journal of Medical Genetics* 50 (5): 271–79. https://doi.org/10.1136/jmedgenet-2012-101448.

Hoeffer, C A, E Sanchez, R J Hagerman, Y Mu, D V Nguyen, H Wong, A M Whelan, R S Zukin, E Klann, and F Tassone. 2012. “Altered MTOR Signaling and Enhanced CYFIP2 Expression Levels in Subjects with Fragile X Syndrome.” *Genes, Brain and Behavior* 11 (3): 332–41. https://doi.org/10.1111/j.1601-183X.2012.00768.x.

Hou, L, and E Klann. 2004. “Activation of the Phosphoinositide 3-Kinase-Akt-Mammalian Target of Rapamycin Signaling Pathway Is Required for Metabotropic Glutamate Receptor-Dependent Long-Term Depression.” *The Journal of Neuroscience* 24 (28): 6352–61. https://doi.org/10.1523/JNEUROSCI.0995-04.2004.

Jackson, R J, C U T Hellen, and T V Pestova. 2010. “The Mechanism of Eukaryotic Translation Initiation and Principles of Its Regulation.” *Nature Reviews Molecular Cell Biology* 11 (2): 113–27. https://doi.org/10.1038/nrm2838.

Jang, S H, J K Byun, W I Jeon, S Y Choi, J Park, B H Lee, J E Yang, et al. 2015. “Nuclear Localization and Functional Characteristics of Voltage-Gated Potassium Channel Kv1.3.” *The Journal of Biological Chemistry* 290 (20): 12547–57. https://doi.org/10.1074/jbc.M114.561324.

Jarero-Basulto, J J, Y Gasca-Martinez, M Rivera-Cervantes, M Ureña-Guerrero, A I Feria-Valesco, and C Beas-Zarate. 2018. “Interactions Between Epilepsy and Plasticity.” *Pharmaceuticals* 11 (1): 1–18. https://doi.org/10.3390/ph11010017.

Jenkins, H T, R Baker-Wilding, and T A Edwards. 2009. “Structure and RNA Binding of the Mouse Pumilio-2 Puf Domain.” *Journal of Structural Biology* 167 (3): 271–76. https://doi.org/10.1016/j.jsb.2009.06.007.

Jung, H, C G Gkogkas, N Sonenberg, and C E Holt. 2014. “Remote Control of Gene Function by Local Translation.” *Cell* 157 (1): 26-40. https://doi.org/10.1016/j.cell.2014.03.005.

Kepert, I, and M A Kiebler. 2013. “MoniTORing Neuronal Excitability at the Synapse.” *The Journal of Cell Biology* 202 (1): 7–9. https://doi.org/10.1083/jcb.201304183.

Kidd, S A, A Lachiewicz, D Barbouth, R Blitz, C Delahunty, D McBrien, J Visootsak, and E Berry-Kravis. 2014. “Fragile X Syndrome: A Review of Associated Medical Problems.” *Pediatrics* 134 (5): 995–1005. https://doi.org/10.1542/peds.2013-4301.

Kiebler, M A, and L DesGroseillers. 2000. “Molecular Insights into MRNA Transport and Local Translation in the Mammalian Nervous System.” *Neuron* 25 (1): 19–28.

https://doi.org/10.1016/s0896-6273(00)80868-5.

Kim, J, S C Jung, A M Clemens, R S Petralia, and D A Hoffman. 2007. “Regulation of Dendritic Excitability by Activity-Dependent Trafficking of the A-Type K+ Channel Subunit Kv4.2 in Hippocampal Neurons.” *Neuron* 54 (6): 933–47. https://doi.org/10.1016/j.neuron.2007.05.026.

Kirchheim, F, S Tinnes, C A Haas, M Stegen, and J Wolfart. 2013. “Regulation of Action Potential Delays via Voltage-Gated Potassium Kv1.1 Channels in Dentate Granule Cells during Hippocampal Epilepsy.” *Frontiers in Cellular Neuroscience* 7: 248. https://doi.org/10.3389/fncel.2013.00248.

Klein, M E, P E Castillo, and B A Jordan. 2015. “Coordination between Translation and Degradation Regulates Inducibility of MGluR-LTD.” *Cell Reports* 10 (9): 1459–66. https://doi.org/10.1016/j.celrep.2015.02.020.

Kohnhorst, C L, D L Schmitt, A Sundaram, and S An. 2016. “Subcellular Functions of Proteins under Fluorescence Single-Cell Microscopy.” *Biochimica et Biophysica Acta - Proteins and Proteomics* 1864 (1): 77–84. https://doi.org/10.1016/j.bbapap.2015.05.014.

Koyama, R, and Y Ikegaya. 2018. “The Molecular and Cellular Mechanisms of Axon Guidance in Mossy Fiber Sprouting.” *Frontiers in Neurology* 9 (29): 832. https://doi.org/10.3389/fneur.2018.00382.

Krymskaya, V P, and E A Goncharova. 2009. “PI3K/MTORC1 Activation in Hamartoma Syndromes: Therapeutic Prospects.” *Cell Cycle* 8 (3): 403–13. https://doi.org/10.4161/cc.8.3.7555.

Laplante, M, and D M Sabatini. 2009. “MTOR Signaling at a Glance.” *Journal of Cell Science* 122 (Pt 20): 3589–94. https://doi.org/122/20/3589 [pii] 10.1242/jcs.051011.

Laplante, M, and D M Sabatini. 2012. “MTOR Signaling in Growth Control and Disease.” *Cell* 149 (2): 274–93. https://doi.org/10.1016/j.cell.2012.03.017.

Lee, H J, D N Hammond, T H Large, J D Roback, J a Sim, D a Brown, U H Otten, and B H Wainer. 1990. “Neuronal Properties and Trophic Activities of Immortalized Hippocampal Cells from Embryonic and Young Adult Mice.” *The Journal of Neuroscience* 10 (6): 1779–87. https://doi.org/10.1523/JNEUROSCI.10-06-01779.1990.

Lee, Hye Young, Woo-Ping Ge, Wendy Huang, Ye He, Gordon X. Wang, Ashley Rowson-Baldwin, Stephen J. Smith, Yuh Nung Jan, and Lily Yeh Jan. 2011.

"Bidirectional Regulation of Dendritic Voltage-Gated Potassium Channels by the Fragile X Mental Retardation Protein." *Neuron* 72 (6): 1091. https://doi.org/10.1016/j.neuron.2011.11.012.

Lee, M H, B Hook, G Pan, A M Kershner, C Merritt, G Seydoux, J A Thomson, M Wickens, and J Kimble. 2007. "Conserved Regulation of MAP Kinase Expression by PUF RNA-Binding Proteins." *PLoS Genetics* 3 (12): 2540–50. https://doi.org/10.1371/journal.pgen.0030233.

Lerche, H, M Shah, H Beck, J Noebels, D Johnston, and A Vincent. 2013. "Ion Channels in Genetic and Acquired Forms of Epilepsy." *Journal of Physiology* 591 (4): 753–64. https://doi.org/10.1113/jphysiol.2012.240606.

Li, Yi, Zechun Peng, Bo Xiao, and Carolyn R. Houser. 2010. "Activation of ERK by Spontaneous Seizures in Neural Progenitors of the Dentate Gyrus in a Mouse Model of Epilepsy." *Experimental Neurology* 224 (1): 133–45. https://doi.org/10.1016/j.expneurol.2010.03.003.

Lin, MC A, S C Cannon, and D M Papazian. 2018. "Kv4.2 Autism and Epilepsy Mutation Enhances Inactivation of Closed Channels but Impairs Access to Inactivated State after Opening." *Proceedings of the National Academy of Sciences the United States of America* 115 (15): 3559–68. https://doi.org/10.1073/pnas.1717082115.

Linden, D J. 1996. "A Protein Synthesis-Dependent Late Phase of Cerebellar Long-Term Depression." *Neuron* 17 (3): 483–490. https://doi.org/10.1016/S0896-6273(00)80180-4.

Lipton, J O, and M Sahin. 2014. "The Neurology of MTOR." *Neuron* 84 (2): 275–91. https://doi.org/10.1016/j.neuron.2014.09.034.

Liu-Yesucevitz, L, G J Bassell, A D Gitler, A C Hart, E Klann, J D Richter, S T Warren, and B Wolozin. 2011. "Local RNA Translation at the Synapse and in Disease." *The Journal of Neuroscience* 31 (49): 16086–16093. https://doi.org/10.1523/JNEUROSCI.4105-11.2011.

Ljungberg, M C, C N Sunnen, J N Lugo, A E Anderson, and G D'Arcangelo. 2009. "Rapamycin Suppresses Seizures and Neuronal Hypertrophy in a Mouse Model of Cortical Dysplasia." *Disease Models & Mechanisms* 2 (7–8): 389–98. https://doi.org/10.1242/dmm.002386.

Löscher, W, H Potschka, S M Sisodiya, and A Vezzani. 2020. "Drug Resistance in Epilepsy: Clinical Impact, Potential Mechanisms, and New Innovative Treatment

Options.” *Pharmacological Reviews* 72 (3): 606–38. https://doi.org/10.1124/pr.120.019539.

Lugo, J N, L F Barnwell, Y Ren, W L Lee, L D Johnston, R Kim, R A Hrachovy, J D Sweatt, and A E Anderson. 2008. “Altered Phosphorylation and Localization of the A-Type Channel, Kv4.2 in Status Epilepticus.” *Journal of Neurochemistry* 106 (4): 1929–40. https://doi.org/10.1111/j.1471-4159.2008.05508.x.

Ma, X M, and J Blenis. 2009. “Molecular Mechanisms of MTOR-Mediated Translational Control.” *Nature Reviews. Molecular Cell Biology* 10 (5): 307–18. https://doi.org/10.1038/nrm2672.

Macchi, P, A M Brownawell, B Grunewald, L DesGroseillers, I G Macara, and M A Kiebler. 2004. “The Brain-Specific Double-Stranded RNA-Binding Protein Staufen2. Nucleolar Accumulation and Isoform-Specific Exportin-5-Dependent Export.” *The Journal of Biological Chemistry* 279 (30): 31440–44. https://doi.org/10.1074/jbc.C400226200.

Martínez, J C, L K Randolph, D M Iascone, H F Pernice, F Polleux, and U Hengst. 2019. “Pum2 Shapes the Transcriptome in Developing Axons through Retention of Target MRNAs in the Cell Body.” *Neuron* 104 (5): 931–46. https://doi.org/10.1016/j.neuron.2019.08.035.

Matsushita, Yuki, Yasunari Sakai, Mitsunori Shimmura, Hiroshi Shigeto, Miki Nishio, Satoshi Akamine, Masafumi Sanefuji, et al. 2016. “Hyperactive MTOR Signals in the Proopiomelanocortin-Expressing Hippocampal Neurons Cause Age-Dependent Epilepsy and Premature Death in Mice.” *Scientific Reports* 6: 1–12.

McDaniel, S S, and M Wong. 2011. “Therapeutic Role of Mammalian Target of Rapamycin (MTOR) Inhibition in Preventing Epileptogenesis.” *Neuroscience Letters* 497 (3): 231-239. https://doi.org/10.1016/j.neulet.2011.02.037.

Meng, X F, J T Yu, J H Song, S Chi, and L Tan. 2013. “Role of the MTOR Signaling Pathway in Epilepsy.” *Journal of the Neurological Sciences* 332 (1.2): 4-15. https://doi.org/10.1016/j.jns.2013.05.029.

Menon, K P, S Sanyal, Y Habara, R Sanchez, R P Wharton, M Ramaswami, and K Zinn. 2004. “The Translational Repressor Pumilio Regulates Presynaptic Morphology and Controls Postsynaptic Accumulation of Translation Factor EIF-4E.” *Neuron* 44 (4): 663–76. https://doi.org/10.1016/j.neuron.2004.10.028.

Monaghan, M M, J S Trimmer, and K J Rhodes. 2001. “Experimental Localization of Kv1 Family Voltage-Gated K + Channel α and β Subunits in Rat Hippocampal

Formation.” *The Journal of Neuroscience* 21 (16): 5973–5983. https://doi.org/10.1523/jneurosci.21-16-05973.2001.

Moon, I S, SJ Cho, DH Seog, and R Walikonis. 2009. “Neuronal Activation Increases the Density of Eukaryotic Translation Initiation Factor 4E MRNA Clusters in Dendrites of Cultured Hippocampal Neurons.” *EXPERIMENTAL and MOLECULAR MEDICINE* 41 (8): 601–10. https://doi.org/10.3858/emm.2009.41.8.066.

Narayanan, U, V Nalavadi, M Nakamoto, D C Pallas, S Ceman, G J Bassell, and S T Warren. 2007. “FMRP Phosphorylation Reveals an Immediate-Early Signaling Pathway Triggered by Group I MGluR and Mediated by PP2A.” *The Journal of Neuroscience* 27 (52): 14349 –14357. https://doi.org/10.1523/JNEUROSCI.2969-07.2007.

Narayanan, U, V Nalavadi, M Nakamoto, G Thomas, S Ceman, G J Bassell, and S T Warren. 2008. “S6K1 Phosphorylates and Regulates FMRP with the Neuronal Protein Synthesis-Dependent MTOR Signaling Cascade.” *The Journal of Biological Chemistry* 283 (27): 18478–82. https://doi.org/10.1074/jbc.C800055200.

Navidhamidi, M, M Ghasimi, and N Mehranfard. 2017. “Epilepsy-Associated Alterations in Hippocampal Excitability.” *Rev. Neuroscience* 28 (3): 307–34. https://doi.org/10.1515/revneuro-2016-0059.

Nguyen, L H, and A E Anderson. 2018. “MTOR-Dependent Alterations of Kv1.1 Subunit Expression in the Neuronal Subset-Specific Pten Knockout Mouse Model of Cortical Dysplasia with Epilepsy.” *Scientific Reports* 8 (1): 1–12. https://doi.org/10.1038/s41598-018-21656-8.

Niere, F, and K F Raab-Graham. 2017. “MTORC1 Is a Local, Postsynaptic Voltage Sensor Regulated by Positive and Negative Feedback Pathways.” *Frontiers in Cellular Neuroscience* 11 (152): 1–15. https://doi.org/10.3389/fncel.2017.00152.

Osterweil, E K, D D Krueger, K Reinhold, and M F Bear. 2010. “Hypersensitivity to MGluR5 and ERK1/2 Leads to Excessive Protein Synthesis in the Hippocampus of a Mouse Model of Fragile X Syndrome.” *The Journal of Neuroscience* 30 (46): 15616–27. https://doi.org/10.1523/JNEUROSCI.3888-10.2010.

Pan, T, P Rawal, Y Wu, W Xie, J Jankovic, and W Le. 2009. “Rapamycin Protects against Rotenone-Induced Apoptosis through Autophagy Induction.” *Neuroscience* 164 (2): 541–51.

https://doi.org/10.1016/j.neuroscience.2009.08.014.

Parras, A, H Anta, M Santos-Galindo, V Swarup, A Elorza, J L Nieto-González, S Picó, et al. 2018. “Autism-like Phenotype and Risk Gene MRNA Deadenylation by CPEB4 Mis-Splicing.” *Nature* 560 (7719): 441–46. https://doi.org/10.1038/s41586-018-0423-5.

Paulhus, K, L Ammerman, and E Glasscock. 2020. “Clinical Spectrum of KCNA1 Mutations: New Insights into Episodic Ataxia and Epilepsy Comorbidity.” *International Journal of Molecular Sciences* 21 (8): 2802. https://doi.org/10.3390/ijms21082802.

Pernice, H F, R Schieweck, M A Kiebler, and B Popper. 2016. “MTOR and MAPK: From Localized Translation Control to Epilepsy.” *BMC Neuroscience* 17 (1): 73. https://doi.org/10.1186/s12868-016-0308-1.

Perrone-Bizzozero, N, and C W Bird. 2013. “Role of HuD in Nervous System Function and Pathology.” *Front. Biosci.* 5 (1): 554–63. https://doi.org/10.2741/S389.

Popper, B, A Demleitner, V J Bolivar, G Kusek, A Snyder-Keller, R Schieweck, S Temple, and M A Kiebler. 2018. “Staufen2 Deficiency Leads to Impaired Response to Novelty in Mice.” *Neurobiology of Learning and Memory* 150 (2018): 107–15. https://doi.org/10.1016/j.nlm.2018.02.027.

Pun, R Y K, I J Rolle, C L LaSarge, B E Hosford, J M Rosen, J D Uhl, S N Schmeltzer, et al. 2012. “Excessive Activation of MTOR in Postnatally Generated Granule Cells Is Sufficient to Cause Epilepsy.” *Neuron* 75 (6): 1022–34. https://doi.org/10.1016/j.neuron.2012.08.002.

Raab-Graham, K F, P C G Haddick, Y N Jan, and L Y Jan. 2006. “Activity- and MTOR-Dependent Suppression of Kv1.1 Channel MRNA Translation in Dendrites.” *Science (New York, N.Y.)* 314 (5796): 144–48. https://doi.org/10.1126/science.1131693.

Ravanidis, S, F G Kattan, and E Doxakis. 2018. “Unraveling the Pathways to Neuronal Homeostasis and Disease: Mechanistic Insights into the Role of RNA-Binding Proteins and Associated Factors.” *International Journal of Molecular Sciences* 19 (8): 2280. https://doi.org/10.3390/ijms19082280.

Rhodes, K J, B W Strassle, M M Monaghan, Z Bekele-Arcuri, M F Matos, and James S. Trimmer. 1997. “Association and Colocalization of the Kvbeta1 and Kvbeta2 Beta-Subunits with Kv1 Alpha-Subunits in Mammalian Brain K+ Channel Complexes.” *The Journal of Neuroscience* 17 (21): 8246–58.

https://doi.org/ 10.1523/JNEUROSCI.17-21-08246.1997

Richter, J D, and N Sonenberg. 2005. “Regulation of Cap-Dependent Translation by EIF4E Inhibitory Proteins.” *Nature* 433 (7025): 477–80. https://doi.org/10.1038/nature03205.

Rodriguez, L, J B Mdzomba, S Joly, M Boudreau-Laprise, E Planel, and V Pernet. 2018. “Human Tau Expression Does Not Induce Mouse Retina Neurodegeneration, Suggesting Differential Toxicity of Tau in Brain vs. Retinal Neurons.” *Frontiers in Molecular Neuroscience* 11: 293. https://doi.org/10.3389/fnmol.2018.00293.

Rong, R, J Y Ahn, H Huang, E Nagata, D Kalman, J A Kapp, J Tu, P F Worley, S H Snyder, and K Ye. 2003. “PI3 Kinase Enhancer-Homer Complex Couples MGluRI to PI3 Kinase, Preventing Neuronal Apoptosis.” *Nature Neuroscience* 6 (11): 1153–61. https://doi.org/10.1038/nn1134.

Saxton, R A, and D M Sabatini. 2017. “MTOR Signaling in Growth, Metabolism, and Disease.” *Cell* 168 (6): 960–76. https://doi.org/10.1016/j.cell.2017.02.004.

Scheffer, I E, S Berkovic, G Capovilla, M B Connolly, J French, L Guilhoto, E Hirsch, et al. 2017. “ILAE Classification of the Epilepsies: Position Paper of the ILAE Commission for Classification and Terminology.” *Epilepsia* 48 (5): 512–521. https://doi.org/10.1111/epi.13709.

Schindelin, J, C T Rueden, M C Hiner, and K W Eliceiri. 2015. “The ImageJ Ecosystem: An Open Platform for Biomedical Image Analysis.” *Molecular Reproduction and Development* 82 (7–8): 518–29. https://doi.org/10.1002/mrd.22489.

Sendrowski, K, and W Sobaniec. 2013. “Hippocampus, Hippocampal Sclerosis and Epilepsy.” *Pharmacological Reports* 65 (3): 555–65. https://doi.org/10.1016/S1734-1140(13)71033-8.

Shakirullah, N Ali, A Khan, and M Nabi. 2014. “The Prevalence, Incidence and Etiology of Epilepsy.” *International Journal of Clinical and Experimental Neurology* 88 (3): 296–303. https://doi.org/10.12691/IJCEN-2-2-3.

Sharangdhar, T, Y Sugimoto, J Heraud-Farlow, S M Fernández-Moya, J Ehses, I Ruiz de los Mozos, J Ule, and M A Kiebler. 2017. “A Retained Intron in the 3′-UTR of Calm3 MRNA Mediates Its Staufen2- and Activity-dependent Localization to Neuronal Dendrites.” *EMBO Reports* 18 (10): 1762–74. https://doi.org/10.15252/embr.201744334.

Sharma, A, C A Hoeffer, Y Takayasu, T Miyawaki, S M McBride, E Klann, and R S

Zukin. 2010. “Dysregulation of MTOR Signaling in Fragile X Syndrome.” *The Journal of Neuroscience* 30 (2): 694–702. https://doi.org/30/2/694 [pii]\r10.1523/JNEUROSCI.3696-09.2010.

Shigeoka, T, B Lu, and C E Holt. 2013. “RNA-Based Mechanisms Underlying Axon Guidance.” *The Journal of Cell Biology* 202 (7): 991–99. https://doi.org/10.1083/jcb.201305139.

Shirokikh, N E, and T Preiss. 2018. “Translation Initiation by Cap-Dependent Ribosome Recruitment: Recent Insights and Open Questions.” *Wiley Interdisciplinary Reviews: RNA* 9 (4): 1–45. https://doi.org/10.1002/wrna.1473.

Shuyan, Q, G Weijun, X Jianin, W Congxiao, W Luyi, and Y Shouwei. 2019. “Glia Activation of Eukaryotic Translation Initiation Factor 4e-Binding Protein 1 in Temporal Lobe Epilepsy.” *Neuroreport* 30 (3): 222–226. https://doi.org/10.1097/WNR.0000000000001188.

Siemen, H, D Colas, H C Heller, O Brüstle, and R A Reijo Pera. 2011. “Pumilio-2 Function in the Mouse Nervous System.” *PLoS ONE* 6 (10): e25932. https://doi.org/10.1371/journal.pone.0025932.

Smart, S L, V Lopantsev, C L Zhang, C A Robbins, H Wang, S Y Chiu, P A Schwartzkroin, A Messing, and B L Tempel. 1998. “Deletion of the K(v)1.1 Potassium Channel Causes Epilepsy in Mice.” *Neuron* 20 (4): 809–19. https://doi.org/10.1016/S0896-6273(00)81018-1.

Sosanya, M N, D H Brager, S Wolfe, F Niere, and K F Raab-Graham. 2015. “Rapamycin Reveals an MTOR-Independent Repression of Kv1.1 Expression during Epileptogenesis.” *Neurobiology of Disease* 73: 96–105. https://doi.org/10.1016/j.nbd.2014.09.011.

Sosanya, N, P P C Huang, L P Cacheaux, C J Chen, K Nguyen, N I Perrone-Bizzozero, and K F Raab-Graham. 2013. “Degradation of High Affinity HuD Targets Releases Kv1.1 MRNA from MiR-129 Repression by MTORC1.” *The Journal of Cell Biology* 202 (1): 53–69. https://doi.org/10.1083/jcb.201212089.

Stoica, L, P J Zhu, W Huang, H Zhou, S C Kozma, and M Costa-Mattioli. 2011. “Selective Pharmacogenetic Inhibition of Mammalian Target of Rapamycin Complex I (MTORC1) Blocks Long-Term Synaptic Plasticity and Memory Storage.” *Proceedings of the National Academy of Sciences of the United States of America* 108 (9): 3791–96. https://doi.org/10.1073/pnas.1014715108.

Stoll, G, O P H Pietiläinen, B Linder, J Suvisaari, C Brosi, W Hennah, V Leppä, et al.

2013. “Deletion of TOP3β, a Component of FMRP-Containing MRNPs, Contributes to Neurodevelopmental Disorders.” *Nature Neuroscience* 16 (9): 1228–37. https://doi.org/10.1038/nn.3484.

Su, T, W D Cong, Y S Long, A H Luo, W W Sun, W Y Deng, and W P Liao. 2008. “Altered Expression of Voltage-Gated Potassium Channel 4.2 and Voltage-Gated Potassium Channel 4-Interacting Protein, and Changes in Intracellular Calcium Levels Following Lithium-Pilocarpine-Induced Status Epilepticus.” *Neuroscience* 157 (3): 566–76. https://doi.org/10.1016/j.neuroscience.2008.09.027.

Swiech, L, M Perycz, A Malik, and J Jaworski. 2008. “Role of MTOR in Physiology and Pathology of the Nervous System.” *Biochimica et Biophysica Acta - Proteins and Proteomics* 1784 (1): 116-132. https://doi.org/10.1016/j.bbapap.2007.08.015.

Takei, N, and H Nawa. 2014. “MTOR Signaling and Its Roles in Normal and Abnormal Brain Development.” *Frontiers in Molecular Neuroscience* 24 (7): 28. https://doi.org/10.3389/fnmol.2014.00028.

Talos, D M, L M Jacobs, S Gourmaud, C A Coto, H Sun, KC Lim, T H Lucas, K A Davis, M Martinez-Lage, and F E Jensen. 2018. “Mechanistic Target of Rapamycin Complex 1 and 2 in Human Temporal Lobe Epilepsy.” *Annual Neurology* 83 (2): 311–27. https://doi.org/10.1002/ana.25149.

Tang, C M, and S M Thompson. 2010. “Perturbations of Dendritic Excitability in Epilepsy.” *Epilepsia* 51 (5): 44. https://doi.org/10.1111/j.1528-1167.2010.02830.x.

Tang, H, H Long, C Zeng, Y Li, F Bi, J Wang, H Qian, and B Xiao. 2012. “Rapamycin Suppresses the Recurrent Excitatory Circuits of Dentate Gyrus in a Mouse Model of Temporal Lobe Epilepsy.” *Biochemical and Biophysical Research Communications* 420 (1): 199–204. https://doi.org/10.1016/j.bbrc.2012.02.143.

Tang, S J, G Reis, H Kang, AC Gingras, N Sonenberg, and E M Schuman. 2002. “A Rapamycin-Sensitive Signaling Pathway Contributes to Long-Term Synaptic Plasticity in the Hippocampus.” *Proceedings of the National Academy of Sciences of the United States of America* 99 (1): 467–72. https://doi.org/10.1073/pnas.012605299.

Tao-Cheng, J H, S Thein, Y Yang, T S Reese, and P E Gallant. 2014. “Homer Is Concentrated at the Postsynaptic Density and Does Not Redistribute after Acute Synaptic Stimulation.” *Neuroscience* 266: 80–90. https://doi.org/10.1016/j.neuroscience.2014.01.066.

Terenzio, M, S Koley, N Samra, I Rishal, Q Zhao, P K Sahoo, A Urisman, et al. 2018.

"Locally Translated MTOR Controls Axonal Local Translation in Nerve Injury." *Science* 359 (6382): 1416–21. https://doi.org/10.1126/science.aan1053.

Tiruchinapalli, D M, M G Caron, and J D Keene. 2008. "Activity-Dependent Expression of ELAV/Hu RBPs and Neuronal MRNAs in Seizure and Cocaine Brain." *Journal of Neurochemistry* 107 (6): 1529–43. https://doi.org/10.1111/j.1471-4159.2008.05718.x.

Tiruchinapalli, D M, M D Ehlers, and J D Keene. 2008. "Activity-Dependent Expression of RNA Binding Protein HuD and Its Association with MRNAs in Neurons." *RNA Biology* 5 (3): 157–68. https://doi.org/10.4161/rna.5.3.6782.

Tsokas, P, T Ma, R Iyengar, E M Landau, and R D Blitzer. 2007. "Mitogen-Activated Protein Kinase Upregulates the Dendritic Translation Machinery in Long-Term Potentiation by Controlling the Mammalian Target of Rapamycin Pathway." *The Journal of Neuroscience* 27 (22): 5885–94. https://doi.org/10.1523/JNEUROSCI.4548-06.2007.

Urbanska, M, A Gozdz, M Macias, I A Cymerman, E Liszewska, I Kondratiuk, H Devijver, B Lechat, F Van Leuven, and J Jaworski. 2018. "GSK3β Controls MTOR and Prosurvival Signaling in Neurons." *Molecular Neurobiology* 55 (7): 6050–62. https://doi.org/10.1007/s12035-017-0823-9.

Vacher, H, D P Mohapatra, and J S Trimmer. 2008. "Localization and Targeting of Voltage-Dependent Ion Channels in Mammalian Central Neurons." *Physiological Reviews* 88 (4): 1407–47. https://doi.org/10.1152/physrev.00002.2008.

Veh, R W, R Lichtinghagen, S Sewing, F Wunder, I M Grumbach, and O Pongs. 1995. "Immunohistochemical Localization of Five Members of the KV1 Channel Subunits: Contrasting Subcellular Locations and Neuron-specific Co-localizations in Rat Brain." *European Journal of Neuroscience* 7 (11): 2189–2205. https://doi.org/10.1111/j.1460-9568.1995.tb00641.x.

Venigalla, R K C, and M Turner. 2012. "RNA-Binding Proteins as a Point of Convergence of the PI3K and P38 MAPK Pathways." *Frontiers in Immunology* 3 (398): 1–9. https://doi.org/10.3389/fimmu.2012.00398.

Vessey, J P, L Schoderboeck, E Gingl, E Luzi, J Riefler, F Di Leva, D Karra, S Thomas, M A Kiebler, and P Macchi. 2010. "Mammalian Pumilio 2 Regulates Dendrite Morphogenesis and Synaptic Function." *Proceedings of the National Academy of Sciences of the United States of America* 107 (7): 3222–27. https://doi.org/10.1073/pnas.0907128107.

Vessey, J P, A Vaccani, Y Xie, R Dahm, D Karra, M A Kiebler, and P Macchi. 2006. “Dendritic Localization of the Translational Repressor Pumilio 2 and Its Contribution to Dendritic Stress Granules.” *The Journal of Neuroscience* 26 (24): 6496–6508. https://doi.org/10.1523/JNEUROSCI.0649-06.2006.

Vickers, C A, K S Dickson, and D J A Wyllie. 2005. “Induction and Maintenance of Late-Phase Long-Term Potentiation in Isolated Dendrites of Rat Hippocampal CA1 Pyramidal Neurones.” *Journal of Physiology* 568 (3): 803–13. https://doi.org/10.1113/jphysiol.2005.092924.

Wahl, D, S M Solon-Biet, Q P Wang, J A Wali, T Pulpitel, X Clark, D Raubenheimer, et al. 2018. “Comparing the Effects of Low-Protein and High-Carbohydrate Diets and Caloric Restriction on Brain Aging in Mice.” *Cell Reports* 25 (8): 2234–43. https://doi.org/10.1016/j.celrep.2018.10.070.

Weiss, A, A Roscic, and P Paganetti. 2009. “Inducible Mutant Huntingtin Expression in HN10 Cells Reproduces Huntington’s Disease-like Neuronal Dysfunction.” *Molecular Neurodegeneration* 4: 11. https://doi.org/1750-1326-4-11 [pii]\r10.1186/1750-1326-4-11.

Wickens, M, D S Bernstein, J Kimble, and R Parker. 2002. “A PUF Family Portrait: 3′UTR Regulation as a Way of Life.” *Trends in Genetics* 18 (3): 150–57. https://doi.org/10.1016/S0168-9525(01)02616-6.

Wolff, M, P Czorlich, C Nagaraj, R Schnöbel-Ehehalt, Y Li, G Kwapiszewska, H Olschewski, S Heschl, and A Olschewski. 2016. “Amitriptyline and Carbamazepine Utilize Voltage-Gated Ion Channel Suppression to Impair Excitability of Sensory Dorsal Horn Neurons in Thin Tissue Slice: An in Vitro Study.” *Neuroscience Research* 109: 16–27. https://doi.org/10.1016/j.neures.2016.02.006.

Wu, XL, H Huang, YY Huang, JX Yuan, X Zhou, and YM Chen. 2015. “Reduced Pumilio-2 Expression in Patients with Temporal Lobe Epilepsy and in the Lithium-Pilocarpine Induced Epilepsy Rat Model.” *Epilepsy & Behavior* 50: 31–39. https://doi.org/10.1016/j.yebeh.2015.05.017.

Xiong, L, F Wu, Q Wu, L Xu, O K Cheung, W Kang, M T Mok, et al. 2019. “Aberrant Enhancer Hypomethylation Contributes to Hepatic Carcinogenesis through Global Transcriptional Reprogramming.” *Nature Communications* 10 (1): 335. https://doi.org/10.1038/s41467-018-08245-z.

Yamawaki, R, K Thind, and P S Buckmaster. 2015. “Blockade of Excitatory

Synaptogenesis with Proximal Dendrites of Dentate Granule Cells Following Rapamycin Treatment in a Mouse Model of Temporal Lobe Epilepsy." *Journal of Comparative Neurology* 523 (2): 281–97. https://doi.org/10.1002/cne.23681.

Yang, Guo Shuai, Xiao Yan Zhou, Xue Fang An, Xuan Jun Liu, Yan Jun Zhang, and Dan Yu. 2018. "MTOR Is Involved in Stroke-Induced Seizures and the Anti-Seizure Effect of Mild Hypothermia." *Molecular Medicine Reports* 17 (4): 5821–29. https://doi.org/10.3892/mmr.2018.8629.

Yao, JJ, J Sun, QR Zhao, CY Wang, and YA Mei. 2013. "Neuregulin-1/ErbB4 Signaling Regulates Kv4.2-Mediated Transient Outward K+ Current through the Akt/MTOR Pathway." *American Journal of Physiology. Cell Physiology* 305 (2): C197-206. https://doi.org/10.1152/ajpcell.00041.2013.

Yoon, Y J, B Wu, A R Buxbaum, S Das, A Tsai, B P English, J B Grimm, L D Lavis, and R H Singer. 2016. "Glutamate-Induced RNA Localization and Translation in Neurons." *Proceedings of the National Academy of Sciences of the United States of America* 113 (44): E6877–86. https://doi.org/10.1073/pnas.1614267113.

Zeng, LH, N R Rensing, and M Wong. 2009. "The Mammalian Target of Rapamycin Signaling Pathway Mediates Epileptogenesis in a Model of Temporal Lobe Epilepsy." *The Journal of Neuroscience* 29 (21): 6964–72. https://doi.org/10.1523/JNEUROSCI.0066-09.2009.

Zhang, M, D Chen, J Xia, W Han, X Cui, N Neuenkirchen, G Hermes, N Sestan, and H Lin. 2017. "Post-Transcriptional Regulation of Mouse Neurogenesis by Pumilio Proteins." *Genes and Development* 31 (13): 1354–69. https://doi.org/10.1101/gad.298752.117.

Zhang, X, D Peng, Y Xi, C Yuan, C A Sagum, B J Klein, K Tanaka, et al. 2016. "G9a-Mediated Methylation of ERα Links the PHF20/MOF Histone Acetyltransferase Complex to Hormonal Gene Expression." *Nature Communications* 7: 10810. https://doi.org/10.1038/ncomms10810.

Zhou, J, and L F Parada. 2012. "PTEN Signaling in Autism Spectrum Disorders." *Current Opinion in Neurobiology* 22 (5): 873–79. https://doi.org/10.1016/j.conb.2012.05.004.

List of figures

List of tables

List of Abbreviations

3'-UTR: 3'-untranslated region
7mG: 7-methylguanine
4EBP: eIF4e binding protein
AKT: protein kinase B (also: PKB)
APS: ammonium persulfate
BES: 2-(Bis[2-hydroxyethyl]amino) ethanesulfonic acid
BBS: BES buffered saline
BSA: bovine serum albumin
CA: cornu amonis
CaMKIIa: Ca^{2+}/calmodulin-dependent protein kinase II alpha
CCR4-Not complex: carbon catabolite repression—negative on TATA-less complex
cDNA: complementary DNA
CPBP4: cytoplasmic polyadenylation binding protein 4
CREB: cAMP response element-binding protein
DEPTOR: DEP domain containing mTOR-interacting protein
ddH_2O: double distilled water
DG: dentate gyrus
DGC: dentate gyrus cell
DIV15: day in vitro 15
DMEM: Dulbecco's modified Eagle's medium
DMSO: dimethylsufloxide
dNTP: desoxynucleoside triphosphate
DTT: 1,4–Dithiothreitol
DAPI: 4′,6-Diamidin-2-phenylindol
GFP: green fluorescent protein
DMEM: Dulbecco's modified Eagle's medium
DNA: deoxyribonucleic acid
DRG: dorsal root ganglion
E17: embryonic day 17
eIF4e: eukaryotic initiation factor 4e
ERK: extracellular-signal regulated kinases (also: MAPK)
FCS: fetal calf serum
FKBP12: FK506 binding protein of 12 kDa
fmr1: fragile X mental retardation mRNA
FMRP: fragile X mental retardation protein

$GABA_AR$: gamma aminobutyric acid type A receptor
GSK3: glycogen synthase kinase 3
GTP: guanosine-5'-triphosphate
HBSS: Hank´s balanced salt solution
Hepes: 2-(4-(2-Hydroxyethyl)-piperazinyl-ethanosulfonic acid
HeLa cells: immortal cell line derived from cancer cells of Henrietta Lacks
HN10e: hippocampal neuroblastoma cell line of embryonic day 10
HS: horse serum
HuD: ELAV-like protein 4 (also: ELAVL4)
HuR: ELAV-like protein 1 (also: ELAVL1)
HyD: hybrid photodetector (Leica)
IHC: immunohistochemistry
IMM objective: multi-immersion objective (Leica)
KD: knock down
KO: knock out
$K_v1.1$: voltage-gated potassium channel 1.1
$K_v4.2$: voltage-gated potassium channel 4.2
LB media: lysogeny broth media
LTP: long-term potentiation
MAPK: mitogen-activated protein kinase (also: ERK)
MEM: minimum essential medium
mGluR: metabolic glutamate receptor
mLST8: mammalian lethal with Sec13 protein 8 (also: GßL)
mSin1: mammalian stress-activated map kinase-interacting protein 1
mRNA: messenger RNA
mTOR: mechanistic target of rapamycin
mTORC1,2: mTOR complex 1 or 2
Na_v: voltage-gated sodium channel
NMDA: N-methyl-D-aspartic acid
NMDAR: NMDA receptor
NTC: non-targeting control
PBS: phosphate buffered saline
PBST: PBS +Tween buffer
PCR: polymerase chain reaction
PFA: paraformaldehyde
PI3K: Phosphoinositide 3-kinase
PIP2: Phosphatidylinositol 4,5-bisphosphate

PIP3:	Phosphatidylinositol (3,4,5)-trisphosphate
PKB:	protein kinase B (also: AKT)
pmTOR:	phosphorylated mTOR (also: p-mTOR)
PRAS40:	proline-rich Akt substrate 40kDa
protor1/2:	protein observed with rictor 1 and 2
pS6:	phosphorylated S6 (also: p-S6)
PSD95:	postsynaptic density protein 95
PTEN:	Phosphatase and tensine homologue
Pum1:	Pumilio1
Pum2:	Pumilio2
$Pum2^{GT}$:	Pum2 gene trap mouse
PUF:	FBF repressor protein
qRT-PCR:	Quantitative real-time polymerase chain reaction
RA:	retinoic acid
Raptor:	regulatory protein associated with mTOR
Ras:	rat sarcoma
RBFOX1:	RNA binding protein fox1 homolog 1
RBP:	RNA-binding protein
Rheb:	ras homolog enriched in brain
Rictor:	rapamycin-insensitive companion of mTOR
RNA:	ribonucleic acid
RNP:	ribonucleoprotein particle
ROI:	region of interest
RT:	room temperature
S6:	40S ribosomal protein S6
S6K:	ribosomal protein S6 kinase
SEM:	standard error of the mean
SDS:	alpha-Dodecylsulfate
SDS page:	SDS polyacrylamide gel electrophoresis
SGK:	Serine/Threonine protein kinases
shNTC:	shRNA construct for non-targeting control
shPum2:	shRNA construct directed against Pum2
shRNA:	short hairpin RNA
SLM:	stratum lacunosum moleculare
tagRFP:	Tag red fluorescent protein
TBS:	tris buffered saline
TEMED:	N,N,N',N-Tetramethylethylenediamine

TLE:	temporal lobe epilepsy
TSC1/2:	Tuberous complex 1/2
WT:	wild type
YFP:	yellow fluorescent protein

Acknowledgements

I am sincerely grateful to my supervisor, Prof. Dr. Michael Kiebler for the opportunity to realize my thesis work in his laboratory. I thank him for his support, patience, and teaching throughout my laboratory work, as well as for all the discussions, meetings, read throughs, advises, and corrections beyond that. This and his generous recommendations for scholarships and projects beyond my thesis, enabled me to grow as a scientist in the medical society.

A special thanks goes to my supervisor and mentor Dr. Bastian Popper, whom I owe not only being accepted to the FöFoLe program, but also numerous opportunities, such as publications of projects beyond my thesis, as well as participation and presentations at multiple scientific conferences and meetings. I want to thank him for guiding my research, for always being available for even the smallest questions and for always pushing me to go further. I feel humbled by the dedication and generosity with which the entire Kiebler-AG has taught me to be able to independently perform laboratory work. Especially, I thank Rico Schieweck, who has helped me with the simplest and the most difficult of problems, advised me with his impressive experience and knowledge, and taught me almost everything I now know about laboratory work.

I also thank all the collaborating labs, especially the Zentrale Versuchstierhaltung LMU Innenstadt and the BMC Core Facility Bio Imaging for providing me with the resources to perform all my experiences.

Without the FöFoLe program and their interesting lectures, I would not have been able to participate and grow so much in the scientific community. I also want to thank my Promotionskommitee including Prof. Dr. Axel Imhof for his support and availability during the FöFoLe program.

Finally, without the endless support of my genius family, especially my parents and my big brothers Leon and Maxi, who inspired me to choose the world of science and never stopped supporting me and pushing me to reach my goals, I probably never would stand where I do now. Without my incredible friends, their endless love, support, and advice, none of this would have been possible.

Affidavit

LMU LUDWIG-MAXIMILIANS-UNIVERSITÄT MÜNCHEN | Promotionsbüro Medizinische Fakultät | MMRS

Eidesstattliche Versicherung

Ich , Helena Franziska Pernice, erkläre hiermit an Eides statt, dass ich die vorliegende Dissertation mit dem Titel:

“The role of the kinase mechanistic Target Of Rapamycin – mTOR – and the RNA-binding protein Pumilio2 in epileptogenesis”

selbständig verfasst, mich außer der angegebenen keiner weiteren Hilfsmittel bedient und alle Erkenntnisse, die aus dem Schrifttum ganz oder annähernd übernommen sind, als solche kenntlich gemacht und nach ihrer Herkunft unter Bezeichnung der Fundstelle einzeln nachgewiesen habe.

Ich erkläre des Weiteren, dass die hier vorgelegte Dissertation nicht in gleicher oder in ähnlicher Form bei einer anderen Stelle zur Erlangung eines akademischen Grades eingereicht wurde.

Berlin, 29.11.2021
Ort, Datum

Pernice, Helena Franziska
Name, Vorname

List of Publications

03.2021 Educational Article: „HIV-Patient:innen mit Dysästhesien – An Polyneuropathien denken!“ Hahn K, Pernice HF. *doctors|today, 2021 Mar*; *1(3):*28-30

12.2019 Research Article: “Pum2 shapes the transcriptome in developing axons through retention of target mRNAs in the cell body.” Martínez J C, Randolph L K, Iascone DM, Pernice H F, Polleux F, Hengst U. *Neuron, 2019 Dec 4, 104(5):931-946.*

04.2019 Research Article: "Altered Glutamate Receptor Ionotropic Delta Subunit 2 Expression in Stau2-Deficient Cerebellar Purkinje Cells in the Adult Brain" Pernice H F, Schieweck R, Jafari M, Straub T, Bilban M, Kiebler M A, Popper B. *International Journal of Molecular Sciences, 2019 Apr; 20(7): 1797.*

11.2016 Review Article: „mTOR and MAPK: from localized translation control to epilepsy“ Pernice H F, Schieweck R, Kiebler M A, Popper B. *BMC Neuroscience, 2016 Nov; 17: 73.*